

Whole-genome sequencing reveals host factors underlying critical COVID-19

<https://doi.org/10.1038/s41586-022-04576-6>

Received: 2 September 2021

Accepted: 23 February 2022

Published online: 7 March 2022

Open access

 Check for updates

Athanasios Kousathanas^{1,556}, Erola Pairo-Castineira^{2,3,556}, Konrad Rawlik², Alex Stuckey¹, Christopher A. Odhams¹, Susan Walker¹, Clark D. Russell^{2,4}, Tomas Malinauskas⁵, Yang Wu⁶, Jonathan Millar², Xia Shen^{7,8}, Katherine S. Elliott⁵, Fiona Griffiths², Wilna Oosthuyzen², Kirstie Morrice⁹, Sean Keating¹⁰, Bo Wang², Daniel Rhodes¹, Lucija Klaric³, Marie Zechner², Nick Parkinson², Afshan Siddiq¹, Peter Goddard¹, Sally Donovan¹, David Maslove¹¹, Alistair Nichol¹², Malcolm G. Semple^{13,14}, Tala Zainy¹, Fiona Maleady-Crowe¹, Linda Todd¹, Shahla Salehi¹, Julian Knight⁵, Greg Elgar¹, Georgia Chan¹, Prabhu Arumugam¹, Christine Patch¹, Augusto Rendon¹, David Bentley¹⁵, Clare Kingsley¹⁵, Jack A. Kosmicki¹⁶, Julie E. Horowitz¹⁶, Aris Baras¹⁶, Goncalo R. Abecasis¹⁶, Manuel A. R. Ferreira¹⁶, Anne Justice¹⁷, Tooraj Mirshahi¹⁷, Matthew Oetjens¹⁷, Daniel J. Rader¹⁸, Marylyn D. Ritchie¹⁸, Anurag Verma¹⁸, Tom A. Fowler^{1,19}, Manu Shankar-Hari²⁰, Charlotte Summers²¹, Charles Hinds²², Peter Horby²³, Lowell Ling²⁴, Danny McAuley^{25,26}, Hugh Montgomery²⁷, Peter J. M. Openshaw^{28,29}, Paul Elliott³⁰, Timothy Walsh¹⁰, Albert Tenesa^{2,3,8}, GenOMICC investigators*, 23andMe investigators*, COVID-19 Human Genetics Initiative*, Angie Fawkes⁹, Lee Murphy⁹, Kathy Rowan³¹, Chris P. Ponting³, Veronique Vitart³, James F. Wilson^{3,8}, Jian Yang^{32,33}, Andrew D. Bretherick³, Richard H. Scott^{1,3,4}, Sara Clohisey Hendry^{2,557}, Loukas Moutsianas^{1,557}, Andy Law^{2,557}, Mark J. Caulfield^{1,35,557} & J. Kenneth Baillie^{2,3,4,10,557}

Critical COVID-19 is caused by immune-mediated inflammatory lung injury. Host genetic variation influences the development of illness requiring critical care¹ or hospitalization^{2–4} after infection with SARS-CoV-2. The GenOMICC (Genetics of Mortality in Critical Care) study enables the comparison of genomes from individuals who are critically ill with those of population controls to find underlying disease mechanisms. Here we use whole-genome sequencing in 7,491 critically ill individuals compared with 48,400 controls to discover and replicate 23 independent variants that significantly predispose to critical COVID-19. We identify 16 new independent associations, including variants within genes that are involved in interferon signalling (*IL10RB* and *PLSCR1*), leucocyte differentiation (*BCL11A*) and blood-type antigen secretor status (*FUT2*). Using transcriptome-wide association and colocalization to infer the effect of gene expression on disease severity, we find evidence that implicates multiple genes—including reduced expression of a membrane flippase (*ATP11A*), and increased expression of a mucin (*MUC1*)—in critical disease. Mendelian randomization provides evidence in support of causal roles for myeloid cell adhesion molecules (*SELE*, *ICAM5* and *CD209*) and the coagulation factor *F8*, all of which are potentially druggable targets. Our results are broadly consistent with a multi-component model of COVID-19 pathophysiology, in which at least two distinct mechanisms can predispose to life-threatening disease: failure to control viral replication; or an enhanced tendency towards pulmonary inflammation and intravascular coagulation. We show that comparison between cases of critical illness and population controls is highly efficient for the detection of therapeutically relevant mechanisms of disease.

Critical illness in COVID-19 is both an extreme disease phenotype and a relatively homogeneous clinical definition; it includes patients with hypoxaemic respiratory failure⁵ with acute lung injury⁶, and excludes many patients with non-pulmonary clinical presentations⁷, who are known to have divergent responses to therapy⁸. In the UK, individuals in the critically ill group are younger, less likely to have significant

comorbidity and more severely affected than a general hospitalized cohort⁵, characteristics which may amplify observed genetic effects. In addition, as development of critical illness is in itself a key clinical end-point for therapeutic trials⁸, using critical illness as a phenotype in genetic studies enables the detection of directly therapeutically relevant genetic effects¹.

A list of affiliations appears at the end of the paper.

Table 1 | Lead variants from independent association signals in the per-population GWAS and multi-ancestry meta-analysis

| chr:pos (hg38) | rsID | REF | ALT | RAF | OR | OR _{CI} | P | P _{Hglib2.23m} | P _{reg} | Consequence | Gene | Cit. |
|--------------------------|-------------|-----|------|--------|-----|------------------|-------------------------|-------------------------|------------------|-------------|-----------|--------------|
| 1:155066988 | rs114301457 | C | T* | 0.0058 | 2.4 | 1.82–3.16 | 6.8×10 ⁻¹⁰ | 0.00011* | – | Synonymous | EFNA4 | – |
| 1:155175305 [†] | rs7528026 | G | A* | 0.032 | 1.4 | 1.24–1.55 | 7.16×10 ⁻⁹ | 0.00012* | – | Intron | TRIM46 | – |
| 1:155197995 | rs41264915 | A* | G | 0.89 | 1.3 | 1.19–1.37 | 1.02×10 ⁻¹² | 1.51×10 ^{-9*} | – | Intron | THBS3 | ³ |
| 2:60480453 [†] | rs1123573 | A* | G | 0.61 | 1.1 | 1.09–1.18 | 9.85×10 ⁻¹⁰ | 0.000018* | – | Intron | BCL11A | – |
| 3:45796521 | rs2271616 | G | T* | 0.14 | 1.3 | 1.21–1.37 | 9.9×10 ⁻¹⁷ | 4.95×10 ^{-9*} | – | 5' UTR | SLC6A20 | ³ |
| 3:45859597 | rs73064425 | C | T* | 0.077 | 2.7 | 2.51–2.94 | 1.97×10 ⁻¹³³ | 1.02×10 ^{-77*} | – | Intron | LZTFL1 | ² |
| 3:146517122 | rs343320 | G | A* | 0.081 | 1.2 | 1.16–1.35 | 4.94×10 ⁻⁹ | 0.00028* | – | Missense | PLSCR1 | – |
| 5:131995059 | rs56162149 | C | T* | 0.17 | 1.2 | 1.13–1.26 | 7.65×10 ⁻¹¹ | 0.00074* | – | Intron | ACSL6 | – |
| 6:32623820 | rs9271609 | T* | C | 0.65 | 1.1 | 1.09–1.19 | 3.26×10 ⁻⁹ | 0.89 | – | – | HLA-DRB1 | – |
| 6:41515007 [†] | rs2496644 | A* | C | 0.015 | 1.4 | 1.32–1.60 | 7.59×10 ⁻¹⁵ | 3.17×10 ^{-7*} | – | Intron | LINC01276 | ³ |
| 9:21206606 | rs28368148 | C | G* | 0.013 | 1.7 | 1.45–2.09 | 1.93×10 ⁻⁹ | 0.0024 | 0.00089 | Missense | IFNA10 | – |
| 11:34482745 | rs61882275 | G* | A | 0.62 | 1.1 | 1.10–1.20 | 1.61×10 ⁻¹⁰ | 1.9×10 ^{-10*} | – | Intron | ELF5 | – |
| 12:132489230 | rs56106917 | GC | G* | 0.49 | 1.1 | 1.09–1.18 | 2.08×10 ⁻⁹ | 0.00047* | – | Upstream | FBRSL1 | – |
| 13:112889041 | rs9577175 | C | T* | 0.23 | 1.2 | 1.12–1.24 | 3.71×10 ⁻¹¹ | 1.29×10 ^{-6*} | – | Downstream | ATP11A | – |
| 15:93046840 [†] | rs4424872 | T* | A | 0.0079 | 2.4 | 1.87–3.01 | 8.61×10 ⁻¹³ | – | 0.29 | Intron | RGMA | – |
| 16:89196249 | rs117169628 | G | A* | 0.15 | 1.2 | 1.12–1.26 | 4.4×10 ⁻⁹ | 6.57×10 ^{-9*} | – | Missense | SLC22A31 | – |
| 17:46152620 | rs2532300 | T* | C | 0.77 | 1.2 | 1.10–1.22 | 4.19×10 ⁻⁹ | 2.49×10 ^{-9*} | – | Intron | KANSL1 | ⁹ |
| 17:49863260 | rs3848456 | C | A* | 0.029 | 1.5 | 1.33–1.70 | 4.19×10 ⁻¹¹ | 1.34×10 ^{-7*} | – | Regulatory | . | ³ |
| 19:4717660 | rs12610495 | A | G* | 0.31 | 1.3 | 1.27–1.38 | 3.91×10 ⁻³⁶ | 5.74×10 ^{-19*} | – | Intron | DPP9 | ¹ |
| 19:10305768 | rs73510898 | G | A* | 0.093 | 1.3 | 1.19–1.37 | 1.57×10 ⁻¹¹ | 0.00016* | – | Intron | ZGLP1 | – |
| 19:10352442 | rs34536443 | G | C* | 0.05 | 1.5 | 1.36–1.65 | 6.98×10 ⁻¹⁷ | 4.06×10 ^{-11*} | – | Missense | TYK2 | ¹ |
| 19:48697960 | rs368565 | C | T* | 0.44 | 1.1 | 1.1–1.2 | 3.55×10 ⁻¹¹ | 0.00087* | – | Intron | FUT2 | – |
| 21:33230000 | rs17860115 | C | A* | 0.32 | 1.2 | 1.19–1.3 | 9.69×10 ⁻²² | 1.77×10 ^{-18*} | – | 5' UTR | IFNAR2 | ¹ |
| 21:33287378 | rs8178521 | C | T* | 0.27 | 1.2 | 1.12–1.23 | 3.53×10 ⁻¹² | 8.02×10 ^{-6*} | – | Intron | IL10RB | – |
| 21:33959662 | rs35370143 | T | TAC* | 0.083 | 1.3 | 1.17–1.36 | 1.24×10 ⁻⁹ | 2.33×10 ^{-7*} | – | Intron | LINC00649 | – |

Variants and the reference and alternative allele are reported according to GRCh38. The three variants discovered in multi-ancestry meta-analysis but not in the European ancestry GWAS are labelled with †, and † indicates genome-wide significant heterogeneity. REF and ALT columns indicate the reference and alternative alleles; an asterisk (*) indicates the risk allele. For each variant, we report the risk allele frequency in Europeans (RAF), the odds ratio and 95% confidence interval (OR and OR_{CI}), and the association P value. 'Consequence' indicates the predicted worst consequence type across GENCODE basic transcripts predicted by VEP (v104), and 'Gene' indicates the VEP-predicted gene, but not necessarily the causal mediator. For the HLA locus, the gene that was identified by HLA allele analysis is displayed. An asterisk (*) next to the replication P value (P_{Hglib2.23m} - HGI B2 and 23andMe; or P_{reg} - Regeneron) indicates that the lead signal (from multi-ancestry meta-analysis) is replicated with a Bonferroni-corrected P < 0.002 (0.05/25) with a concordant direction of effect. The 'Cit.' column lists citation numbers for the first publication of confirmed genome-wide associations with critical illness or (in brackets) any COVID-19 phenotype.

Using microarray genotyping in 2,244 cases, we previously discovered that critical COVID-19 is associated with genetic variation in the host immune response to viral infection (*OAS1*, *IFNAR2* and *TYK2*) and the inflammasome regulator *DPP9*⁹. In collaboration with international groups, we extended these findings to include a variant near *TAC4* (rs77534576)³. Several variants have been associated with milder phenotypes, including the ABO blood-type locus², a pleiotropic inversion in chr17q21.31⁹ and associations in five additional loci, including the T lymphocyte-associated transcription factor, *FOXP4*³. An enrichment of rare loss-of-function variants in candidate interferon signalling genes has been reported⁴, but this has yet to be replicated at genome-wide significance thresholds^{10,11}.

In partnership with Genomics England, we performed whole-genome sequencing (WGS) to improve the resolution and deepen the fine-mapping of significant signals and thereby provide further biological insight into critical COVID-19. Here we present results from a cohort of 7,491 critically ill patients from 224 intensive care units, compared with 48,400 control individuals, describing the discovery and validation of 23 gene loci for susceptibility to critical COVID-19 (Extended Data Fig. 1).

Genome-wide association study analysis

After quality control procedures, we used a logistic mixed model regression, implemented in SAIGE¹², to perform association analyses with unrelated individuals (critically ill cases, *n* = 7,491; controls, *n* = 48,400 (100,000 Genomes Project (100k) cohort, *n* = 46,770; mild COVID-19, *n* = 1,630) (Methods, Supplementary Table 2). A total of 1,339 of these cases were included in the primary analysis for our previous report¹. Genome-wide association studies (GWASs) were performed separately for genetic ancestry groups (*n*_{cases}/*n*_{controls}: European (EUR) 5,989/42,891; South Asian (SAS) 788/3,793; African (AFR) 440/1,350; East Asian (EAS) 274/366), and combined by inverse-variance-weighted fixed effects meta-analysis using METAL (Methods). We established the independence of signals using GCTA-cojo, and we validated this with conditional analysis using individual-level data with SAIGE (Methods, Supplementary Table 6). To reduce the risk of spurious associations arising from genotyping or pipeline errors, we required supporting evidence from variants in linkage disequilibrium (LD) for all genome-wide-significant variants: observed z-scores for each variant were compared with imputed z-scores for the same variant, with discrepant values being excluded (see Methods, Supplementary Fig. 2).

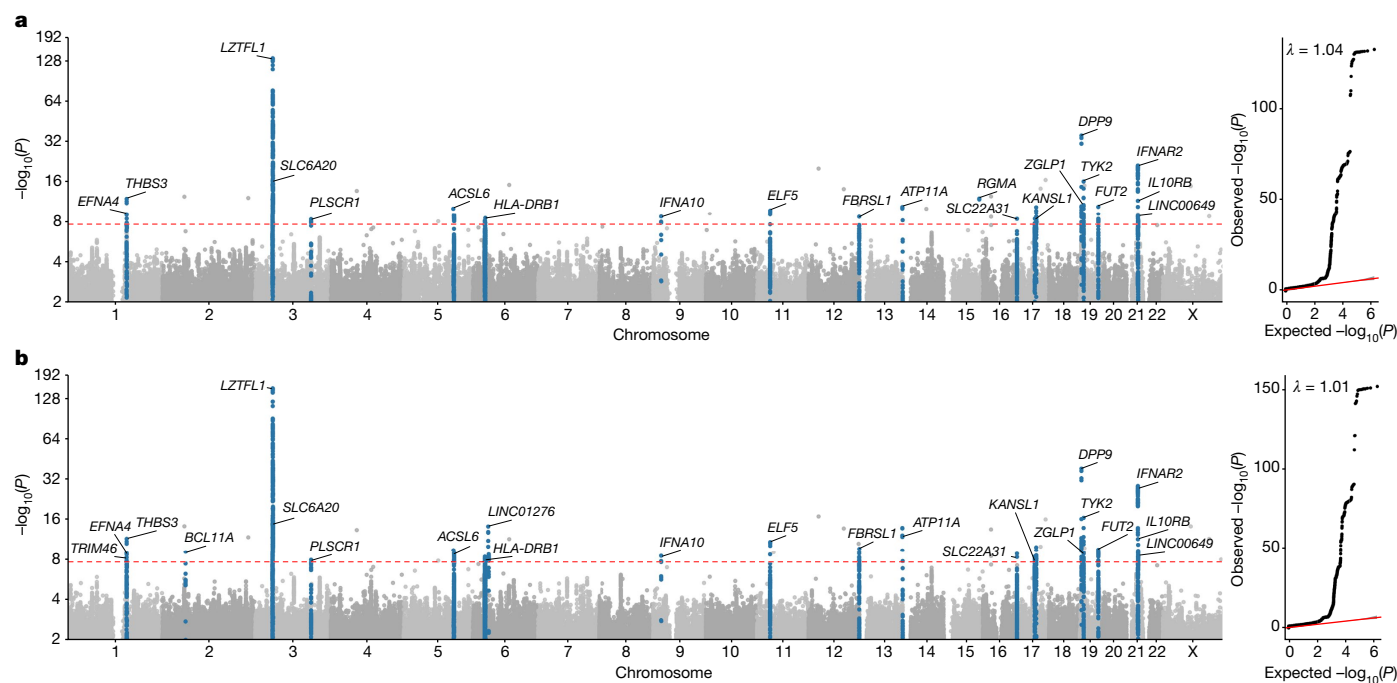


Fig. 1 | GWAS results for the EUR ancestry group, and multi-ancestry meta-analysis. Manhattan plots are shown on the left and quantile–quantile (QQ) plots of observed versus expected P values on the right, with genomic inflation (λ) displayed for each analysis. Highlighted results in blue in the Manhattan plots indicate variants that are LD-clumped ($r^2 = 0.1$, $P_2 = 0.01$, EUR LD) with the lead variants at each locus. Gene name annotation indicates genes

that are affected by the predicted worst consequence type of each lead variant (annotation by Variant Effect Predictor (VEP)). For the HLA locus, the gene that was identified by HLA allele analysis is annotated. The GWAS was performed using logistic regression and meta-analysed by the inverse variant method. The red dashed line shows the Bonferroni-corrected P value: $P = 2.2 \times 10^{-8}$.

In population-specific analyses, we discovered 22 independent genome-wide-significant associations in the EUR ancestry group (Fig. 1, Supplementary Fig. 11, Table 1) at a P value threshold adjusted for multiple testing (2.2×10^{-8} , Supplementary Table 5). In multi-ancestry meta-analysis, we identified an additional three independent genome-wide-significant association signals (Fig. 1, Table 1).

To assess the sensitivity of our results to mismatches of demographic characteristics between cases and controls (Supplementary Figs. 9, 10), we performed an age-, sex- and body mass index (BMI)-matched case-control analysis (Supplementary Figs. 18–21). As there is a theoretical risk of mismatch between cases and 100,000 Genomes Project participants in risk factors for exposure (for example, shielding behaviour) or susceptibility to critical COVID-19 (for example, immunosuppression), we performed a sensitivity analysis using only the cohort with mild COVID-19 (see above; Supplementary Table 10). In both of these analyses, allele frequencies and directions of effect were concordant for all lead signals.

We inferred credible sets of variants using Bayesian fine-mapping with susieR¹³, by analysing the GWAS summaries of 17 regions of genomic length 3 Mb that were flanking groups of lead signals. We obtained 22 independent credible sets of variants for EUR and an additional 2 from the trans-ancestry meta-analysis with a posterior inclusion probability greater than 0.95 (Extended Data Table 1, Supplementary Information). Fine-mapping of the association signals revealed putative causal variants for both previously reported and novel association signals (see Supplementary Information, Extended Data Table 1). In 12 out of the 24 fine-mapped signals, the credible sets included 5 or fewer variants, and for 8 signals we detected variants with predicted missense or worse consequence across each credible set (Extended Data Table 1). We were able to fine-map multiple independent signals at previously identified loci (Fig. 3, Extended Data Figs. 2, 4). For example, the signal in the 3p21.31 region², was fine-mapped into two independent associations, with the credible set for the first refined to a single variant in the

5' untranslated region (UTR) of *SLC6A20* (chr3:45796521:G:T, rs2271616, odds ratio (OR): 1.29, 95% confidence interval (CI):1.21–1.37), and the second credible set including multiple variants in downstream and intronic regions of *LZTFL1* (Fig. 3). Among the novel signals, at 3q24 and 9p21.3 we detected missense variants that affect *PLSCR1* and *IFNA10*, respectively (chr3:146517122:G:A, rs343320, p.His262Tyr, OR: 1.24, 95% CI: 1.15–1.33, CADD: 22.6; chr9:21206606:C:G, rs28368148, p.Trp164Cys, OR: 1.74, 95% CI: 1.45–2.09, CADD: 23.9). Both are predicted to be deleterious by the Combined Annotation Dependent Depletion (CADD) tool¹⁴. Structural predictions for these variants suggest functional effects (Extended Data Fig. 5). We assessed whether the main signals of this study were underlain by rarer variants with a lower minor allele frequency (MAF) (less than 0.02%) than our GWAS default threshold (less than 0.5%), by including rarer variant summaries when fine-mapping, but no additional variants were added to the main credible sets (Supplementary Table 9).

Consistent with our expectation that genetic susceptibility has a stronger role in younger individuals, age-stratified analysis (individuals of younger than 60 years old versus individuals of 60 years old or above) in the EUR group revealed a signal in the 3p21.31 region with a significantly stronger effect in the younger age group (chr3:45801750:G:A, rs13071258, OR: 3.34, 95% CI: 2.98–3.75 versus OR: 2.1, 95% CI: 1.88–2.34), which is in strong LD ($r^2 = 0.947$) with the main GWAS signal indexed by rs73064425. Sex-specific analysis did not reveal significant effects (Supplementary Fig. 17).

Replication

For replication, we performed a meta-analysis of summary statistics generously shared by 23andMe and the COVID-19 Host Genetics Initiative (HGI) data freeze 6 (B2). As a previous analysis of GenOMICC¹ contributes a substantial part of the signal at each locus in HGI v.6, and leave-one-out analyses were not available, we removed the signal

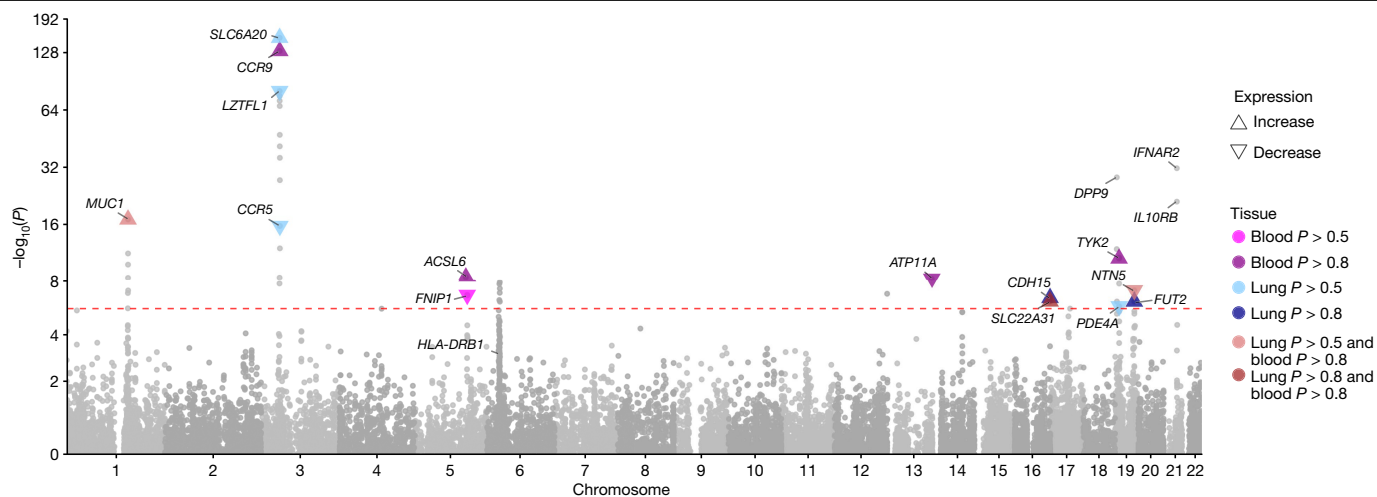


Fig. 2 | Gene-level Manhattan plot showing results from the TWAS meta-analysis and highlighting genes that colocalize with GWAS signals or have strong metaTAS associations. The highlighting colour is different for the lung and blood tissue data that were used for colocalization, and we also distinguish loci that were significant in both. Results are grouped according to two classes for the posterior probability of colocalization (PP_{H4}): $P > 0.5$ and

$P > 0.8$. If a variant is placed in both classes, then the colour that corresponds to the higher probability class is shown. Arrowheads indicate the direction of change in gene expression associated with an increased disease risk. The red dashed line shows the Bonferroni-corrected significance threshold for the metaTAS analysis at $P = 2.3 \times 10^{-6}$.

from GenOMICC cases in HGI v.6 using mathematical subtraction to ensure independence (Methods). Using LD clumping to find variants genotyped in both the discovery and replication studies, we required $P < 0.002$ (0.05/25) and concordant direction of effect (Table 1, Supplementary Table 8) for replication. We interrogated two variants that failed replication in this set in a second GWAS meta-analysis of hospitalized patients with COVID-19 from UK Biobank, AncestryDNA, Penn Medicine Biobank and Geisinger Health Systems, which included a total of 9,937 individuals who were hospitalized with COVID-19 and 1,059,390 control individuals. This led to a further successful replicated finding, in *IFNA10* (Table 1).

We replicated 23 of the 25 significant associations that were identified in the population-specific and/or multi-ancestry GWASs. One of the non-replicated signals (rs4424872) corresponds to a rare variant that may not be well represented in the replication datasets—which are dominated by single-nucleotide polymorphism (SNP) genotyping data—but which also had significant heterogeneity among ancestries. The second non-replicated signal is within the human leukocyte antigen (HLA) locus, which has complex LD (see below).

HLA region

The lead variant in the HLA region, rs9271609, lies upstream of the *HLA-DQA1* and *HLA-DRB1* genes. To investigate the contribution of specific HLA alleles to the observed association in the HLA region, we imputed HLA alleles at a four-digit (two-field) level using HIBAG¹⁵. The only allele that reached genome-wide significance was *HLA-DRB1*04:01* (OR: 0.80, 95% CI: 0.75–0.86, $P = 1.6 \times 10^{-10}$ in EUR), which has a stronger P value than the lead SNP in the region (OR: 0.88, 95% CI: 0.84–0.92, $P = 3.3 \times 10^{-9}$ in EUR) and is a better fit to the data (Akaike information criterion (AIC): $AIC_{DRB1*04:01} = 30,241.34$; $AIC_{leadSNP} = 30,252.93$) (Extended Data Fig. 6). *HLA-DRB1*04:01* has been previously reported to confer protection against severe disease in a small cohort of European ancestry¹⁶.

Gene burden testing

To assess the contribution of rare variants to critical illness, we performed gene-based analysis using SKAT-O as implemented in

SAIGE-GENE¹⁷ on a subset of 12,982 individuals from our cohort (7,491 individuals with critical COVID-19 and 5,391 control individuals), for which the genome-sequencing data were processed with the same alignment and variant calling pipeline. We tested the burden of rare (MAF < 0.5%) variants considering the predicted variant consequence type (tested variant counts provided in the Supplementary Information). We assessed burden using a strict definition for damaging variants (high-confidence putative loss-of-function (pLoF) variants as identified by LOFTEE¹⁸) and a lenient definition (pLoF plus missense variants with CADD ≥ 10)¹⁴, but found no significant associations at a gene-wide-significance level. Moreover, all individual rare variants included in the tests had P values greater than 10^{-5} .

Consistent with other recent work¹¹, we did not find any significant gene burden test associations among the 13 genes previously reported from an interferon-pathway-focused study⁴ (tests for all genes had $P > 0.05$; Supplementary Information), and we did not replicate the reported association^{19–21} in *TLR7* (EUR $P = 0.30$ for pLoF and $P = 0.075$ for missense variants).

Transcriptome-wide association study analysis

To infer the effect of genetically determined variation in gene expression on disease susceptibility, we performed a transcriptome-wide association study (TWAS) using gene expression data (GTEx v.8; ref. ²²) for two disease-relevant tissues: lung and whole blood. We found significant associations between critical COVID-19 and predicted expression in lung (14 genes) and blood (6 genes) (Supplementary Fig. 23) and in an all-tissue meta-analysis (GTEx v.8; 51 genes) (Supplementary Fig. 24). Expression signals for 16 genes significantly colocalized with susceptibility (Fig. 2). As the LD structure of the HLA is complex, we only assessed colocalization for the significant association, *HLA-DRB1*. Although it was not significant in our TWAS analysis, expression quantitative trait loci (eQTLs) in the proximity of the association significantly colocalize with the GWAS signal for both blood and lung (both $PP_{H4} > 0.8$; Supplementary Information).

We repeated the TWAS analysis using models of intron excision rate from GTEx v.8 to obtain a splicing TWAS, which revealed significant signals in lung (16 genes) and whole blood (9 genes), and in an all-tissue meta-analysis (33 genes); 11 of these had strongly colocalizing splicing signals (Supplementary Information).

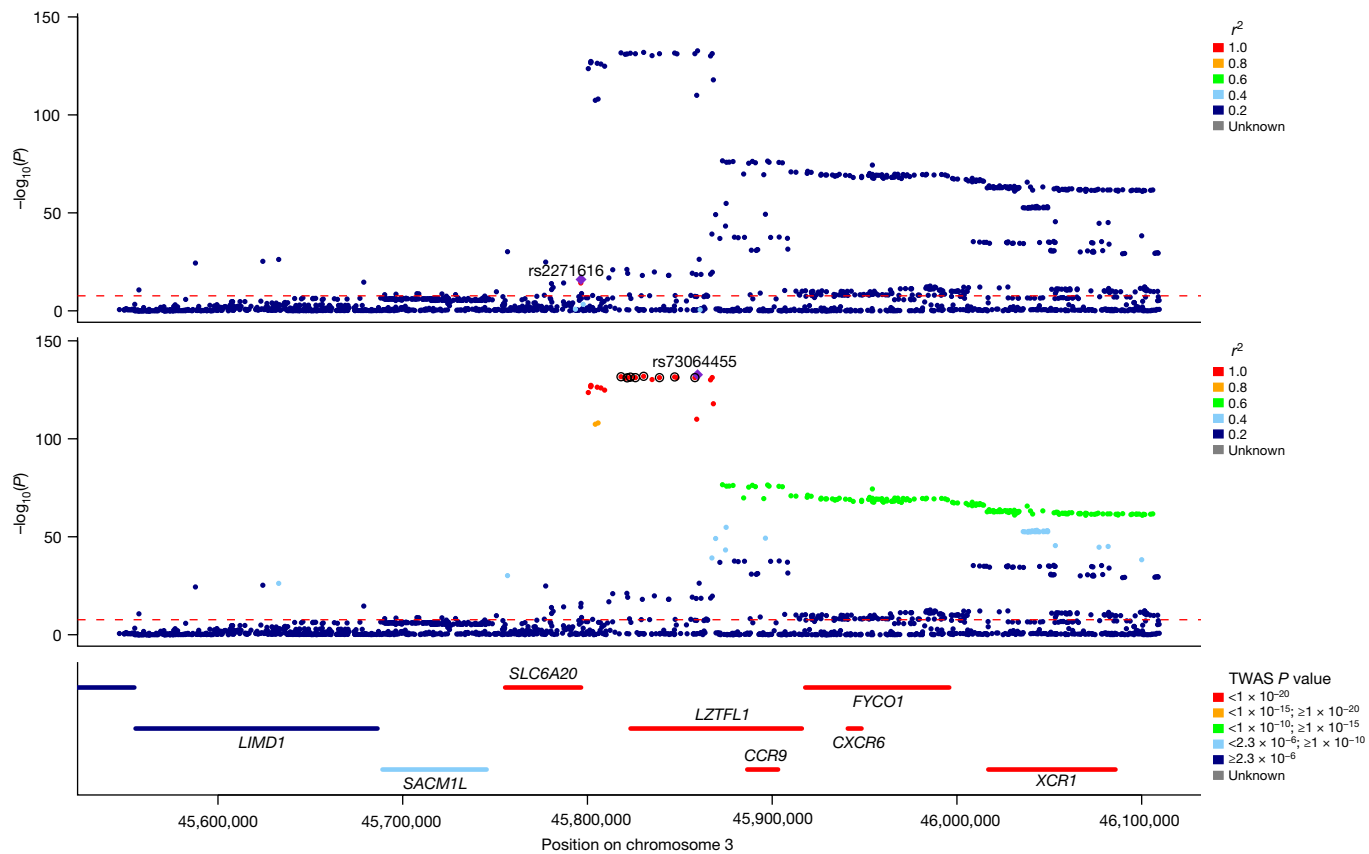


Fig. 3 | Regional detail showing fine-mapping to identify two adjacent independent signals on chromosome 3. Top two panels, variants in LD with the lead variants shown. The variants that are included in two independent credible sets are displayed with black outline circles. The r^2 values in the key

denote upper limits; that is, 0.2 = [0, 0.2], 0.4 = [0.2, 0.4], 0.6 = [0.4, 0.6], 0.8 = [0.6, 0.8], 1 = [0.8, 1]. Bottom, locations of protein-coding genes, coloured by TWAS P value. The red dashed line shows the Bonferroni-corrected P value: $P = 2.2 \times 10^{-8}$ for individuals of European ancestry.

Mendelian randomization

We performed generalized summary-data-based Mendelian randomization (GSMR)²³ in a replicated outcome study design using the protein quantitative trait loci (pQTLs) from the INTERVAL study²⁴. GSMR incorporates information from multiple independent SNPs and provides stronger evidence of a causal relationship than single-SNP-based approaches. Of 16 proteome-wide-significant associations in this study, 8 were replicated in an external dataset at a Bonferroni-corrected P value threshold of $P < 0.0031$ ($P < 0.05/16$; Extended Data Table 2, Extended Data Fig. 7).

Discussion

We report 23 replicated genetic associations with critical COVID-19, which were discovered in only 7,491 cases. This demonstrates the efficiency of the design of the GenOMICC study, an open-source²⁵ international research programme (<https://genomicc.org>) that focuses on extreme phenotypes: patients with life-threatening infectious disease, sepsis, pancreatitis and other critical illness phenotypes. GenOMICC detects greater heritability and stronger effect sizes than other study designs across all variants (Supplementary Figs. 22, 14). In COVID-19, critical illness is not only an extreme susceptibility phenotype, but also a more homogeneous one: we have shown previously that critically ill patients with COVID-19 are more likely to have the primary disease process—hypoxaemic respiratory failure⁵—and that patients in this group have a divergent response to immunosuppressive therapy compared to other hospitalized patients⁸. We detect distinct signals at several of the associated loci, in some cases implicating different biological mechanisms.

Five of the variants associated with critical COVID-19 have direct roles in interferon signalling and broadly concordant predicted biological effects. These include a probable destabilizing amino acid substitution in a ligand, *IFNA10* (Trp164Cys, Extended Data Fig. 5), and—as we reported previously¹—reduced expression of a subunit of its receptor *IFNAR2* (Fig. 2). *IFNAR2* signals through a kinase that is encoded by *TYK2*¹. Although the lead variant in *TYK2* in WGS is a protein-coding variant with reduced STAT1 phosphorylation activity²⁶, it is also associated with significantly increased expression of *TYK2* (Fig. 2, Methods). Fine-mapping reveals a significant association with an independent missense variant in *IL1ORB*, a receptor for type III (lambda) interferons (rs8178521; Table 1). Finally, we detected a lead risk variant in phospholipid scramblase 1 (chr3:146517122:G:A, rs343320; *PLSCR1*) which disrupts a nuclear localization signal that is important for the antiviral effect of interferons²⁷ (Extended Data Fig. 5). *PLSCR1* controls the replication of other RNA viruses, including vesicular stomatitis virus, encephalomyocarditis virus and influenza A virus^{29,30}.

Although our genome-wide gene-based association tests did not replicate any findings from a previous pathway-specific study of rare deleterious variants⁴, our results provide robust evidence implicating reduced interferon signalling in susceptibility to critical COVID-19. Notably, systemic administration of interferon in two large clinical trials, albeit late in disease, did not reduce mortality^{29,30}.

We found significant associations in genes that are implicated in lymphopoiesis and in the differentiation of myeloid cells. *BCL11A* is essential for B and T lymphopoiesis³¹ and promotes the differentiation of plasmacytoid dendritic cells³². *TAC4*, reported previously³, encodes a regulator of B cell lymphopoiesis³³ and antibody production³⁴, and promotes the survival of dendritic cells³⁵. Finally, although the strongest

fine-mapping signal at 5q31.1 (chr5:131995059:C:T, rs56162149) is in an intron of *ACSL6* with significant effects on expression (Supplementary Information), the credible set includes a missense variant in *CSF2* (encoding granulocyte–macrophage colony stimulating factor; GM-CSF) of uncertain significance (chr5:132075767:T:C; Extended Data Table 1). We have previously shown that GM-CSF is strongly up-regulated in critical COVID-19³⁶, and it is already under investigation as a target for therapy³⁷. Mendelian randomization results are consistent with a direct link between the plasma levels of a closely related cytokine receptor subunit, IL3RA, and critical COVID-19 (Extended Data Table 2).

Fine-mapping, colocalization and TWAS analyses provide evidence for increased expression of *MUC1* as the mediator of the association with rs41264915 (Supplementary Table 12). This suggests that mucins could have a therapeutically important role in the development of critical illness in COVID-19.

Mendelian randomization provides genetic evidence in support of a causal role for coagulation factors (*F8*) and platelet activation (*PDGFRL*) in critical COVID-19 (Extended Data Table 2, Extended Data Fig. 7), consistent with autopsy⁶, proteomic³⁸ and therapeutic³⁹ evidence. Perhaps more importantly, we identify specific and closely related intercellular adhesion molecules that have known roles in the recruitment of inflammatory cells to sites of inflammation, including E-selectin (*SELE*), intercellular adhesion molecule 5 (*ICAM5*) and DC-SIGN (dendritic-cell-specific ICAM3-grabbing non-integrin; *CD209*), which may provide additional therapeutic targets. DC-SIGN (*CD209*) mediates pathogen endocytosis and antigen presentation, and is known to be involved in multiple viral infections, including SARS-CoV and influenza A virus. It has affinity for SARS-CoV-2^{40,41}.

Our previous report of an association between the OAS gene cluster and severe disease was robustly replicated in an external cohort¹, but does not meet genome-wide significance in the present analysis (Supplementary Table 7). This may indicate a change in the observed effect size because any effect that is detected in GWASs is more likely to have been sampled from the larger end of the range of possible effect sizes—the ‘winner’s curse’. Alternatively, it may indicate either a change in the population of patients (cases or controls) or a change in the pathogen. For example it is possible that—as with the other coronaviruses that are known to infect humans⁴²—more recent variants of SARS-CoV-2 have evolved to overcome this host antiviral defence mechanism.

Limitations

In contrast to microarray genotyping, WGS is a rapidly evolving and relatively new technology for GWASs, with relatively few sources of population controls. We selected a control cohort from the 100,000 Genomes Project, which was sequenced and analysed using a different platform and bioinformatics pipeline compared with the case cohort (Extended Data Fig. 1). However, to minimize the risk of false-positive associations due to technical artifacts, extensive quality measures were used (Methods). In brief, we masked low-quality genotypes, filtered for genotype signal using a low threshold for missingness and performed a control–control relative allele frequency filter using a subset of samples processed with both bioinformatics pipelines. Finally, we required all significant associations to be supported by local variants in LD, which may be excessively stringent (Methods). Although this approach may remove some true associations, our priority is to maximize confidence in the reported signals. Of 25 variants that meet this requirement, 23 are externally replicated, and the remaining 2 may be true associations that are yet to be replicated owing to a lack of coverage or power in the replication datasets.

The design of our study incorporates genetic signals for every stage in the disease progression into a single phenotype. This includes establishment of infection, viral replication, inflammatory lung injury and hypoxaemic respiratory failure. Although we can have considerable confidence that the replicated associations with critical COVID-19 we report are robust, we cannot determine at which stage in the disease process, or in which tissue, the relevant biological mechanisms are active.

Conclusions

These genetic associations identify biological mechanisms that may underlie the development of life-threatening COVID-19, several of which may be amenable to therapeutic targeting. Furthermore, we demonstrate the value of WGS for fine-mapping loci in a complex trait. In the context of the ongoing global pandemic, translation to clinical practice is an urgent priority. As with our previous work, biological and molecular studies—and, where appropriate, large-scale randomized trials—will be essential before our findings can be translated into clinical practice.

Online content

Any methods, additional references, Nature Research reporting summaries, source data, extended data, supplementary information, acknowledgements, peer review information; details of author contributions and competing interests; and statements of data and code availability are available at <https://doi.org/10.1038/s41586-022-04576-6>.

- Pairo-Castineira, E. et al. Genetic mechanisms of critical illness in COVID-19. *Nature* **591**, 92–98 (2021).
- Ellinghaus, D. et al. Genomewide association study of severe Covid-19 with respiratory failure. *N. Engl. J. Med.* **383**, 1522–1534 (2020).
- COVID-19 Host Genetics Initiative. Mapping the human genetic architecture of COVID-19. *Nature* **600**, 472–477 (2021).
- Zhang, Q. et al. Inborn errors of type I IFN immunity in patients with life-threatening COVID-19. *Science* **370**, eabd4570 (2020).
- Docherty, A. B. et al. Features of 20,133 UK patients in hospital with covid-19 using the ISARIC WHO Clinical Characterisation Protocol: prospective observational cohort study. *BMJ* **369**, m1985 (2020).
- Dorward, D. A. et al. Tissue-specific immunopathology in fatal COVID-19. *Am. J. Respir. Crit. Care Med.* **203**, 192–201 (2021).
- Millar, J. E. et al. Distinct clinical symptom patterns in patients hospitalised with COVID-19 in an analysis of 59,011 patients in the ISARIC-4C study. *Sci. Rep.* **12**, 6843 (2022).
- The RECOVERY Collaborative Group. Dexamethasone in hospitalized patients with Covid-19. *N. Engl. J. Med.* **384**, 693–704 (2021).
- Degenhardt, F. et al. New susceptibility loci for severe COVID-19 by detailed GWAS analysis in European populations. Preprint at medRxiv <https://doi.org/10.1101/2021.07.21.21260624> (2021).
- Povysil, G. et al. Rare loss-of-function variants in type I IFN immunity genes are not associated with severe COVID-19. *J. Clin. Invest.* **131**, e147834 (2021).
- Kosmicki, J. A. et al. Pan-ancestry exome-wide association analyses of COVID-19 outcomes in 586,157 individuals. *Am. J. Hum. Genet.* **108**, 1350–1355 (2021).
- Zhou, W. et al. Efficiently controlling for case-control imbalance and sample relatedness in large-scale genetic association studies. *Nat. Genet.* **50**, 1335–1341 (2018).
- Wang, G., Sarkar, A., Carbonetto, P. & Stephens, M. A simple new approach to variable selection in regression, with application to genetic fine mapping. *J. R. Stat. Soc. B* **82**, 1273–1300 (2020).
- Rentzsch, P., Witten, D., Cooper, G. M., Shendure, J. & Kircher, M. CADD: predicting the deleteriousness of variants throughout the human genome. *Nucleic Acids Res.* **47**, D886–D894 (2018).
- Zheng, X. et al. HIBAG—HLA genotype imputation with attribute bagging. *Pharmacogenomics J.* **14**, 192–200 (2014).
- Langton, D. J. et al. The influence of HLA genotype on the severity of COVID-19 infection. *HLA* **98**, 14–22 (2021).
- Zhou, W. et al. Scalable generalized linear mixed model for region-based association tests in large biobanks and cohorts. *Nat. Genet.* **52**, 634–639 (2020).
- Karczewski, K. J. et al. The mutational constraint spectrum quantified from variation in 141,456 humans. *Nature* **581**, 434–443 (2020).
- Asano, T. et al. X-linked recessive TLR7 deficiency in ~1% of men under 60 years old with life-threatening COVID-19. *Sci. Immunol.* **6**, eabl4348 (2021).
- Fallerini, C. et al. Association of toll-like receptor 7 variants with life-threatening COVID-19 disease in males: findings from a nested case-control study. *eLife* **10**, e67569 (2021).
- van der Made, C. I. et al. Presence of genetic variants among young men with severe COVID-19. *J. Am. Med. Assoc.* **324**, 663–673 (2020).
- The GTEx Consortium. The GTEx Consortium atlas of genetic regulatory effects across human tissues. *Science* **369**, 1318–1330 (2020).
- Zhu, Z. et al. Causal associations between risk factors and common diseases inferred from GWAS summary data. *Nat. Commun.* **9**, 224 (2018).
- Sun, B. B. et al. Genomic atlas of the human plasma proteome. *Nature* **558**, 73–79 (2018).
- Dunning, J. W. et al. Open source clinical science for emerging infections. *Lancet Infect. Dis.* **14**, 8–9 (2014).
- Dendrou, C. A. et al. Resolving TYK2 locus genotype-to-phenotype differences in autoimmunity. *Sci. Transl. Med.* **8**, 363ra149 (2016).
- Dong, B. et al. Phospholipid scramblase 1 potentiates the antiviral activity of interferon. *J. Virol.* **78**, 8983–8993 (2004).
- Luo, W. et al. Phospholipid scramblase 1 interacts with influenza A virus NP, impairing its nuclear import and thereby suppressing virus replication. *PLoS Pathog.* **14**, e1006851 (2018).
- WHO Solidarity Trial Consortium. Repurposed antiviral drugs for Covid-19—interim WHO Solidarity trial results. *N. Engl. J. Med.* **384**, 497–511 (2021).

30. Kalil, A. C. et al. Efficacy of interferon beta-1a plus remdesivir compared with remdesivir alone in hospitalised adults with COVID-19: a double-blind, randomised, placebo-controlled, phase 3 trial. *Lancet Respir. Med.* **12**, 1365–1376 (2021).
31. Yu, Y. et al. Bcl11a is essential for lymphoid development and negatively regulates p53. *J. Exp. Med.* **209**, 2467–2483 (2012).
32. Reizis, B. Plasmacytoid dendritic cells: development, regulation, and function. *Immunity* **50**, 37–50 (2019).
33. Zhang, Y., Lu, L., Furlonger, C., Wu, G. E. & Paige, C. J. Hemokinin is a hematopoietic-specific tachykinin that regulates B lymphopoiesis. *Nat. Immunol.* **1**, 392–397 (2000).
34. Wang, W. et al. Hemokinin-1 activates the MAPK pathway and enhances B cell proliferation and antibody production. *J. Immunol.* **184**, 3590–3597 (2010).
35. Janelsins, B. M. et al. Proinflammatory tachykinins that signal through the neurokinin 1 receptor promote survival of dendritic cells and potent cellular immunity. *Blood* **113**, 3017–3026 (2009).
36. Thwaites, R. S. et al. Inflammatory profiles across the spectrum of disease reveal a distinct role for GM-CSF in severe COVID-19. *Sci. Immunol.* **6**, eabg9873 (2021).
37. Lang, F. M., Lee, K. M.-C., Teijaro, J. R., Becher, B. & Hamilton, J. A. GM-CSF-based treatments in COVID-19: reconciling opposing therapeutic approaches. *Nat. Rev. Immunol.* **20**, 507–514 (2020).
38. Reyes, L. et al. A type I IFN, prothrombotic hyperinflammatory neutrophil signature is distinct for COVID-19 ARDS. *Wellcome Open Res.* **6**, 38 (2021).
39. Lawler, P. R. et al. Therapeutic anticoagulation with heparin in noncritically ill patients with Covid-19. *N. Engl. J. Med.* **385**, 790–802 (2021).
40. Amraei, R. et al. CD209L/L-SIGN and CD209/DC-SIGN act as receptors for SARS-CoV-2. *ACS Cent. Sci.* **7**, 1156–1165 (2021).
41. Thépaut, M. et al. DC/L-SIGN recognition of spike glycoprotein promotes SARS-CoV-2 trans-infection and can be inhibited by a glycomimetic antagonist. *PLoS Pathog.* **17**, e1009576 (2021).
42. Silverman, R. H. & Weiss, S. R. Viral phosphodiesterases that antagonize double-stranded RNA signaling to RNase L by degrading 2-5A. *J. Interferon Cytokine Res.* **34**, 455–463 (2014).

Publisher's note Springer Nature remains neutral with regard to jurisdictional claims in published maps and institutional affiliations.



Open Access This article is licensed under a Creative Commons Attribution 4.0 International License, which permits use, sharing, adaptation, distribution and reproduction in any medium or format, as long as you give appropriate credit to the original author(s) and the source, provide a link to the Creative Commons license, and indicate if changes were made. The images or other third party material in this article are included in the article's Creative Commons license, unless indicated otherwise in a credit line to the material. If material is not included in the article's Creative Commons license and your intended use is not permitted by statutory regulation or exceeds the permitted use, you will need to obtain permission directly from the copyright holder. To view a copy of this license, visit <http://creativecommons.org/licenses/by/4.0/>.

© The Author(s) 2022

¹Genomics England, London, UK. ²Roslin Institute, University of Edinburgh, Edinburgh, UK. ³MRC Human Genetics Unit, Institute of Genetics and Cancer, University of Edinburgh, Western General Hospital, Edinburgh, UK. ⁴Centre for Inflammation Research, The Queen's Medical Research Institute, University of Edinburgh, Edinburgh, UK. ⁵Wellcome Centre for Human Genetics, University of Oxford, Oxford, UK. ⁶Institute for Molecular Bioscience, The University of Queensland, Brisbane, Queensland, Australia. ⁷Biostatistics Group, Greater Bay Area Institute of Precision Medicine (Guangzhou), Fudan University, Guangzhou, China. ⁸Centre for Global Health Research, Usher Institute of Population Health Sciences and Informatics, Edinburgh, UK. ⁹Edinburgh Clinical Research Facility, Western General Hospital, University of Edinburgh, Edinburgh, UK. ¹⁰Intensive Care Unit, Royal Infirmary of Edinburgh, Edinburgh, UK. ¹¹Department of Critical Care Medicine, Queen's University and Kingston Health Sciences Centre, Kingston, Ontario, Canada. ¹²Clinical Research Centre at St Vincent's University Hospital, University College Dublin, Dublin, Ireland. ¹³NIHR Health Protection Research Unit for Emerging and Zoonotic Infections, Institute of Infection, Veterinary and Ecological Sciences, University of Liverpool, Liverpool, UK. ¹⁴Respiratory Medicine and Institute in the Park, Alder Hey Children's Hospital and University of Liverpool, Liverpool, UK. ¹⁵Illumina Cambridge, Great Abington, UK. ¹⁶Regeneron Genetics Center, Tarrytown, NY, USA. ¹⁷Geisinger, Danville, PA, USA. ¹⁸Department of Genetics, Perelman School of Medicine, University of Pennsylvania, Philadelphia, PA, USA. ¹⁹Test and Trace, the Health Security Agency, Department of Health and Social Care, London, UK. ²⁰Department of Intensive Care Medicine, Guy's and St Thomas' NHS Foundation Trust, London, UK. ²¹Department of Medicine, University of Cambridge, Cambridge, UK. ²²William Harvey Research Institute, Barts and the London School of Medicine and Dentistry, Queen Mary University of London, London, UK. ²³Centre for Tropical Medicine and Global Health, Nuffield Department of Medicine, University of Oxford, Oxford, UK. ²⁴Department of Anaesthesia and Intensive Care, The Chinese University of Hong Kong, Prince of Wales Hospital, Hong Kong, China. ²⁵Wellcome–Wolfson Institute for Experimental Medicine, Queen's University Belfast, Belfast, UK. ²⁶Department of Intensive Care Medicine, Royal Victoria Hospital, Belfast, UK. ²⁷UCL Centre for Human Health and Performance, London, UK. ²⁸National Heart and Lung Institute, Imperial College London, London, UK. ²⁹Imperial College Healthcare NHS Trust: London, London, UK. ³⁰Imperial College, London, UK. ³¹Intensive Care National Audit and Research Centre, London, UK. ³²School of Life Sciences, Westlake University, Hangzhou, China. ³³Westlake Laboratory of Life Sciences and Biomedicine, Hangzhou, China. ³⁴Great Ormond Street Hospital, London, UK. ³⁵William Harvey Research Institute, Queen Mary University of London, London, UK. ⁵⁵⁶These authors contributed equally: Athanasios Kousathanas, Erola Pairo-Castineira. ⁵⁵⁷These authors jointly supervised this work: Sara Clohisey Hendry, Loukas Moutsianas, Andy Law, Mark J. Caulfield, J. Kenneth Baillie. *Lists of authors and their affiliations appear online. ⁵⁵⁸e-mail: m.j.caulfield@qmul.ac.uk; j.k.baillie@ed.ac.uk

Article

GenOMICC investigators

GenOMICC co-investigators

J. Kenneth Baillie^{36,37}, Colin Begg³⁸, Sara Clohisey Hendry³⁶, Charles Hinds³⁹, Peter Horby⁴⁰, Julian Knight⁴¹, Lowell Ling⁴², David Maslove⁴³, Danny McAuley^{44,45}, Johnny Millar³⁶, Hugh Montgomery⁴⁶, Alistair Nichol⁴⁷, Peter J. M. Openshaw^{48,49}, Alexandre C. Pereira⁵⁰, Chris P. Ponting⁵¹, Kathy Rowan⁵², Malcolm G. Semple^{53,54}, Manu Shankar-Hari⁵⁵, Charlotte Summers⁵⁶ & Timothy Walsh³⁷

Management, laboratory and data team

Latha Aravindan⁵⁷, Ruth Armstrong³⁶, J. Kenneth Baillie^{36,37}, Heather Biggs⁵⁸, Ceilia Boz³⁶, Adam Brown³⁶, Richard Clark⁵⁹, Sara Clohisey Hendry³⁶, Audrey Coutts⁵⁹, Judy Coyle³⁶, Louise Cullum³⁶, Sukamal Das⁵⁷, Nicky Day³⁶, Lorna Donnelly⁵⁹, Esther Duncan³⁶, Angie Fawkes⁵⁹, Paul Fineran³⁶, Max Head Fourman³⁶, Anita Furlong⁵⁸, James Furniss³⁶, Bernadette Gallagher³⁶, Tammy Gilchrist⁵⁹, Ailsa Golightly³⁶, Fiona Griffiths³⁶, Katarzyna Hafez⁵⁹, Debbie Hamilton³⁶, Ross Hendry³⁶, Andy Law³⁶, Dawn Law³⁶, Rachel Law³⁶, Sarah Law³⁶, Rebecca Lidstone-Scott³⁶, Louise Macgillivray⁵⁹, Alan Maclean⁵⁹, Hanning Mal³⁶, Sarah McCafferty⁵⁹, Ellie McMaster³⁶, Jen Meikle³⁶, Shona C. Moore⁵³, Kirstie Morrice⁵⁹, Lee Murphy⁵⁹, Sheena Murphy⁵⁷, Mybaya Hellen³⁶, Wilna Oosthuizen³⁶, Chenqing Zheng⁶⁰, Jiantao Chen⁶⁰, Nick Parkinson³⁶, Trevor Paterson³⁶, Katherine Schon⁵⁸, Andrew Stenhouse³⁶, Mihaela Das⁵⁷, Maaike Swets^{36,61}, Helen Szoor-McElhinney³⁶, Filip Taneski³⁶, Lance Turtle⁵³, Tony Wackett³⁶, Mairi Ward³⁶, Jane Weaver³⁶, Nicola Wrobel⁵⁹, Marie Zechner³⁶ & Mybaya Hellen³⁶

Guy's and St Thomas' Hospital team

Gill Arbane⁶², Aneta Bociek⁶², Sara Campos⁶², Neus Grau⁶², Tim Owen Jones⁶², Rosario Lim⁶², Martina Marotti⁶², Marlies Ostermann⁶², Manu Shankar-Hari⁶² & Christopher Whitton⁶²

Barts Health NHS Trust team

Zoe Alldis⁶³, Raine Astin-Chamberlain⁶³, Fatima Bibi⁶³, Jack Biddle⁶³, Sarah Blow⁶³, Matthew Bolton⁶³, Catherine Borra⁶³, Ruth Bowles⁶³, Maudrian Burton⁶³, Yasmin Choudhury⁶³, David Collier⁶³, Amber Cox⁶³, Amy Easthope⁶³, Patrizia Ebano⁶³, Stavros Fotiadis⁶³, Jana Gurasashvili⁶³, Rosslyn Halls⁶³, Pippa Hartridge⁶³, Delordson Kallon⁶³, Jamila Kassam⁶³, Ivone Lancoma-Malcolm⁶³, Maninderpal Matharu⁶³, Peter May⁶³, Oliver Mitchelmore⁶³, Tabitha Newman⁶³, Mital Patel⁶³, Jane Pheby⁶³, Irene Pinzut⁶³, Zoe Prime⁶³, Oleksandra Prysazhna⁶³, Julian Shiel⁶³, Melanie Taylor⁶³, Carey Tierney⁶³, Suzanne Wood⁶³, Anne Zak⁶³ & Olivier Zongo⁶³

James Cook University Hospital team

Stephen Bonner⁶⁴, Keith Hugill⁶⁴, Jessica Jones⁶⁴, Steven Liggett⁶⁴ & Evie Headlam⁶⁴

Royal Stoke University Hospital team

Nageswar Bandla⁶⁵, Minnie Gellamucho⁶⁵, Michelle Davies⁶⁵ & Christopher Thompson⁶⁵

North Middlesex University Hospital NHS Trust team

Marwa Abdelrazik⁶⁶, Dhanalakshmi Baktavatsalam⁶⁶, Munzir Elhassan⁶⁶, Arunkumar Ganesan⁶⁶, Anne Haldeos⁶⁶, Jeronimo Moreno-Cuesta⁶⁶, Dharam Purohit⁶⁶, Rachel Vincent⁶⁶, Kugan Xavier⁶⁶, Rohit Kumar⁶⁷, Alasdair Frater⁶⁶, Malik Saleem⁶⁶, David Carter⁶⁶, Samuel Jenkins⁶⁶, Zoe Lamond⁶⁶ & Alanna Wall⁶⁶

The Royal Liverpool University Hospital team

Jaime Fernandez-Roman⁶⁸, David O. Hamilton⁶⁸, Emily Johnson⁶⁸, Brian Johnston⁶⁸, Maria Lopez Martinez⁶⁸, Suleman Mulla⁶⁸, David Shaw⁶⁸, Alicia A. C. Waite⁶⁸, Victoria Waugh⁶⁸, Ingeborg D. Welters⁶⁸ & Karen Williams⁶⁸

King's College Hospital team

Anna Cavazza⁶⁹, Maeve Cockrell⁶⁹, Eleanor Corcoran⁶⁹, Maria Depante⁶⁹, Clare Finney⁶⁹, Ellen Jerome⁶⁹, Mark McPhail⁶⁹, Monalisa Nayak⁶⁹, Harriet Noble⁶⁹, Kevin O'Reilly⁶⁹, Evita Pappa⁶⁹, Rohit Saha⁶⁹, Sian Saha⁶⁹, John Smith⁶⁹ & Abigail Knighton⁶⁹

Charing Cross Hospital team

David Antcliffe⁷⁰, Dorota Banach⁷⁰, Stephen Brett⁷⁰, Phoebe Coghlan⁷⁰, Ziortza Fernandez⁷⁰, Anthony Gordon⁷⁰, Roceld Rojo⁷⁰, Sonia Sousa Arias⁷⁰ & Maie Templeton⁷⁰

Nottingham University Hospital team

Megan Meredith⁷¹, Lucy Morris⁷¹, Lucy Ryan⁷¹, Amy Clark⁷¹, Julia Sampson⁷¹, Cecilia Peters⁷¹, Martin Dent⁷¹, Margaret Langley⁷¹, Saima Ashraf⁷¹, Shuying Wei⁷¹ & Angela Andrew⁷¹

John Radcliffe Hospital team

Archana Bashyal⁷², Neil Davidson⁷², Paula Hutton⁷², Stuart McKechnie⁷² & Jean Wilson⁷²

Kingston Hospital team

David Baptista⁷³, Rebecca Crowe⁷³, Rita Fernandes⁷³, Rosaleen Herdman-Grant⁷³, Anna Joseph⁷³, Denise O'Connor⁷⁴, Meryem Allen⁷³, Adam Loveridge⁷³, India McKenley⁷³, Eriko Morino⁷³, Andres Naranjo⁷³, Richard Simms⁷³, Kathryn Sollesta⁷³, Andrew Swain⁷³, Harish Venkatesh⁷³, Jacyntha Khera⁷³ & Jonathan Fox⁷³

Royal Infirmary of Edinburgh team

Gillian Andrew⁷⁵, J. Kenneth Baillie⁷⁵, Lucy Barclay⁷⁵, Marie Callaghan⁷⁵, Rachael Campbell⁷⁵, Sarah Clark⁷⁵, Dave Hope⁷⁵, Lucy Marshal⁷⁵, Corrienne McCulloch⁷⁵, Kate Briton⁷⁵, Jo Singleton⁷⁵ & Sophie Birch⁷⁵

Queen Alexandra Hospital team

Lutece Brimfield⁷⁶, Zoe Daly⁷⁶, David Pogson⁷⁶, Steve Rose⁷⁶ & Angela Nown⁷⁶

Morrison Hospital team

Ceri Battle⁷⁷, Elaine Brinkworth⁷⁷, Rachel Harford⁷⁷, Carl Murphy⁷⁷, Luke Newey⁷⁷, Tabitha Rees⁷⁷, Marie Williams⁷⁷ & Sophie Arnold⁷⁷

Addenbrooke's Hospital team

Petra Polgarova⁷⁸, Katerina Stroud⁷⁸, Charlotte Summers⁷⁸, Eoghan Meaney⁷⁸, Megan Jones⁷⁸, Anthony Ng⁷⁸, Shruti Agrawal⁷⁸, Nazima Pathan⁷⁸, Deborah White⁷⁸, Esther Daubney⁷⁸ & Kay Elston⁷⁸

BHRUT (Barking Havering)—Queen's Hospital and King George Hospital team

Lina Grauslyte⁷⁹, Musarat Hussain⁷⁹, Mandeep Phull⁷⁹, Tatiana Pogreban⁷⁹, Lace Rosaroso⁷⁹, Erika Salciute⁷⁹, George Franke⁷⁹, Joanna Wong⁷⁹ & Aparna George⁷⁹

Royal Sussex County Hospital team

Laura Ortiz-Ruiz de Gordoa⁸⁰, Emily Peasgood⁸⁰ & Claire Phillips⁸⁰

Queen Elizabeth Hospital team

Michelle Bates⁸¹, Jo Dasgin⁸¹, Jaspreet Gill⁸¹, Annette Nilsson⁸¹, James Scriven⁸¹, Amy Collins⁸², Waqas Khaliq⁸² & Estefania Treus Gude⁸²

St George's Hospital team

Carlos Castro Delgado⁸³, Deborah Dawson⁸³, Lijun Ding⁸³, Georgia Durrant⁸³, Obiageri Ezeobu⁸³, Sarah Farnell-Ward⁸³, Abiola Harrison⁸³, Rebecca Kanu⁸³, Susannah Leaver⁸³, Elena Maccacari⁸³, Soumendru Manna⁸³, Romina Pepermans Saluzzio⁸³, Joana Queiroz⁸³, Tinashe Samakomva⁸³, Christine Sicat⁸³, Joana Teixeira⁸³, Edna Fernandes Da Gloria⁸³, Ana Lisboa⁸³, John Rawlins⁸³, Jisha Mathew⁸³, Ashley Kinch⁸³, William James Hurt⁸³, Nirav Shah⁸³, Victoria Clark⁸³, Maria Thanasi⁸³, Nikki Yun⁸³ & Kamal Patel⁸³

Stepping Hill Hospital team

Sara Bennett⁸⁴, Emma Goodwin⁸⁴, Matthew Jackson⁸⁴, Alissa Kent⁸⁴, Clare Tibke⁸⁴, Wiesia Woodyatt⁸⁴ & Ahmed Zak⁸⁴

Countess of Chester Hospital team

Azmerelda Abraheem⁸⁵, Peter Bamford⁸⁵, Kathryn Cawley⁸⁵, Charlie Dunmore⁸⁵, Maria Faulkner⁸⁵, Rumanah Girach⁸⁵, Helen Jeffrey⁸⁵, Rhianna Jones⁸⁵, Emily London⁸⁵, Imrun Nagra⁸⁵, Farah Nasir⁸⁵, Hannah Sainsbury⁸⁵ & Clare Smedley⁸⁵

Royal Blackburn Teaching Hospital team

Tahera Patel⁸⁶, Matthew Smith⁸⁶, Srikanth Chukkambotla⁸⁶, Aayesha Kazi⁸⁶, Janice Hartley⁸⁶, Joseph Dykes⁸⁶, Muhammad Hijazi⁸⁶, Sarah Keith⁸⁶, Meherunnisa Khan⁸⁶, Janet Ryan-Smith⁸⁶, Philippa Springle⁸⁶, Jacqueline Thomas⁸⁶, Nick Truman⁸⁶, Samuel Saad⁸⁶, Dabheoc Coleman⁸⁶, Christopher Fine⁸⁶, Roseanna Matt⁸⁶, Bethan Gay⁸⁶, Jack Dalziel⁸⁶, Syamlan Ali⁸⁶, Drew Goodchild⁸⁶, Rhiannan Harling⁸⁶, Ravi Bhatteejee⁸⁶, Wendy Goddard⁸⁶, Chloe Davison⁸⁶, Stephen Duberly⁸⁶, Jeanette Hargreaves⁸⁶ & Rachel Bolton⁸⁶

The Tunbridge Wells Hospital and Maidstone Hospital team

Miriam Davey⁸⁷, David Golden⁸⁷ & Rebecca Seaman⁸⁷

Royal Gwent Hospital team

Shiney Cherian⁸⁸, Sean Cutler⁸⁸, Anne Emma Heron⁸⁸, Anna Roynon-Reed⁸⁸, Tamas Szakmany⁸⁸, Gemma Williams⁸⁸, Owen Richards⁸⁸ & Yusuf Cheema⁸⁸

Pinderfields General Hospital team

Hollie Brooke⁸⁹, Sarah Buckley⁸⁹, Jose Cebrian Suarez⁸⁹, Ruth Charlesworth⁸⁹, Karen Hansson⁸⁹, John Norris⁸⁹, Alice Poole⁸⁹, Alastair Rose⁸⁹, Rajdeep Sandhu⁸⁹, Brendan Sloan⁸⁹, Elizabeth Smithson⁸⁹, Muthu Thirumaran⁸⁹, Veronica Wagstaff⁸⁹ & Alexandra Metcalfe⁸⁹

Royal Berkshire NHS Foundation Trust team

Mark Brunton⁹⁰, Jess Caterson⁹⁰, Holly Coles⁹⁰, Matthew Frise⁹⁰, Sabi Gurung Rai⁹⁰, Nicola Jacques⁹⁰, Liza Keating⁹⁰, Emma Tilney⁹⁰, Shauna Bartley⁹⁰ & Parminder Bhuie⁹⁰

Broomfield Hospital team

Sian Gibson⁹¹, Amanda Lyle⁹¹, Fiona McNeela⁹¹, Jayachandran Radhakrishnan⁹¹ & Alistair Hughes⁹¹

Northumbria Healthcare NHS Foundation Trust team

Bryan Yates⁹², Jessica Reynolds⁹², Helen Campbell⁹², Maria Thompson⁹², Steve Dodds⁹² & Stacey Duffy⁹²

Whiston Hospital team

Sandra Greer⁹³, Karen Shuker⁹³ & Ascanio Tridente⁹³

Croydon University Hospital team

Reena Khade⁹⁴, Ashok Sundar⁹⁴ & George Tsinaslanidis⁹⁴

York Hospital team

Isobel Birkinshaw⁹⁵, Joseph Carter⁹⁵, Kate Howard⁹⁵, Joanne Ingham⁹⁵, Rosie Joy⁹⁵, Harriet Pearson⁹⁵, Samantha Roche⁹⁵ & Zoe Scott⁹⁵

Heartlands Hospital team

Hollie Bancroft⁹⁶, Mary Bellamy⁹⁶, Margaret Carmody⁹⁶, Jacqueline Daglish⁹⁶, Faye Moore⁹⁶, Joanne Rhodes⁹⁶, Mirriam Sangombe⁹⁶, Salma Kadiiri⁹⁶ & James Scriven⁹⁶

Ashford and St Peter's Hospital team

Maria Croft⁹⁷, Ian White⁹⁷, Victoria Frost⁹⁷ & Maia Aquino⁹⁷

Barnet Hospital team

Rajeev Jha⁹⁸, Vinodh Krishnamurthy⁹⁸, Lai Lim⁹⁸, Rajeev Jha⁹⁸, Vinodh Krishnamurthy⁹⁸ & Li Lim⁹⁸

East Surrey Hospital team

Edward Combes⁹⁹, Teishel Joefield⁹⁹, Sonja Monnery⁹⁹, Valerie Beech⁹⁹ & Sallyanne Trotman⁹⁹

Newells Hospital team

Christine Almaden-Boyle¹⁰⁰, Pauline Austin¹⁰⁰, Louise Cabrelli¹⁰⁰, Stephen Cole¹⁰⁰, Matt Casey¹⁰⁰, Susan Chapman¹⁰⁰, Stephen Cole¹⁰⁰ & Clare Whyte¹⁰⁰

Worthing Hospital team

Yolanda Baird^{101,102}, Aaron Butler^{101,102}, Indra Chadbourn^{101,102}, Linda Folkes^{101,102}, Heather Fox^{101,102}, Amy Gardner^{101,102}, Raquel Gomez^{101,102}, Gillian Hobden^{101,102}, Luke Hodgson^{101,102}, Kirsten King^{101,102}, Michael Margaron^{101,102}, Tim Martindale^{101,102}, Emma Meadows^{101,102}, Dana Raynard^{101,102}, Yvette Thirlwall^{101,102}, David Helm^{101,102} & Jordi Margalef^{101,102}

Southampton General Hospital team

Kristine Criste¹⁰³, Rebecca Cusack¹⁰³, Kim Golder¹⁰³, Hannah Golding¹⁰³, Oliver Jones¹⁰³, Samantha Leggett¹⁰³, Michelle Male¹⁰³, Martyna Marani¹⁰³, Kirsty Prager¹⁰³, Toran Williams¹⁰³, Belinda Roberts¹⁰³ & Karen Salmon¹⁰³

The Alexandra Hospital team

Peter Anderson¹⁰⁴, Katie Archer¹⁰⁴, Karen Austin¹⁰⁴, Caroline Davis¹⁰⁴, Alison Durie¹⁰⁴, Olivia Kelsall¹⁰⁴, Jessica Thrush¹⁰⁴, Charlie Vigurs¹⁰⁴, Laura Wild¹⁰⁴, Hannah-Louise Wood¹⁰⁴, Helen Tranter¹⁰⁴, Alison Harrison¹⁰⁴, Nicholas Cowley¹⁰⁴, Michael McAlindon¹⁰⁴, Andrew Burtenshaw¹⁰⁴, Stephen Digby¹⁰⁴, Emma Low¹⁰⁴, Aled Morgan¹⁰⁴, Naiara Cother¹⁰⁴, Tobias Rankin¹⁰⁴, Sarah Clayton¹⁰⁴ & Alex McCurdy¹⁰⁴

Sandwell General Hospital and City Hospital team

Cecilia Ahmed¹⁰⁵, Balvinder Baines¹⁰⁵, Sarah Clamp¹⁰⁵, Julie Colley¹⁰⁵, Risna Haq¹⁰⁵, Anne Hayes¹⁰⁵, Jonathan Hulme¹⁰⁵, Samia Hussain¹⁰⁵, Sibet Joseph¹⁰⁵, Rita Kumar¹⁰⁵, Zahira Maqsood¹⁰⁵ & Manjit Purewal¹⁰⁵

Blackpool Victoria Hospital team

Leonie Benham¹⁰⁶, Zena Bradshaw¹⁰⁶, Joanna Brown¹⁰⁶, Melanie Caswell¹⁰⁶, Jason Cupitt¹⁰⁶, Sarah Melling¹⁰⁶, Stephen Preston¹⁰⁶, Nicola Slawson¹⁰⁶, Emma Stoddard¹⁰⁶ & Scott Warden¹⁰⁶

Royal Glamorgan Hospital team

Bethan Deacon¹⁰⁷, Ceri Lynch¹⁰⁷, Carla Potheccary¹⁰⁷, Lisa Roche¹⁰⁷, Gwenllian Sera Howe¹⁰⁷, Jayaprakash Singh¹⁰⁷, Keri Turner¹⁰⁷, Hannah Ellis¹⁰⁷ & Natalie Stroud¹⁰⁷

The Royal Oldham Hospital team

Jodie Hunt¹⁰⁸, Joy Dearden¹⁰⁸, Emma Dobson¹⁰⁸, Andy Drummond¹⁰⁸, Michelle Mulcahy¹⁰⁸, Sheila Munt¹⁰⁸, Grainne O'Connor¹⁰⁸, Jennifer Philbin¹⁰⁸, Chloe Rishton¹⁰⁸, Redmond Tully¹⁰⁸ & Sarah Winnard¹⁰⁸

Glasgow Royal Infirmary team

Susanne Cathcart¹⁰⁹, Katharine Duffy¹⁰⁹, Alex Puxty¹⁰⁹, Kathryn Puxty¹⁰⁹, Lynne Turner¹⁰⁹, Jane Ireland¹⁰⁹ & Gary Semple¹⁰⁹

St James's University Hospital and Leeds General Infirmary team

Kate Long¹¹⁰, Simon Whiteley¹¹⁰, Elizabeth Wilby¹¹⁰ & Bethan Ogg¹¹⁰

University Hospital North Durham team

Amanda Cowton^{111,112}, Andrea Kay^{111,112}, Melanie Kent^{111,112}, Kathryn Potts^{111,112}, Ami Wilkinson^{111,112}, Suzanne Campbell^{111,112} & Ellen Brown^{111,112}

Fairfield General Hospital team

Julie Melville¹¹³, Jay Naisbitt¹¹³, Rosane Joseph¹¹³, Maria Lazo¹¹³, Olivia Walton¹¹³ & Alan Neal¹¹³

Wythenshawe Hospital team

Peter Alexander¹¹⁴, Schvearn Allen¹¹⁴, Joanne Bradley-Potts¹¹⁴, Craig Brantwood¹¹⁴, Jasmine Egan¹¹⁴, Timothy Felton¹¹⁴, Grace Padden¹¹⁴, Luke Ward¹¹⁴, Stuart Moss¹¹⁴ & Susannah Glasgow¹¹⁴

Royal Alexandra Hospital team

Lynn Abel¹¹⁵, Michael Brett¹¹⁵, Brian Digby¹¹⁵, Lisa Gemmel¹¹⁵, James Hornsby¹¹⁵, Patrick MacGoe¹¹⁵, Pauline O'Neil¹¹⁵, Richard Price¹¹⁵, Natalie Rodden¹¹⁵, Kevin Rooney¹¹⁵, Radha Sundaram¹¹⁵ & Nicola Thomson¹¹⁵

Good Hope Hospital team

Bridget Hopkins¹¹⁶, James Scriven¹¹⁶, Laura Thrasyloulou¹¹⁶ & Heather Willis¹¹⁶

Tameside General Hospital team

Martyn Clark¹¹⁷, Martina Coulding¹¹⁷, Edward Jude¹¹⁷, Jacqueline McCormick¹¹⁷, Oliver Mercer¹¹⁷, Darsh Potla¹¹⁷, Hafiz Rehman¹¹⁷, Heather Savill¹¹⁷ & Victoria Turner¹¹⁷

Royal Derby Hospital team

Charlotte Downes¹¹⁸, Kathleen Holding¹¹⁸, Katie Riches¹¹⁸, Mary Hilton¹¹⁸, Mel Hayman¹¹⁸, Deepak Subramanian¹¹⁸ & Priya Daniel¹¹⁸

Medway Maritime Hospital team

Oluronke Adanini¹¹⁹, Nikhil Bhatia¹¹⁹, Maines Msiska¹¹⁹ & Rebecca Collins¹¹⁹

Royal Victoria Infirmary team

Ian Clement¹²⁰, Bijal Patel¹²⁰, A. Gulati¹²⁰, Carole Hays¹²⁰, K. Webster¹²⁰, Anne Hudson¹²⁰, Andrea Webster¹²⁰, Elaine Stephenson¹²⁰, Louise McCormack¹²⁰, Victoria Slater¹²⁰, Rachel Nixon¹²⁰, Helen Hanson¹²⁰, Maggie Fearby¹²⁰, Sinead Kelly¹²⁰, Victoria Bridgett¹²⁰ & Philip Robinson¹²⁰

Pooler Hospital team

Julie Camsooksa¹²¹, Charlotte Humphrey¹²¹, Sarah Jenkins¹²¹, Henrik Reschreiter¹²¹, Beverley Wadams¹²¹ & Yasmin Death¹²¹

Bedford Hospital team

Victoria Bastion¹²², Daphene Clarke¹²², Beena David¹²², Harriet Kent¹²², Rachel Lorusso¹²², Gamu Lubimbi¹²², Sophie Murdoch¹²², Melchizedek Penacerrada¹²², Alastair Thomas¹²², Jennifer Valentine¹²², Ana Vochin¹²², Retno Wulandari¹²² & Brice Djegum¹²²

Queens Hospital Burton team

Gillian Bell¹²³, Katy English¹²³, Amro Katary¹²³ & Louise Wilcox¹²³

North Manchester General Hospital team

Michelle Bruce¹²⁴, Karen Connolly¹²⁴, Tracy Duncan¹²⁴, Helen T. Michael¹²⁴, Gabriella Lindergard¹²⁴, Samuel Hey¹²⁴, Claire Fox¹²⁴, Jordan Alfonso¹²⁴, Laura Jayne Durrans¹²⁴, Jacinta Guerin¹²⁴, Bethan Blackledge¹²⁴, Jade Harris¹²⁴, Martin Hruska¹²⁴, Ayaa Eltayeb¹²⁴, Thomas Lamb¹²⁴, Tracey Hodgkiss¹²⁴, Lisa Cooper¹²⁴ & Joanne Rothwell¹²⁴

Aberdeen Royal Infirmary team

Angela Allan¹²⁵, Felicity Anderson¹²⁵, Callum Kaye¹²⁵, Jade Liew¹²⁵, Jasmine Medhora¹²⁵, Teresa Scott¹²⁵, Erin Trumper¹²⁵ & Adriana Botello¹²⁵

Derriford Hospital team

Liana Lankester¹²⁶, Nikitas Nikitas¹²⁶, Colin Wells¹²⁶, Bethan Stowe¹²⁶ & Kayleigh Spencer¹²⁶

Manchester Royal Infirmary team

Craig Brandwood¹²⁷, Lara Smith¹²⁷, Richard Clark¹²⁷, Katie Birchall¹²⁷, Laurel Kolakaluri¹²⁷, Deborah Baines¹²⁷ & Anila Sukumaran¹²⁷

Salford Royal Hospital team

Elena Apetri¹²⁸, Cathrine Basikolo¹²⁸, Bethan Blackledge¹²⁸, Laura Catlow¹²⁸, Bethan Charles¹²⁸, Paul Dark¹²⁸, Reece Doonan¹²⁸, Jade Harris¹²⁸, Alice Harvey¹²⁸, Daniel Horner¹²⁸, Karen Knowles¹²⁸, Stephanie Lee¹²⁸, Diane Lomas¹²⁸, Chloe Lyons¹²⁸, Tracy Marsden¹²⁸, Danielle McLaughlan¹²⁸, Liam McMorrow¹²⁸, Jessica Pendlebury¹²⁸, Jane Perez¹²⁸, Maria Poulaka¹²⁸, Nicola Proudfoot¹²⁸, Melanie Slaughter¹²⁸, Kathryn Slevin¹²⁸, Melanie Taylor¹²⁸, Vicky Thomas¹²⁸, Danielle Walker¹²⁸, Angiy Michael¹²⁸ & Matthew Collis¹²⁸

William Harvey Hospital team

Tracey Cosier¹²⁹, Gemma Millen¹²⁹, Neil Richardson¹²⁹, Natasha Schumacher¹²⁹, Heather Weston¹²⁹ & James Rand¹²⁹

Queen Elizabeth University Hospital team

Nicola Baxter¹³⁰, Steven Henderson¹³⁰, Sophie Kennedy-Hay¹³⁰, Christopher McParland¹³⁰, Laura Rooney¹³⁰, Malcolm Sim¹³⁰ & Gordan McCreath¹³⁰

Bradford Royal Infirmary team

Louise Akeroyd¹³¹, Shereen Bano¹³¹, Matt Bromley¹³¹, Lucy Gurr¹³¹, Tom Lawton¹³¹, James Morgan¹³¹, Kirsten Sellick¹³¹, Deborah Warren¹³¹, Brian Wilkinson¹³¹, Janet McGowan¹³¹, Camilla Ledgard¹³¹, Amelia Stacey¹³¹, Kate Pye¹³¹, Ruth Bellwood¹³¹ & Michael Bentley¹³¹

Bristol Royal Infirmary team

Jeremy Bewley¹³², Zoe Garland¹³², Lisa Grimmer¹³², Bethany Gumbrell¹³², Rebekah Johnson¹³², Katie Sweet¹³², Denise Webster¹³² & Georgia Efford¹³²

Norfolk and Norwich University Hospital (NNUH) team

Karen Convery¹³³, Deirdre Fottrell-Gould¹³³, Lisa Hudig¹³³, Jocelyn Keshet-Price¹³³, Georgina Randell¹³³ & Katie Stammers¹³³

Queen Elizabeth Hospital Gateshead team

Maria Bokhari¹³⁴, Vanessa Linnett¹³⁴, Rachael Lucas¹³⁴, Wendy McCormick¹³⁴, Jenny Ritzema¹³⁴, Amanda Sanderson¹³⁴ & Helen Wild¹³⁴

Article

Sunderland Royal Hospital team

Anthony Rostron¹³⁵, Alistair Roy¹³⁵, Lindsey Woods¹³⁵, Sarah Cornell¹³⁵, Fiona Wakinshaw¹³⁵, Kimberley Rogerson¹³⁵ & Jordan Jarman¹³⁵

Aintree University Hospital team

Robert Parker¹³⁶, Amie Reddy¹³⁶, Ian Turner-Bone¹³⁶, Laura Wilding¹³⁶ & Peter Harding¹³⁶

Hull Royal Infirmary team

Caroline Abernathy¹³⁷, Louise Foster¹³⁷, Andrew Gratrix¹³⁷, Vicky Martinson¹³⁷, Priyai Parkinson¹³⁷, Elizabeth Stones¹³⁷ & LluCIA Carbral-Ortega¹³⁸

University College Hospital team

Georgia Bercades¹³⁹, David Brealey¹³⁹, Ingrid Hass¹³⁹, Niall MacCallum¹³⁹, Gladys Martir¹³⁹, Eamon Raith¹³⁹, Anna Reyes¹³⁹ & Deborah Smyth¹³⁹

Royal Devon and Exeter Hospital team

Letizia Zitter¹⁴⁰, Sarah Benyon¹⁴⁰, Suzie Marriott¹⁴⁰, Linda Park¹⁴⁰, Samantha Keenan¹⁴⁰, Elizabeth Gordon¹⁴⁰, Helen Quinn¹⁴⁰ & Kizzy Baines¹⁴⁰

The Royal Papworth Hospital team

Lenka Cagova¹⁴¹, Adama Fofano¹⁴¹, Lucie Garner¹⁴¹, Helen Holcombe¹⁴¹, Sue Mepham¹⁴¹, Alice Michael Mitchell¹⁴¹, Lucy Mwaura¹⁴¹, Krithivasan Praman¹⁴¹, Alain Vuylsteke¹⁴¹ & Julie Zamikula¹⁴¹

Ipswich Hospital team

Bally Purewal¹⁴², Vanessa Rivers¹⁴² & Stephanie Bell¹⁴²

Southmead Hospital team

Hayley Blakemore¹⁴³, Borislava Borislavova¹⁴³, Beverley Faulkner¹⁴³, Emma Gendall¹⁴³, Elizabeth Goff¹⁴³, Kati Hayes¹⁴³, Matt Thomas¹⁴³, Ruth Worner¹⁴³, Kerry Smith¹⁴³ & Deanna Stephens¹⁴³

Milton Keynes University Hospital team

Louise Mew¹⁴⁴, Esther Mwaura¹⁴⁴, Richard Stewart¹⁴⁴, Felicity Williams¹⁴⁴, Lynn Wren¹⁴⁴ & Sara-Beth Sutherland¹⁴⁴

Royal Hampshire County Hospital team

Emily Bevan¹⁴⁵, Jane Martin¹⁴⁵, Dawn Trodd¹⁴⁵, Geoff Watson¹⁴⁵ & Caroline Wrey Brown¹⁴⁵

Great Ormond St Hospital and UCL Great Ormond St Institute of Child Health NIHR Biomedical Research Centre team

Olugbenga Akinkugbe¹⁴⁶, Alasdair Bamford¹⁴⁶, Emily Beech¹⁴⁶, Holly Belfield¹⁴⁶, Michael Bell¹⁴⁶, Charlene Davies¹⁴⁶, Gareth A. L. Jones¹⁴⁶, Tara McHugh¹⁴⁶, Hamza Meghari¹⁴⁶, Lauran O'Neill¹⁴⁶, Mark J. Peters¹⁴⁶, Samiran Ray¹⁴⁶ & Ana Luisa Tomas¹⁴⁶

Stoke Mandeville Hospital team

Iona Burn¹⁴⁷, Geraldine Hambrook¹⁴⁷, Katarina Manso¹⁴⁷, Ruth Penn¹⁴⁷, Pradeep Shanmugasundaram¹⁴⁷, Julie Tebbutt¹⁴⁷ & Danielle Thornton¹⁴⁷

University Hospital of Wales team

Jade Cole¹⁴⁸, Michelle Davies¹⁴⁸, Rhys Davies¹⁴⁸, Donna Duffin¹⁴⁸, Helen Hill¹⁴⁸, Ben Player¹⁴⁸, Emma Thomas¹⁴⁸ & Angharad Williams¹⁴⁸

Basingstoke and North Hampshire Hospital team

Denise Griffin¹⁴⁹, Nycola Muchenje¹⁴⁹, Mcdonald Mupudzi¹⁴⁹, Richard Partridge¹⁴⁹, Jo-Anna Conyngham¹⁴⁹, Rachel Thomas¹⁴⁹, Mary Wright¹⁴⁹ & Maria Alvarez Corral¹⁴⁹

Arrove Park Hospital team

Reni Jacob¹⁵⁰, Cathy Jones¹⁵⁰ & Craig Denmade¹⁵⁰

Chesterfield Royal Hospital Foundation Trust team

Sarah Beavis¹⁵¹, Katie Dale¹⁵¹, Rachel Gascoyne¹⁵¹, Joanne Hawes¹⁵¹, Kelly Pritchard¹⁵¹, Lesley Stevenson¹⁵¹ & Amanda Whileman¹⁵¹

Musgrove Park Hospital team

Patricia Doble¹⁵², Joanne Hutter¹⁵², Corinne Pawley¹⁵², Charmaine Shovelton¹⁵² & Marius Vaida¹⁵²

Peterborough City Hospital team

Deborah Butcher^{153,154}, Susie O'Sullivan^{153,154} & Nicola Butterworth-Cowin^{153,154}

Royal Hallamshire Hospital and Northern General Hospital team

Norfaizan Ahmad¹⁵⁵, Joann Barker¹⁵⁵, Kris Bauchmuller¹⁵⁵, Sarah Bird¹⁵⁵, Kay Cawthron¹⁵⁵, Kate Harrington¹⁵⁵, Yvonne Jackson¹⁵⁵, Faith Kibutu¹⁵⁵, Becky Lenagh¹⁵⁵, Becky Masuko¹⁵⁵, Gary H. Mills¹⁵⁵, Ajay Raithatha¹⁵⁵, Matthew Wiles¹⁵⁵, Jayne Willson¹⁵⁵, Helen Newell¹⁵⁵, Alison Lye¹⁵⁵, Lorenza Nwafor¹⁵⁵, Claire Jarman¹⁵⁵, Sarah Rowland-Jones¹⁵⁵, David Foote¹⁵⁵, Joby Cole¹⁵⁵, Roger Thompson¹⁵⁵, James Watson¹⁵⁵, Lisa Hesseldon¹⁵⁵, Irene Macharia¹⁵⁵, Luke Chetam¹⁵⁵, Jacqui Smith¹⁵⁵, Amber Ford¹⁵⁵, Samantha Anderson¹⁵⁵, Kathryn Birchall¹⁵⁵, Kay Housley¹⁵⁵, Sara Walker¹⁵⁵, Leanne Milner¹⁵⁵, Helena Hanratty¹⁵⁵, Helen Trower¹⁵⁵, Patrick Phillips¹⁵⁵, Simon Oxspring¹⁵⁵ & Ben Donne¹⁵⁵

Dumfries and Galloway Royal Infirmary team

Catherine Jardine¹⁵⁶, Dewi Williams¹⁵⁶ & Alasdair Hay¹⁵⁶

Royal Bolton Hospital team

Rebecca Flanagan¹⁵⁷, Gareth Hughes¹⁵⁷, Scott Latham¹⁵⁷, Emma McKenna¹⁵⁷, Jennifer Anderson¹⁵⁷, Robert Hull¹⁵⁷ & Kat Rhead¹⁵⁷

Lister Hospital team

Carina Cruz¹⁵⁸ & Natalie Pattison¹⁵⁸

Craigavon Area Hospital team

Rob Charnock¹⁵⁹, Denise McFarland¹⁵⁹ & Denise Cosgrove¹⁵⁹

Southport and Formby District General Hospital team

Ashar Ahmed¹⁶⁰, Anna Morris¹⁶⁰, Srinivas Jakkula¹⁶⁰ & Arvind Nune¹⁶⁰

Calderdale Royal Hospital team

Asifa Ali^{161,162}, Megan Brady^{161,162}, Sam Dale^{161,162}, Annalisa Dance^{161,162}, Lisa Gledhill^{161,162}, Jill Greig^{161,162}, Kathryn Hanson^{161,162}, Kelly Holdroyd^{161,162}, Marie Home^{161,162}, Diane Kelly^{161,162}, Ross Kitson^{161,162}, Lear Matapure^{161,162}, Deborah Melia^{161,162}, Samantha Mellor^{161,162}, Tonicha Nortcliffe^{161,162}, Jez Pinnell^{161,162}, Matthew Robinson^{161,162}, Lisa Shaw^{161,162}, Ryan Shaw^{161,162}, Lesley Thomis^{161,162}, Alison Wilson^{161,162}, Tracy Wood^{161,162}, Lee-Ann Bayo^{161,162}, Ekta Merwaha^{161,162}, Tahira Ishaq^{161,162} & Sarah Hanley^{161,162}

Prince Charles Hospital team

Bethan Deacon¹⁶³, Meg Hibbert¹⁶³, Carla Potheary¹⁶³, Dariusz Tetla¹⁶³, Christopher Woodford¹⁶³, Latha Durga¹⁶³ & Gareth Kennard-Holden¹⁶³

Royal Bournemouth Hospital team

Debbie Branney¹⁶⁴, Jordan Frankham¹⁶⁴, Sally Pitts¹⁶⁴ & Nigel White¹⁶⁴

Royal Preston Hospital team

Shondipon Laha¹⁶⁵, Mark Verlander¹⁶⁵ & Alexandra Williams¹⁶⁵

Whittington Hospital team

Abdelhakim Altabaibeh¹⁶⁶, Ana Alvaro¹⁶⁶, Kayleigh Gilbert¹⁶⁶, Louise Ma¹⁶⁶, Loreta Mostoles¹⁶⁶, Chetan Parmar¹⁶⁶, Kathryn Simpson¹⁶⁶, Champa Jetha¹⁶⁶, Lauren Booker¹⁶⁶ & Anezka Pratley¹⁶⁶

Princess Royal Hospital team

Colene Adams¹⁶⁷, Anita Agasou¹⁶⁷, Tracie Arden¹⁶⁷, Amy Bowes¹⁶⁷, Pauline Boyle¹⁶⁷, Mandy Beekes¹⁶⁷, Heather Button¹⁶⁷, Nigel Capps¹⁶⁷, Mandy Carnahan¹⁶⁷, Anne Carter¹⁶⁷, Danielle Childs¹⁶⁷, Denise Donaldson¹⁶⁷, Kelly Hard¹⁶⁷, Fran Hurford¹⁶⁷, Yasmin Hussain¹⁶⁷, Ayesha Javaid¹⁶⁷, James Jones¹⁶⁷, Sanal Jose¹⁶⁷, Michael Leigh¹⁶⁷, Terry Martin¹⁶⁷, Helen Millward¹⁶⁷, Nichola Motherwell¹⁶⁷, Rachel Rikunenko¹⁶⁷, Jo Stickley¹⁶⁷, Julie Summers¹⁶⁷, Louise Ting¹⁶⁷, Helen Tivenan¹⁶⁷, Louise Tonks¹⁶⁷, Rebecca Wilcox¹⁶⁷, Denise Skinner¹⁶⁸, Jane Gaylard¹⁶⁸, Dee Mullan¹⁶⁸ & Julie Newman¹⁶⁸

Macclesfield District General Hospital team

Maureen Holland¹⁶⁹, Natalie Keenan¹⁶⁹, Marc Lyons¹⁶⁹, Helen Wassall¹⁶⁹, Chris Marsh¹⁶⁹, Mervin Mahenthran¹⁶⁹, Emma Carter¹⁶⁹ & Thomas Kong¹⁶⁹

Royal Surrey County Hospital team

Helen Blackman¹⁷⁰, Ben Creagh-Brown¹⁷⁰, Sinead Donton¹⁷⁰, Natalia Michalak-Glinska¹⁷⁰, Sheila Mtuwa¹⁷⁰, Veronika Pristopan¹⁷⁰, Armored Salberg¹⁷⁰, Eleanor Smith¹⁷⁰, Sarah Stone¹⁷⁰, Charles Piercy¹⁷⁰, Jerik Verula¹⁷⁰, Dorota Burda¹⁷⁰, Rugia Montaser¹⁷⁰, Lesley Harden¹⁷⁰, Irving Mayangao¹⁷⁰, Cheryl Marriott¹⁷⁰, Paul Bradley¹⁷⁰ & Celia Harris¹⁷⁰

Hereford County Hospital team

Susan Anderson¹⁷¹, Eleanor Andrews¹⁷¹, Janine Birch¹⁷¹, Emma Collins¹⁷¹, Kate Hammerton¹⁷¹ & Ryan O'Leary¹⁷¹

University Hospital of North Tees team

Michele Clark¹⁷² & Sarah Purvis¹⁷²

Lincoln County Hospital team

Russell Barber¹⁷³, Claire Hewitt¹⁷³, Annette Hilldrith¹⁷³, Karen Jackson-Lawrence¹⁷³, Sarah Shepardson¹⁷³, Maryanne Wills¹⁷³, Susan Butler¹⁷³, Silvia Tavares¹⁷³, Amy Cunningham¹⁷³, Julia Hindale¹⁷³ & Sarwat Arif¹⁷³

Royal Cornwall Hospital team

Sarah Bean¹⁷⁴, Karen Burt¹⁷⁴ & Michael Spivey¹⁷⁴

Royal United Hospital team

Carrie Demetriou¹⁷⁵, Charlotte Eckbad¹⁷⁵, Sarah Hierons¹⁷⁵, Lucy Howie¹⁷⁵, Sarah Mitchard¹⁷⁵, Lidia Ramos¹⁷⁵, Alfredo Serrano-Ruiz¹⁷⁵, Katie White¹⁷⁵ & Fiona Kelly¹⁷⁵

Royal Brompton Hospital team

Daniele Cristiano¹⁷⁶, Natalie Dormand¹⁷⁶, Zohreh Farzad¹⁷⁶, Mahitha Gummadi¹⁷⁶, Kamal Liyanage¹⁷⁶, Brijesh Patel¹⁷⁶, Sara Salmi¹⁷⁶, Geraldine Sloane¹⁷⁶, Vicky Thwaites¹⁷⁶, Mathew Varghese¹⁷⁶ & Anelise C. Zborowski¹⁷⁶

University Hospital Crosshouse team

John Allan¹⁷⁷, Tim Geary¹⁷⁷, Gordon Houston¹⁷⁷, Alistair Meikle¹⁷⁷ & Peter O'Brien¹⁷⁷

Basildon Hospital team

Miranda Forsey¹⁷⁸, Agilan Kaliappan¹⁷⁸, Anne Nicholson¹⁷⁸, Joanne Riches¹⁷⁸, Mark Vertue¹⁷⁸, Miranda Forsey¹⁷⁸, Agilan Kaliappan¹⁷⁸, Anne Nicholson¹⁷⁸, Joanne Riches¹⁷⁸ & Mark Vertue¹⁷⁸

Glan Clwyd Hospital team

Elizabeth Allan¹⁷⁹, Kate Darlington¹⁷⁹, Ffyon Davies¹⁷⁹, Jack Easton¹⁷⁹, Sumit Kumar¹⁷⁹, Richard Lean¹⁷⁹, Daniel Menzies¹⁷⁹, Richard Pugh¹⁷⁹, Xinyi Qiu¹⁷⁹, Llinos Davies¹⁷⁹, Hannah Williams¹⁷⁹, Jeremy Scanlon¹⁷⁹, Gwyneth Davies¹⁷⁹, Callum Mackay¹⁷⁹, Joanne Lewis¹⁷⁹ & Stephanie Rees¹⁷⁹

West Middlesex Hospital team

Metod Oblak¹⁸⁰, Monica Popescu¹⁸⁰ & Mini Thankachen¹⁸⁰

Royal Lancaster Infirmary team

Andrew Higham¹⁸¹, Kerry Simpson¹⁸¹ & Jayne Craig¹⁸¹

Western General Hospital team

Rosie Baruah¹⁸², Sheila Morris¹⁸², Susie Ferguson¹⁸² & Amy Shepherd¹⁸²

Chelsea and Westminster NHS Foundation Trust team

Luke Stephen Prockter Moore¹⁸³, Marcela Paola Vizcaychipi¹⁸³, Laura Gomes de Almeida Martins¹⁸³ & Jaime Carungcong¹⁸³

The Queen Elizabeth Hospital team

Inthakab Ali Mohamed Ali¹⁸⁴, Karen Beaumont¹⁸⁴, Mark Blunt¹⁸⁴, Zoe Coton¹⁸⁴, Hollie Curgenvin¹⁸⁴, Mohamed Elsaadany¹⁸⁴, Kay Fernandes¹⁸⁴, Sameena Mohamed Ally¹⁸⁴, Harini Rangarajan¹⁸⁴, Varun Sarathy¹⁸⁴, Sivarupan Selvanayagam¹⁸⁴, Dave Vedage¹⁸⁴ & Matthew White¹⁸⁴

King's Mill Hospital team

Mandy Gill¹⁸⁵, Paul Paul¹⁸⁵, Valli Ratnam¹⁸⁵, Sarah Shelton¹⁸⁵ & Inez Wynter¹⁸⁵

Watford General Hospital team

Siobhain Carmody¹⁸⁶ & Valerie Joan Page¹⁸⁶

University Hospital Wishaw team

Claire Marie Beith¹⁸⁷, Karen Black¹⁸⁷, Suzanne Clements¹⁸⁷, Alan Morrison¹⁸⁷, Dominic Strachan¹⁸⁷, Margaret Taylor¹⁸⁷, Michelle Clarkson¹⁸⁷, Stuart D'Sylva¹⁸⁷ & Kathryn Norman¹⁸⁷

Forth Valley Royal Hospital team

Fiona Auld¹⁸⁸, Joanne Donnachie¹⁸⁸, Ian Edmond¹⁸⁸, Lynn Prentice¹⁸⁸, Nikole Runciman¹⁸⁸, Dario Salutous¹⁸⁸, Lesley Symon¹⁸⁸, Anne Todd¹⁸⁸, Patricia Turner¹⁸⁸, Abigail Short¹⁸⁸, Laura Sweeney¹⁸⁸, Euan Murdoch¹⁸⁸ & Dhaneesha Senaratne¹⁸⁸

George Eliot Hospital NHS Trust team

Michaela Hill¹⁸⁹, Thogulava Kannan¹⁸⁹ & Laura Wild¹⁸⁹

Barnsley Hospital team

Rikki Crawley¹⁹⁰, Abigail Crew¹⁹⁰, Mishell Cunningham¹⁹⁰, Allison Daniels¹⁹⁰, Laura Harrison¹⁹⁰, Susan Hope¹⁹⁰, Ken Inweregbu¹⁹⁰, Sian Jones¹⁹⁰, Nicola Lancaster¹⁹⁰, Jamie Matthews¹⁹⁰, Alice Nicholson¹⁹⁰ & Gemma Wray¹⁹⁰

The Great Western Hospital team

Helen Langton¹⁹¹, Rachel Prout¹⁹¹, Malcolm Watters¹⁹¹ & Catherine Novis¹⁹¹

Harefield Hospital team

Anthony Barron¹⁹², Ciara Collins¹⁹², Sundeep Kaul¹⁹², Heather Passmore¹⁹², Claire Prendergast¹⁹², Anna Reed¹⁹², Paula Rogers¹⁹², Rajvinder Shokkar¹⁹², Meriel Woodruff¹⁹², Hayley Middleton¹⁹², Oliver Polgar¹⁹², Claire Nolan¹⁹², Vicky Thwaites¹⁹² & Kanta Mahay¹⁹²

Rotherham General Hospital team

Dawn Collier¹⁹³, Anil Hormis¹⁹³, Victoria Maynard¹⁹³, Cheryl Graham¹⁹³, Rachel Walker¹⁹³ & Victoria Maynard¹⁹³

Ysbyty Gwynedd team

Ellen Knights¹⁹⁴, Alicia Price¹⁹⁴, Alice Thomas¹⁹⁴ & Chris Thorpe¹⁹⁴

Diana Princess of Wales Hospital team

Teresa Behan¹⁹⁵, Caroline Burnett¹⁹⁵, Jonathan Hatton¹⁹⁵, Elaine Heeney¹⁹⁵, Atideb Mitra¹⁹⁵, Maria Newton¹⁹⁵, Rachel Pollard¹⁹⁵ & Rachael Stead¹⁹⁵

Russell's Hall Hospital team

Vishal Amin¹⁹⁶, Elena Anastasescu¹⁹⁶, Vikram Anumakonda¹⁹⁶, Komala Karthik¹⁹⁶, Rizwana Kausar¹⁹⁶, Karen Reid¹⁹⁶, Jacqueline Smith¹⁹⁶, Janet Imeson-Wood¹⁹⁶, Denise Skinner¹⁹⁶, Jane Gaylard¹⁹⁶, Dee Mullan¹⁹⁶ & Julie Newman¹⁹⁶

St Mary's Hospital team

Alison Brown¹⁹⁷, Vikki Crickmore¹⁹⁷, Gabor Debreceni¹⁹⁷, Joy Wilkins¹⁹⁷ & Liz Nicol¹⁹⁷

University Hospital Lewisham team

Waqas Khaliq¹⁹⁸, Rosie Reece-Anthony¹⁹⁸ & Mark Birt¹⁹⁸

Colchester General Hospital team

Alison Ghosh¹⁹⁹ & Emma Williams¹⁹⁹

Queen Elizabeth the Queen Mother Hospital team

Louise Allen²⁰⁰, Eva Beranova²⁰⁰, Nikki Crisp²⁰⁰, Joanne Deery²⁰⁰, Tracy Hazelton²⁰⁰, Alicia Knight²⁰⁰, Carly Price²⁰⁰, Sorrell Tilbey²⁰⁰, Salah Turki²⁰⁰ & Sharon Turney²⁰⁰

Royal Albert Edward Infirmary team

Joshua Cooper²⁰¹, Cheryl Finch²⁰¹, Sarah Litherth²⁰¹, Alison Quinn²⁰¹ & Natalia Waddington²⁰¹

Victoria Hospital team

Tina Coventry²⁰², Susan Fowler²⁰², Michael MacMahon²⁰² & Amanda McGregor²⁰²

Eastbourne District General Hospital team

Anne Cowley^{203,204} & Judith Highgate^{203,204}

Cumberland Infirmary team

Alison Brown²⁰⁵, Jane Gregory²⁰⁵, Susan O'Connell²⁰⁵, Tim Smith²⁰⁵ & Luigi Barberis²⁰⁵

New Cross Hospital team

Shameer Gopal²⁰⁶, Nichola Harris²⁰⁶, Victoria Lake²⁰⁶, Stella Metherell²⁰⁶ & Elizabeth Radford²⁰⁶

The Princess Alexandra Hospital team

Amelia Daniel²⁰⁷, Joanne Finn²⁰⁷, Rajnish Saha²⁰⁷, Nikki White²⁰⁷ & Amy Easthope²⁰⁷

Salisbury District Hospital team

Phil Donnison²⁰⁸, Fiona Trim²⁰⁸ & Beena Eapen²⁰⁸

Dorset County Hospital team

Jenny Birch²⁰⁹, Laura Bough²⁰⁹, Josie Goodsell²⁰⁹, Rebecca Tutton²⁰⁹, Patricia Williams²⁰⁹, Sarah Williams²⁰⁹ & Barbara Winter-Goodwin²⁰⁹

University College Dublin team

Ailstair Nichol²¹⁰, Kathy Brickell²¹⁰, Michelle Smyth²¹⁰ & Lorna Murphy²¹⁰

Glangwili General Hospital team

Samantha Coetzee²¹¹, Alistair Gales²¹¹, Igor Otahal²¹¹, Meena Raj²¹¹ & Craig Sell²¹¹

Gloucestershire Royal Hospital team

Paula Hilltout²¹², Jayne Evitts²¹², Amanda Tyler²¹² & Joanne Waldron²¹²

Yeovil Hospital team

Kate Beesley²¹³, Sarah Board²¹³, Agnieszka Kubisz-Pudelko²¹³, Alison Lewis²¹³, Jess Perry²¹³, Lucy Pippard²¹³, Di Wood²¹³ & Clare Buckley²¹³

Leicester Royal Infirmary team

Peter Barry²¹⁴, Neil Flint²¹⁴, Patel Rekha²¹⁴ & Dawn Hales²¹⁴

Royal Manchester Children's Hospital team

Lara Bunn²¹⁵, Claire Jennings²¹⁵, Monica Latif²¹⁵, Rebecca Marshall²¹⁵ & Gayathri Subramanian²¹⁵

Royal Victoria Hospital team

Peter J. McGuigan²¹⁶, Christopher Wasson²¹⁶, Stephanie Finn²¹⁶, Jackie Green²¹⁶, Erin Collins²¹⁶ & Bernadette King²¹⁶

Wrexham Maelor Hospital team

Andy Campbell²¹⁷, Sara Smuts²¹⁷, Joseph Duffield²¹⁷, Oliver Smith²¹⁷, Lewis Mallon²¹⁷ & Claire Watkins²¹⁷

Walsall Manor Hospital team

Liam Botfield²¹⁸, Joanna Butler²¹⁸, Catherine Dexter²¹⁸, Jo Fletcher²¹⁸, Atul Garg²¹⁸, Aditya Kuravi²¹⁸, Poonam Ranga²¹⁸ & Emma Virgilio²¹⁸

Darent Valley Hospital team

Zakula Belagodu²¹⁹, Bridget Fuller²¹⁹, Anca Gherman²¹⁹, Olumide Olufuwa²¹⁹, Remi Paramsothy²¹⁹, Carmel Stuart²¹⁹, Naomi Oakley²¹⁹, Charlotte Kamundi²¹⁹, David Tyl²¹⁹, Katy Collins²¹⁹, Pedro Silva²¹⁹, June Taylor²¹⁹, Laura King²¹⁹, Charlotte Coates²¹⁹, Maria Crowley²¹⁹, Philippa Wakefield²¹⁹, Jane Beadle²¹⁹, Laura Johnson²¹⁹, Janet Sargeant²¹⁹ & Madeleine Anderson²¹⁹

Warrington General Hospital team

Ailbhe Brady²²⁰, Rebekah Chan²²⁰, Jeff Little²²⁰, Shane McIvor²²⁰, Helena Prady²²⁰, Helen Whittle²²⁰ & Bijoy Mathew²²⁰

Article

Warwick Hospital team

Ben Attwood²²¹ & Penny Parsons²²¹

University Hospitals Coventry and Warwickshire NHS Trust team

Geraldine Ward²²² & Pamela Bremner²²²

University Hospital Monklands team

West Joe²²³, Baird Tracy²²³ & Ruddy Jim²²³

Princess of Wales Hospital team

Ellie Davies²²⁴, Lisa Roche²²⁴ & Sonia Sathe²²⁴

Northwick Park Hospital team

Catherine Dennis²²⁵, Alastair McGregor²²⁵, Victoria Parris²²⁵, Sinduya Srikanan²²⁵ & Anisha Sukha²²⁵

Raigmore Hospital team

Rachael Campbell²²⁶, Noreen Clarke²²⁶, Jonathan Whiteside²²⁶, Mairi Mascarenhas²²⁶, Avril Donaldson²²⁶, Joanna Matheson²²⁶, Fiona Barrett²²⁶, Marianne O'Hara²²⁶, Laura O'Keefe²²⁶ & Clare Bradley²²⁶

Royal Free Hospital team

Christine Eastgate-Jackson²²⁷, Helder Filipe²²⁷, Daniel Martin²²⁷, Amitaa Maharajh²²⁷, Sara Mingo Garcia²²⁷, Glykeria Pakou²²⁷ & Mark De Nee²²⁷

Scunthorpe General Hospital team

Kathy Dent²²⁸, Elizabeth Horsley²²⁸, Muhammad Nauman Akhtar²²⁸, Sandra Pearson²²⁸, Dorota Potoczna²²⁸ & Sue Spencer²²⁸

West Cumberland Hospital team

Melanie Clapham²²⁹, Rosemary Harper²²⁹, Una Poultney²²⁹, Polly Rice²²⁹, Tim Smith²²⁹, Rachel Mutch²²⁹ & Luigi Barberis²²⁹

Airedale General Hospital team

Lisa Armstrong²³⁰, Hayley Bates²³⁰, Emma Dooks²³⁰, Fiona Farquhar²³⁰, Brigid Hairsine²³⁰, Chantal McParland²³⁰ & Sophie Packham²³⁰

Birmingham Children's Hospital team

Rehana Bi²³¹, Barney Scholefield²³¹ & Lydia Ashton²³¹

Liverpool Heart and Chest Hospital team

Linsha George²³², Sophie Twiss²³² & David Wright²³²

Pilgrim Hospital team

Manish Chablani²³³, Amy Kirkby²³³ & Kimberley Netherton²³³

Prince Philip Hospital team

Kim Davies²³⁴, Linda O'Brien²³⁴, Zohra Omar²³⁴, Igor Otahal²³⁴, Emma Perkins²³⁴, Tracy Lewis²³⁴ & Isobel Sutherland²³⁴

Furness General Hospital team

Karen Burns²³⁵ & Andrew Higham²³⁵

Scarborough General Hospital team

Ben Chandler²³⁶, Kerry Elliott²³⁶, Janine Mallinson²³⁶ & Alison Turnbull²³⁶

Southend University Hospital team

Prisca Gondo²³⁷, Bernard Hadebe²³⁷, Abdul Kayani²³⁷ & Bridgett Masunda²³⁷

Alder Hey Children's Hospital team

Taya Anderson²³⁸, Dan Hawcutt²³⁸, Laura O'Malley²³⁸, Laura Rad²³⁸, Naomi Rogers²³⁸, Paula Saunderson²³⁸, Kathryn Sian Allison²³⁸, Deborah Afolab²³⁸, Jennifer Whitebread²³⁸, Dawn Jones²³⁸ & Rachael Dore²³⁸

Torbay Hospital team

Matthew Halkes²³⁹, Pauline Mercer²³⁹ & Lorraine Thornton²³⁹

Borders General Hospital team

Joy Dawson²⁴⁰, Sweyn Garrioch²⁴⁰, Melanie Tolson²⁴⁰ & Jonathan Aldridge²⁴⁰

Kent and Canterbury Hospital team

Ritoo Kapoor²⁴¹, David Loader²⁴¹ & Karen Castle²⁴¹

West Suffolk Hospital team

Sally Humphreys²⁴² & Ruth Tampsett²⁴²

James Paget University Hospital NHS Trust team

Katherine Mackintosh²⁴³, Amanda Ayers²⁴³, Wendy Harrison²⁴³ & Julie North²⁴³

The Christie NHS Foundation Trust team

Suzanne Allibone²⁴⁴, Roman Genetu²⁴⁴, Vidya Kasipandian²⁴⁴, Amit Patel²⁴⁴, Ainh Mac²⁴⁴, Anthony Murphy²⁴⁴, Parisa Mahjoob²⁴⁴, Roonak Nazari²⁴⁴, Lucy Worsley²⁴⁴ & Andrew Fagan²⁴⁴

The Royal Marsden Hospital team

Thomas Bemand²⁴⁵, Ethel Black²⁴⁵, Arnold Dela Rosa²⁴⁵, Ryan Howle²⁴⁵, Shaman Jhanji²⁴⁵, Ravishankar Rao Baikady²⁴⁵, Kate Colette Tatham²⁴⁵ & Benjamin Thomas²⁴⁵

University Hospital Hairmyres team

Dina Bell²⁴⁶, Rosalind Boyle²⁴⁶, Katie Douglas²⁴⁶, Lynn Glass²⁴⁶, Emma Lee²⁴⁶, Liz Lennon²⁴⁶ & Austin Ratray²⁴⁶

Withybush General Hospital team

Abigail Taylor²⁴⁷, Rachel Anne Hughes²⁴⁷, Helen Thomas²⁴⁷, Alun Rees²⁴⁷, Michaela Duskova²⁴⁷, Janet Phipps²⁴⁷, Suzanne Brooks²⁴⁷ & Michelle Edwards²⁴⁷

Ealing Hospital team

Victoria Parris²⁴⁸, Sheena Quaid²⁴⁸ & Ekaterina Watson²⁴⁸

North Devon District Hospital team

Adam Brayne²⁴⁹, Emma Fisher²⁴⁹, Jane Hunt²⁴⁹, Peter Jackson²⁴⁹, Duncan Kaye²⁴⁹, Nicholas Love²⁴⁹, Juliet Parkin²⁴⁹, Victoria Tuckey²⁴⁹, Lynne van Koutrik²⁴⁹, Sasha Carter²⁴⁹, Benedict Andrew²⁴⁹, Louise Findlay²⁴⁹ & Katie Adams²⁴⁹

St John's Hospital Livingston team

Jen Service²⁵⁰, Alison Williams²⁵⁰, Claire Cheyne²⁵⁰, Anne Saunderson²⁵⁰, Sam Moultrie²⁵⁰ & Miranda Odam²⁵⁰

Northampton General Hospital NHS Trust team

Kathryn Hall²⁵¹, Isheunesu Mapfunde²⁵¹, Charlotte Willis²⁵¹ & Alex Lyon²⁵¹

Harrogate and District NHS Foundation Trust team

Chunda Sri-Chandana²⁵², Joslan Scherewode²⁵², Lorraine Stephenson²⁵² & Sarah Marsh²⁵²

National Hospital for Neurology and Neurosurgery team

David Brealey²⁵³, John Hardy²⁵³, Henry Houlden²⁵³, Eleanor Moncur²⁵³, Eamon Raith²⁵³, Ambreen Tariq²⁵³ & Arianna Tucci²⁵³

Bronlais General Hospital team

Maria Hobrok²⁵⁴, Ronda Loosley²⁵⁴, Heather McGuinness²⁵⁴, Helen Tench²⁵⁴ & Rebecca Wolf-Roberts²⁵⁴

Golden Jubilee National Hospital team

Val Irvine²⁵⁵ & Benjamin Shelley²⁵⁵

Homerton University Hospital Foundation NHS Trust team

Amy Easthope²⁵⁶, Claire Gorman²⁵⁶, Abhinav Gupta²⁵⁶, Elizabeth Timlick²⁵⁶ & Rebecca Brady²⁵⁶

Royal Hospital for Children team

Colin Begg³⁸ & Barry Milligan³⁸

Sheffield Children's Hospital team

Arianna Bellini²⁵⁷, Jade Bryant²⁵⁷, Anton Mayer²⁵⁷, Amy Pickard²⁵⁷, Nicholas Roe²⁵⁷, Jason Sowter²⁵⁷ & Alex Howlett²⁵⁷

The Royal Alexandra Children's Hospital team

Katy Fidler²⁵⁸, Emma Tagliavini²⁵⁸ & Kevin Donnelly²⁵⁸

³⁶Roslin Institute, University of Edinburgh, Edinburgh, UK. ³⁷Intensive Care Unit, Royal Infirmary of Edinburgh, Edinburgh, UK. ³⁸Royal Hospital for Children, Glasgow, UK. ³⁹William Harvey Research Institute, Barts and the London School of Medicine and Dentistry, Queen Mary University of London, London, UK. ⁴⁰Centre for Tropical Medicine and Global Health, Nuffield Department of Medicine, University of Oxford, Oxford, UK. ⁴¹Wellcome Centre for Human Genetics, University of Oxford, Oxford, UK. ⁴²Prince of Wales Hospital, Hong Kong, China. ⁴³Department of Critical Care Medicine, Queen's University and Kingston Health Sciences Centre, Kingston, Ontario, Canada. ⁴⁴Wellcome-Wolfson Institute for Experimental Medicine, Queen's University Belfast, Belfast, UK. ⁴⁵Department of Intensive Care Medicine, Royal Victoria Hospital, Belfast, UK. ⁴⁶UCL Centre for Human Health and Performance, London, UK. ⁴⁷Clinical Research Centre at St Vincent's University Hospital, University College Dublin, Dublin, Ireland. ⁴⁸National Heart and Lung Institute, Imperial College London, London, UK. ⁴⁹Imperial College Healthcare NHS Trust: London, London, UK. ⁵⁰Heart Institute, University of São Paulo, São Paulo, Brazil. ⁵¹MRC Human Genetics Unit, Institute of Genetics and Molecular Medicine, University of Edinburgh, Western General Hospital, Edinburgh, UK. ⁵²Intensive Care National Audit and Research Centre, London, UK. ⁵³NIHR Health Protection Research Unit for Emerging and Zoonotic Infections, Institute of Infection, Veterinary and Ecological Sciences, University of Liverpool, Liverpool, UK. ⁵⁴Respiratory Medicine and Institute in the Park, Alder Hey Children's Hospital and University of Liverpool, Liverpool, UK. ⁵⁵Department of Intensive Care Medicine, Guy's and St Thomas' NHS Foundation Trust, London, UK. ⁵⁶Department of Medicine, University of Cambridge, Cambridge, UK. ⁵⁷NIHR Clinical Research Network (CRN), Hammersmith Hospital, London, UK. ⁵⁸Cambridge University Hospitals NHS Foundation Trust, Cambridge, UK. ⁵⁹Edinburgh Clinical Research

Facility, Western General Hospital, University of Edinburgh, Edinburgh, UK. ⁶⁰Biostatistics Group, State Key Laboratory of Biocontrol, School of Life Sciences, Sun Yat-sen University, Guangzhou, China. ⁶¹Department of Infectious Diseases, Leiden University Medical Center, Leiden, The Netherlands. ⁶²Guys and St Thomas' Hospital, London, UK. ⁶³Barts Health NHS Trust, London, UK. ⁶⁴James Cook University Hospital, Middlesbrough, UK. ⁶⁵Royal Stoke University Hospital, Stoke-on-Trent, UK. ⁶⁶North Middlesex University Hospital NHS Trust, London, UK. ⁶⁷North Middlesex University Hospital NHS Trust, London, UK. ⁶⁸The Royal Liverpool University Hospital, Liverpool, UK. ⁶⁹King's College Hospital, London, UK. ⁷⁰Charing Cross Hospital, St Mary's Hospital and Hammersmith Hospital, London, UK. ⁷¹Nottingham University Hospital, Nottingham, UK. ⁷²John Radcliffe Hospital, Oxford, UK. ⁷³Kingston Hospital, Kingston-upon-Thames, UK. ⁷⁴Kingston Hospital, Kingston-upon-Thames, UK. ⁷⁵Royal Infirmary of Edinburgh, Edinburgh, UK. ⁷⁶Queen Alexandra Hospital, Portsmouth, UK. ⁷⁷Morrison Hospital, Swansea, UK. ⁷⁸Addenbrooke's Hospital, Cambridge, UK. ⁷⁹BHRUT (Barking Havering)—Queen's Hospital and King George Hospital, Romford, UK. ⁸⁰Royal Sussex County Hospital, Brighton, UK. ⁸¹Queen Elizabeth Hospital, Birmingham, UK. ⁸²Queen Elizabeth Hospital, Woolwich, London, UK. ⁸³St George's Hospital, London, UK. ⁸⁴Stepping Hill Hospital, Stockport, UK. ⁸⁵Countess of Chester Hospital, Chester, UK. ⁸⁶Royal Blackburn Teaching Hospital, Blackburn, UK. ⁸⁷The Tunbridge Wells Hospital and Maidstone Hospital, Tunbridge Wells, UK. ⁸⁸Royal Gwent Hospital, Newport, UK. ⁸⁹Pinderfields General Hospital, Wakefield, UK. ⁹⁰Royal Berkshire NHS Foundation Trust, Reading, UK. ⁹¹Broomfield Hospital, Chelmsford, UK. ⁹²Northumbria Healthcare NHS Foundation Trust, North Shields, UK. ⁹³Whiston Hospital, Prescot, UK. ⁹⁴Croydon University Hospital, Croydon, UK. ⁹⁵York Hospital, York, UK. ⁹⁶Heartlands Hospital, Birmingham, UK. ⁹⁷Ashford and St Peter's Hospital, Chertsey, UK. ⁹⁸Barnet Hospital, London, UK. ⁹⁹East Surrey Hospital, Redhill, UK. ¹⁰⁰Ninewells Hospital, Dundee, UK. ¹⁰¹Worthing Hospital, Worthing, UK. ¹⁰²St Richard's Hospital, Chichester, UK. ¹⁰³Southampton General Hospital, Southampton, UK. ¹⁰⁴The Alexandra Hospital, Redditch and Worcester Royal Hospital, Worcester, UK. ¹⁰⁵Sandwell General Hospital and City Hospital, Birmingham, UK. ¹⁰⁶Blackpool Victoria Hospital, Blackpool, UK. ¹⁰⁷Royal Glamorgan Hospital, Pontyclun, UK. ¹⁰⁸The Royal Oldham Hospital, Manchester, UK. ¹⁰⁹Glasgow Royal Infirmary, Glasgow, UK. ¹¹⁰St James's University Hospital and Leeds General Infirmary, Leeds, UK. ¹¹¹University Hospital North Durham, Durham, UK. ¹¹²Darlington Memorial Hospital, Darlington, UK. ¹¹³Fairfield General Hospital, Bury, UK. ¹¹⁴Wythenshawe Hospital, Manchester, UK. ¹¹⁵Royal Alexandra Hospital, Paisley, UK. ¹¹⁶Good Hope Hospital, Birmingham, UK. ¹¹⁷Tameside General Hospital, Ashton-under-Lyne, UK. ¹¹⁸Royal Derby Hospital, Derby, UK. ¹¹⁹Medway Maritime Hospital, Gillingham, UK. ¹²⁰Royal Victoria Infirmary, Newcastle-upon-Tyne, UK. ¹²¹Poole Hospital, Poole, UK. ¹²²Bedford Hospital, Bedford, UK. ¹²³Queens Hospital Burton, Burton-on-Trent, UK. ¹²⁴North Manchester General Hospital, Manchester, UK. ¹²⁵Aberdeen Royal Infirmary, Aberdeen, UK. ¹²⁶Derriford Hospital, Plymouth, UK. ¹²⁷Manchester Royal Infirmary, Manchester, UK. ¹²⁸Salford Royal Hospital, Manchester, UK. ¹²⁹William Harvey Hospital, Ashford, UK. ¹³⁰Queen Elizabeth University Hospital, Glasgow, UK. ¹³¹Bradford Royal Infirmary, Bradford, UK. ¹³²Bristol Royal Infirmary, Bristol, UK. ¹³³Norfolk and Norwich University Hospital (NNUH), Norwich, UK. ¹³⁴Queen Elizabeth Hospital Gateshead, Gateshead, UK. ¹³⁵Sunderland Royal Hospital, Sunderland, UK. ¹³⁶Aintree University Hospital, Liverpool, UK. ¹³⁷Hull Royal Infirmary, Hull, UK. ¹³⁸Hull Royal Infirmary, Hull, UK. ¹³⁹University College Hospital, London, UK. ¹⁴⁰Royal Devon and Exeter Hospital, Exeter, UK. ¹⁴¹The Royal Papworth Hospital, Cambridge, UK. ¹⁴²Ipswich Hospital, Ipswich, UK. ¹⁴³Southmead Hospital, Bristol, UK. ¹⁴⁴Milton Keynes University Hospital, Milton Keynes, UK. ¹⁴⁵Royal Hampshire County Hospital, Winchester, UK. ¹⁴⁶Great Ormond St Hospital and UCL Great Ormond St Institute of Child Health NIHR Biomedical Research Centre, London, UK. ¹⁴⁷Stoke Mandeville Hospital, Aylesbury, UK. ¹⁴⁸University Hospital of Wales, Cardiff, UK. ¹⁴⁹Basingstoke and North Hampshire Hospital, Basingstoke, UK. ¹⁵⁰Arrows Park Hospital, Wirral, UK. ¹⁵¹Chesterfield Royal Hospital Foundation Trust, Chesterfield, UK. ¹⁵²Musgrove Park Hospital, Taunton, UK. ¹⁵³Peterborough City Hospital, Peterborough, UK. ¹⁵⁴Hinchingsbrooke Hospital, Huntingdon, UK. ¹⁵⁵Royal Hallamshire Hospital and Northern General Hospital, Sheffield, UK. ¹⁵⁶Dumfries and Galloway Royal Infirmary, Dumfries, UK. ¹⁵⁷Royal Bolton Hospital, Bolton, UK. ¹⁵⁸Lister Hospital, Stevenage, UK. ¹⁵⁹Craigavon Area Hospital, Craigavon, UK. ¹⁶⁰Southport and Formby District General Hospital, Ormskirk, UK. ¹⁶¹Calderdale Royal Hospital, Halifax, UK. ¹⁶²Huddersfield Royal Infirmary, Huddersfield, UK. ¹⁶³Prince Charles Hospital, Merthyr Tydfil, UK. ¹⁶⁴Royal Bournemouth Hospital, Bournemouth, UK. ¹⁶⁵Royal Preston Hospital, Preston, UK. ¹⁶⁶Whittington Hospital, London, UK. ¹⁶⁷Princess Royal Hospital, Telford and Royal Shrewsbury Hospital, Shrewsbury, UK. ¹⁶⁸Princess Royal Hospital, Haywards Heath, UK. ¹⁶⁹Macclesfield District General Hospital, Macclesfield, UK. ¹⁷⁰Royal Surrey County Hospital, Guildford, UK. ¹⁷¹Hereford County Hospital, Hereford, UK. ¹⁷²University Hospital of North Tees, Stockton-on-Tees, UK. ¹⁷³Lincoln County Hospital, Lincoln, UK. ¹⁷⁴Royal Cornwall Hospital, Truro, UK. ¹⁷⁵Royal United Hospital, Bath, UK. ¹⁷⁶Royal Brompton Hospital, London, UK. ¹⁷⁷University Hospital Crosshouse, Kilmarnock, UK. ¹⁷⁸Basildon Hospital, Basildon, UK. ¹⁷⁹Glan Clwyd Hospital, Bodelwyddan, UK. ¹⁸⁰West Middlesex Hospital, Isleworth, UK. ¹⁸¹Royal Lancaster Infirmary, Lancaster, UK. ¹⁸²Western General Hospital, Edinburgh, UK. ¹⁸³Chelsea and Westminster NHS Foundation Trust, London, UK. ¹⁸⁴The Queen Elizabeth Hospital, King's Lynn, UK. ¹⁸⁵King's Mill Hospital, Nottingham, UK. ¹⁸⁶Watford General Hospital, Watford, UK. ¹⁸⁷University Hospital Wishaw, Wishaw, UK. ¹⁸⁸Forth Valley Royal Hospital, Falkirk, UK. ¹⁸⁹George Eliot Hospital NHS Trust, Nuneaton, UK. ¹⁹⁰Barnsley Hospital, Barnsley, UK. ¹⁹¹The Great Western Hospital, Swindon, UK. ¹⁹²Harefield Hospital, London, UK. ¹⁹³Rotherham General Hospital, Rotherham, UK. ¹⁹⁴Ysbyty Gwynedd, Bangor, UK. ¹⁹⁵Diana Princess of Wales Hospital, Grimsby, UK. ¹⁹⁶Russell's Hall Hospital, Dudley, UK. ¹⁹⁷St Mary's Hospital, Newport, UK. ¹⁹⁸University Hospital Lewisham, London, UK. ¹⁹⁹Colchester General Hospital, Colchester, UK. ²⁰⁰Queen Elizabeth the Queen Mother Hospital, Margate, UK. ²⁰¹Royal Albert Edward Infirmary, Wigan, UK. ²⁰²Victoria Hospital, Kirkcaldy, UK. ²⁰³Eastbourne District General Hospital, Eastbourne, UK. ²⁰⁴Conquest Hospital, St Leonards-on-Sea, UK. ²⁰⁵Cumberland Infirmary, Carlisle, UK. ²⁰⁶New Cross Hospital, Wolverhampton, UK. ²⁰⁷The Princess Alexandra Hospital, Harlow, UK. ²⁰⁸Salisbury District Hospital, Salisbury, UK. ²⁰⁹Dorset County Hospital, Dorchester, UK. ²¹⁰University College Dublin, St Vincent's University Hospital, Dublin, Ireland. ²¹¹Glangwyl General Hospital, Carmarthen, UK. ²¹²Gloucestershire Royal Hospital, Gloucester, UK. ²¹³Yeovil Hospital, Yeovil, UK. ²¹⁴Leicester Royal Infirmary, Leicester, UK. ²¹⁵Royal Manchester Children's Hospital, Manchester, UK. ²¹⁶Royal Victoria Hospital, Belfast, UK. ²¹⁷Wrexham Maelor Hospital, Wrexham, UK. ²¹⁸Walsall Manor Hospital, Walsall, UK. ²¹⁹Darent Valley Hospital, Dartford, UK. ²²⁰Warrington General Hospital, Warrington, UK. ²²¹Warwick

Hospital, Warwick, UK. ²²²University Hospitals Coventry and Warwickshire NHS Trust, Coventry, UK. ²²³University Hospital Monklands, Airdrie, UK. ²²⁴Princess of Wales Hospital, Llantrisant, UK. ²²⁵Northwick Park Hospital, London, UK. ²²⁶Raigmore Hospital, Inverness, UK. ²²⁷Royal Free Hospital, London, UK. ²²⁸Scunthorpe General Hospital, Scunthorpe, UK. ²²⁹West Cumberland Hospital, Whitehaven, UK. ²³⁰Airedale General Hospital, Keighley, UK. ²³¹Birmingham Children's Hospital, Birmingham, UK. ²³²Liverpool Heart and Chest Hospital, Liverpool, UK. ²³³Pilgrim Hospital, Lincoln, UK. ²³⁴Prince Philip Hospital, Llanelli, UK. ²³⁵Furness General Hospital, Barrow-in-Furness, UK. ²³⁶Scarborough General Hospital, Scarborough, UK. ²³⁷Southend University Hospital, Westcliff-on-Sea, UK. ²³⁸Allder Hey Children's Hospital, Liverpool, UK. ²³⁹Torbay Hospital, Torquay, UK. ²⁴⁰Borders General Hospital, Melrose, UK. ²⁴¹Kent and Canterbury Hospital, Canterbury, UK. ²⁴²West Suffolk Hospital, Bury St Edmunds, UK. ²⁴³James Paget University Hospital NHS Trust, Great Yarmouth, UK. ²⁴⁴The Christie NHS Foundation Trust, Manchester, UK. ²⁴⁵The Royal Marsden Hospital, London, UK. ²⁴⁶University Hospital Hairmyres, East Kilbride, UK. ²⁴⁷Withybush General Hospital, Haverfordwest, Wales, UK. ²⁴⁸Ealing Hospital, Southall, UK. ²⁴⁹North Devon District Hospital, Barnstaple, UK. ²⁵⁰St John's Hospital Livingstone, Livingstone, UK. ²⁵¹Northampton General Hospital NHS Trust, Northampton, UK. ²⁵²Harrogate and District NHS Foundation Trust, Harrogate, UK. ²⁵³National Hospital for Neurology and Neurosurgery, London, UK. ²⁵⁴Bronlais General Hospital, Aberystwyth, UK. ²⁵⁵Golden Jubilee National Hospital, Clydebank, UK. ²⁵⁶Homerton University Hospital Foundation NHS Trust, London, UK. ²⁵⁷Sheffield Children's Hospital, Sheffield, UK. ²⁵⁸The Royal Alexandra Children's Hospital, Brighton, UK.

23andMe investigators

Janie F. Shelton²⁵⁹, Anjali J. Shastri²⁵⁹, Chelsea Ye²⁵⁹, Catherine H. Weldon²⁵⁹, Teresa Filshiein-Sonmez²⁵⁹, Daniella Coker²⁵⁹, Antony Symons²⁵⁹, Jorge Esparza-Gordillo²⁶⁰, Stella Aslibekyan²⁵⁹ & Adam Auton²⁵⁹

²⁵⁹23andMe, Sunnyvale, CA, USA. ²⁶⁰Human Genetics R&D and Target Sciences R&D, GSK Medicines Research Centre, Stevenage, UK.

COVID-19 Human Genetics Initiative

Gita A. Pathak²⁶¹, Juha Karjalainen²⁶², Christine Stevens²⁶³, Shea J. Andrews²⁶⁴, Masahiro Kana²⁶³, Mattia Cordioli²⁶², Renato Polimanti²⁶¹, Matti Pirinen²⁶², Nadia Harerimana²⁶⁴, Kumar Veerapan²⁶³, Brooke Wolford²⁶⁵, Huy Nguyen²⁶³, Matthew Solomonson²⁶³, Rachel G. Liao²⁶³, Karolina Chwialkowska²⁶⁶, Amy Trankiem²⁶³, Mary K. Balacanis²⁶³, Caroline Hayward²⁶⁷, Anne Richmond²⁶⁷, Archie Campbell²⁶⁷, Marcela Morris²⁶⁸, Chloe Fawns-Ritchie²⁶⁷, Joseph T. Glessner^{269,270}, Douglas M. Shaw²⁷¹, Xiao Chang²⁶⁹, Hannah Polikowski²⁷¹, Lauren E. Petty²⁷¹, Hung-Hsin Chen²⁷¹, Zhu Wanying²⁷¹, Hakon Hakonarson^{269,270}, David J. Porteous²⁶⁷, Jennifer Below²⁷¹, Kari North²⁷², Joseph B. McCormick²⁶⁸, Paul R. H. J. Timmers²⁶⁷, James F. Wilson²⁶⁷, Albert Tenesa^{267,273}, Kenton D'Mellow²⁷³, Shona M. Kerr²⁶⁷, Mari E. Niemi²⁶², Lindokuhle Nkambulu^{263,274}, Kathrin Aprile von Hohenstaufen²⁷⁵, Ali Sobh²⁷⁶, Madonna M. Eltoukhy²⁷⁷, Amr M. Yassen²⁷⁸, Mohamed A. F. Hegazy²⁷⁹, Kamal Okasha²⁸⁰, Mohammed A. Eid²⁸¹, Hanteera S. Moahmed²⁸², Doaa Shahin²⁸³, Yasser M. El-Sherbiny^{283,284}, Tamer A. Elhadidi²⁸⁵, Mohamed S. Abd Elghafar²⁸⁶, Jehan J. El-Jawhari^{283,284}, Attia A. S. Mohamed²⁷⁷, Marwa H. Elnagdy²⁸⁷, Amr Samir²⁷⁹, Mahmoud Abdel-Aziz²⁸⁸, Walid T. Khafaga²⁸⁹, Walaa M. El-Lawy²⁸², Mohamed S. Torky²⁸², Mohamed R. El-shanshory²⁹⁰, Chiara Batini²⁹¹, Paul H. Lee²⁹¹, Nick Shrine²⁹¹, Alexander T. Williams²⁹¹, Martin D. Tobin^{291,292}, Anna L. Guyatt²⁹¹, Catherine John²⁹¹, Richard J. Packer²⁹¹, Altaf Ali²⁹¹, Robert C. Free²⁹³, Xueyang Wang²⁹¹, Louise V. Wain²⁹¹, Edward J. Hollox²⁹⁴, Laura D. Venn²⁹¹, Catherine E. Bee²⁹¹, Emma L. Adams²⁹¹, Ahmadreza Niavarani²⁹⁵, Bahareh Sharifard²⁹⁵, Rasoul Aliannejad²⁹⁶, Ali Amiravaddokouhi²⁹⁷, Zeinab Naderpour²⁹⁶, Hengameh Ansoori Tadi²⁹⁸, Afshar Etamad Alaeqha²⁹⁹, Saeideh Ahmadi³⁰⁰, Seyyed Behrooz Mohseni Moghaddam³⁰¹, Alireza Adamsara³⁰², Morteza Saedi³⁰³, Hamed Abdollahi³⁰⁴, Abdolmajid Hosseini³⁰⁵, Pejarek Chariyavilaskul^{306,307}, Monpat Chamnanphon^{306,306}, Thitima B. Suttichee³⁰⁶, Vorasak Shotelersuk^{308,310}, Monnat Pongpanich^{311,312}, Chureerat Phokaeaw^{309,310,313}, Wanna Chetruengchai^{309,310}, Watsamon Jantarabenjakul^{314,315}, Opass Putchareon^{314,316}, Pattama Torvorapanit^{314,316}, Thanayawee Puthanakit^{315,317}, Pintip Suchartlitikwong^{317,318}, Nattiya Hiranran^{319,320}, Voraphoj Nilaratanakul^{316,321}, Pimpayao Sodasath^{319,320}, Ben M. Brumpton^{322,323,324}, Kristian Hveem^{322,323}, Cristen Willer^{265,325,326}, Wei Zhou^{274,327}, Tormod Rogne^{328,329,330}, Erik Solligard^{328,330}, Bjorn Olav Åsvold^{322,323,324}, Malak Abedalthagafi³³¹, Manal Alaamery^{332,333}, Saleh Alqahtani^{334,335}, Duna Barakeh³³⁶, Fawz Al Harthi³³¹, Ebtehal Alsolm³³¹, Leen Abu Safieh³³¹, Albandary M. Alowayn³³¹, Fatimah Alqubaishi³³¹, Amal Al Mutairi³³¹, Serghei Mangut³³⁷, Abdurraheem Alshareef³³⁸, Mona Sawaji³³⁹, Mansour Almutairi^{332,333}, Nora Aljawini³⁴⁰, Nour Albesher³⁴⁰, Yaseen M. Arabi³⁴¹, Ebrahim S. Mahmoud³⁴¹, Amin K. Khattab³⁴², Roaa T. Halawani³⁴², Ziab Z. Alahmady³⁴², Jehad K. Albakr³⁴², Walaa A. Felemban³⁴², Bandar A. Suliman³³⁸, Rana Hasanato³³⁶, Laila Al-Awdah³⁴³, Jahad Alghamdi³⁴⁴, Deema AlZahrani³⁴⁵, Sameera AlJohani³⁴⁶, Hani Al-Afghani³⁴⁷, May Alrashed³⁴⁸, Nouf AlDhawi³⁴⁵, Hadeel AlBardisi³³¹, Sarah Alkwa³⁴⁰, Moneera Alswailm³⁴⁰, Faisal Almaliki³⁴⁵, Maha AlBeldadi³⁴⁵, Imran AlMohammed³⁴⁰, Eman Barhouq³⁴⁹, Anoud Albader³⁴⁵, Salam Massadeh^{332,333}, Abdulaziz AlMalik³⁵⁰, Sara Alotaibi³³¹, Bader Alghamdi³⁵¹, Jingyun Jun³⁵², Mohammad S. Fawzy³³¹, Yunsung Lee³⁵³, Per Magnus³⁵³, Lill-Iren S. Troststad³⁵⁴, Øyvind Helgeland³⁵⁵, Jennifer R. Harris³⁵⁵, Massimo Mangino^{356,357}, Tim D. Spector³⁵⁶, Emma Duncan³⁵⁶, Sandra P. Smieszek³⁵⁸, Bartłomiej P. Przychodzen³⁵⁸, Christos Polymeropoulos³⁵⁸, Vasilios Polymeropoulos³⁵⁸, Mihael H. Polymeropoulos³⁵⁸, Israel Fernandez-Cadenas³⁵⁹, Jordi Perez-Tur^{360,361,362}, Laia Lucía-Carol^{359,363}, Natalia Culléll^{359,364}, Elena Muñio³⁵⁹, Jara Cárcel-Márquez³⁵⁹, Marta L. DeDiego³⁶⁵, Lara Loret Iglesias³⁶⁶, Anna M. Planas^{363,367}, Alex Soriano³⁶⁸, Veronica Rico³⁶⁶, Daiana Agüero³⁶⁸, Josep L. Bedini³⁶⁸, Francisco Lozano³⁶⁸, Carlos Domingo³⁶⁸, Veronica Robles³⁶⁸, Francisca Ruiz-Jaén³⁷⁰, Leonardo Márquez³⁷¹, Juan Gomez³⁷², Eliecer Coto³⁷², Guillermo M. Albaiceta³⁷², Marta García-Clemente³⁷², David Dalmau³⁷³, María J. Arranz³⁷³, Beatriz Dietl³⁷³, Alex Serra-Llovich³⁷³, Pere Soler³⁷⁴, Roger Colobrán³⁷⁴,

Article

Andrea Martin-Nalda³⁷⁴, Alba Parra Martínez³⁷⁴, David Bernardo³⁷⁵, Silvia Rojo³⁷⁶, Aida Fiz-López³⁷⁵, Elisa Arribas³⁷⁵, Paloma de la Cal-Sabater³⁷⁵, Tomás Segura³⁷⁷, Esther González-Villa³⁷⁷, Gemma Serrano-Heras³⁷⁷, Joan Martí-Fàbregas³⁷⁸, Elena Jiménez-Xarrié³⁷⁸, Alicia de Felipe Mimbrenra³⁷⁹, Jaime Masjuan³⁷⁹, Sebastian García-Madrona³⁷⁹, Ana Domínguez-Mayoral^{380,381}, Joan Montaner Villalonga^{380,381}, Paloma Menéndez-Valladares^{380,381}, Daniel I. Chasman^{382,383}, Julie E. Buring^{382,383}, Paul M. Ridker^{382,383}, Giulianini Franco³⁸², Howard D. Sesso^{382,383}, JoAnn E. Manson^{382,383}, Joseph R. Glessner^{382,384}, Hakon Hakonarson^{269,384,385}, Carolina Medina-Gomez³⁸⁶, Andre G. Uitterlinden³⁸⁶, M. Arfan Ikram³⁸⁶, Kati Kristiansson³⁸⁷, Sami Koskelainen³⁸⁷, Markus Perola^{387,388}, Kati Donner²⁶², Katja Kivinen²⁶², Aarno Palotie²⁶², Samuli Ripatti^{262,263,389}, Sanni Ruotsalainen²⁶², Mari Kaunisto²⁶², Tomoko Nakanishi^{390,391,392,393}, Guillaume Butler-Laporte^{390,391}, Vincenzo Forgetta³⁹⁰, David R. Morrison³⁹⁰, Biswarup Ghosh³⁹⁰, Laetitia Laurent³⁹⁰, Alexandre Belisle³⁹⁰, Danielle Henry³⁹⁰, Tala Abdullah³⁹⁰, Olumide Adeleye³⁹⁰, Noor Mamlouk³⁹⁰, Nofar Kimchi³⁹⁰, Zaman Afrasiabi³⁹⁰, Nardin Rezk³⁹⁰, Branka Vulevsic³⁹⁰, Meriem Bouab³⁹⁰, Charlotte Guzman³⁹⁰, Louis Petitjean³⁹⁰, Chris Tselios³⁹⁰, Xiaoqing Xue³⁹⁰, Erwin Schurr³⁹⁰, Jonathan Afilato³⁹⁰, Marc Afilato³⁹⁰, Maureen Oliveira³⁹⁰, Bluma Brenner³⁹⁰, Pierre Lepage³⁹⁰, Jiannis Ragoussis³⁹⁰, Daniel Auld³⁹⁰, Nathalie Brassard³⁹⁰, Madeleine Durand³⁹⁰, Michaël Chasse³⁹⁰, Daniel E. Kaufmann³⁹⁰, G. Mark Lathrop³⁹⁰, Vincent Mooser³⁹⁰, J. Brent Richards³⁹⁰, Rui Li³⁹⁰, Darin Adra³⁹⁰, Souad Rahmouni³⁹⁰, Michel Georges³⁹⁴, Michel Moutschen³⁹⁵, Benoit Misse^{394,395}, Gilles Darcis^{394,395}, Julien Guiot^{394,395}, Julien Guntz³⁹⁵, Samira Azarzar^{394,395}, Stéphanie Gofflot³⁹⁶, Yves Beguin³⁹⁶, Sabine Claassen³⁹⁷, Olivier Malaise³⁹⁵, Pascale Huynen³⁹⁵, Christelle Meuris³⁹⁵, Marie Thys³⁹⁵, Jessica Jacques³⁹⁵, Philippe Léonard³⁹⁵, Frederic Frippia³⁹⁵, Jean-Baptiste Giot³⁹⁵, Anne-Sophie Sauvage³⁹⁵, Christian von Frenczell³⁹⁵, Yasmine Belhaj³⁹⁴, Bernard Lambermont³⁹⁵, Mari E. K. Niemi²⁶², Sara Pigazzini²⁶², Lindokuhle Nkambule^{263,263,274}, Michelle Daya³⁹⁸, Jonathan Shortt³⁹⁸, Nicholas Rafaels³⁹⁸, Stephen J. Wicks³⁹⁸, Kristy Crooks³⁹⁸, Kathleen C. Barnes³⁹⁸, Christopher R. Gignoux³⁹⁸, Sameer Chavan³⁹⁸, Triin Laisk³⁹⁹, Kristi Läll³⁹⁹, Maarja Lepamets³⁹⁹, Reedik Mägi³⁹⁹, Tõnu Esko³⁹⁹, Ene Reimann³⁹⁹, Lili Milani³⁹⁹, Helene Alavere³⁹⁹, Kristjan Metsalu³⁹⁹, Mairo Pusepp³⁹⁹, Andres Metspalu³⁹⁹, Paul Naaber⁴⁰⁰, Edward Laane^{401,402}, Jaana Pensukova⁴⁰¹, Pärt Peterson⁴⁰³, Kai Kisand⁴⁰³, Jekaterina Tabri⁴⁰⁴, Ralli Ailos⁴⁰⁴, Kati Hensen⁴⁰⁴, Joel Starkopf⁴⁰², Inge Ringmets⁴⁰⁵, Anu Tamm⁴⁰², Anne Kallaste⁴⁰², Pierre-Yves Bochud⁴⁰⁶, Carlo Rivolta^{407,408}, Stéphanie Bibert⁴⁰⁶, Mathieu Quinodoz^{407,408}, Dhryata Kamdar^{407,408}, Noémie Boillat⁴⁰⁶, Semira Gonseth Nussle⁴⁰⁹, Werner Albrich⁴¹⁰, Noémie Suh⁴¹¹, Dionysios Neofytos⁴¹², Véronique Erard⁴¹³, Cathy Voide⁴¹⁴, Rafael de Cid⁴¹⁵, Iván Galván-Femenia⁴¹⁵, Natalia Blay⁴¹⁵, Anna Carreras⁴¹⁵, Beatriz Cortés⁴¹⁵, Xavier Farré⁴¹⁵, Lauro Sumoy⁴¹⁵, Victor Moreno⁴¹⁶, Josep Maria Mercader⁴¹⁷, Marta Guindo-Martinez⁴¹⁸, David Torrents⁴¹⁸, Manolis Kogevinas^{419,420,421,422}, Judith Garcia-Aymerich^{419,421,422}, Gemma Castaño-Vinyà^{419,420,421,422}, Carlota Dobaño^{419,422}, Alessandra Renieri^{423,424,425}, Francesca Cari^{423,424,425}, Chiara Fallneri^{423,425}, Sergio Daga^{423,425}, Elisa Benetti⁴²⁵, Margherita Baldassarri^{423,425}, Francesca Fava^{423,424,425}, Elisa Frullanti^{423,425}, Floriana Valentino^{423,425}, Gabriella Doddato^{423,425}, Annarita Gilberti^{423,425}, Rossella Tita⁴²⁴, Sara Amritrano⁴²⁴, Mirella Bruttini^{423,424,425}, Susanna Croci^{423,425}, Iliaria Meloni^{423,425}, Maria Antonietta Mencarelli⁴²⁴, Caterina Lo Rizzo⁴²⁴, Anna Maria Pinto⁴²⁴, Giada Beligni^{423,425}, Andrea Tommasi⁴²⁶, Laura Di Sarno^{423,425}, Maria Palmieri^{423,425}, Miriam Lucia Carriero^{423,425}, Diana Alaverdian^{423,425}, Stefano Busani⁴²⁷, Raffaele Bruno^{428,429}, Marco Vecchia⁴²⁸, Mary Ann Belli⁴³⁰, Nicola Picchiotti^{431,432}, Maurizio Sanarico⁴³³, Marco Gori⁴³², Simone Furini⁴²⁵, Stefania Mantovani⁴²⁸, Serena Ludovisi⁴³⁴, Mario Umberto Mondelli^{428,429}, Francesco Castellani⁴³⁵, Eugenia Quiros-Roldan⁴³⁵, Melania Degli Antoni⁴³⁵, Isabella Zanella^{436,437}, Massimo Vaghi⁴³⁸, Stefano Rusconi^{439,440}, Matteo Siano⁴⁴⁰, Francesca Montagnani^{425,441}, Arianna Emiliozzi⁴⁴², Massimiliano Fabbiani⁴⁴¹, Barbara Rossetti⁴⁴¹, Elena Bargagli⁴⁴³, Laura Bergantini⁴⁴³, Miriana D'Alessandro⁴⁴³, Paolo Cameli⁴⁴³, David Bennett⁴⁴³, Federico Anedda⁴⁴⁴, Simona Marcantonio⁴⁴⁴, Sabino Scolletta⁴⁴⁴, Federico Franchi⁴⁴⁴, Maria Antonietta Mazzei⁴⁴⁵, Susanna Guerrini⁴⁴⁵, Edoardo Conticini⁴⁴⁶, Luca Cantarini⁴⁴⁶, Bruno Frediani⁴⁴⁶, Danilo Tacconi⁴⁴⁷, Chiara Spertilli⁴⁴⁷, Marco Feri⁴⁴⁸, Alice Donati⁴⁴⁸, Raffaele Scala⁴⁴⁹, Luca Guidelli⁴⁴⁹, Genni Spargi⁴⁵⁰, Marta Corridi⁴⁵⁰, Cesira Nencioni⁴⁵¹, Leonardo Croci⁴⁵¹, Maria Bandini⁴⁵², Gian Piero Caldarelli⁴⁵³, Paolo Piacentini⁴⁵², Elena Desanctis⁴⁵², Silvia Cappelli⁴⁵², Anna Canaccini⁴⁵⁴, Agnese Verzuri⁴⁵⁴, Valentina Anemoli⁴⁵⁴, Agostino Ognibene⁴⁵⁵, Alessandro Pancrazzi⁴⁵⁵, Maria Lorbubio⁴⁵⁵, Antonella D'Arminio Monforte⁴⁵⁶, Federica Gaia Miraglia⁴⁵⁶, Massimo Girardis⁴²⁷, Sophie Ventureau⁴²⁷, Andrea Cossarizza⁴⁵⁷, Andrea Antinori⁴⁴², Alessandra Vergori⁴⁴², Arianna Gabrieli⁴⁴⁰, Agostino Riva^{439,440}, Daniela Francisci^{426,458}, Elisabetta Schiaroli^{426,458}, Francesco Paciosi⁴⁵⁸, Pier Giorgio Scotton⁴⁵⁹, Francesca Andretta⁴⁵⁹, Sandro Panese⁴⁶⁰, Renzo Scaggiante⁴⁶¹, Francesca Gatti⁴⁶¹, Saverio Giuseppe Parisi⁴⁶², Stefano Baratti⁴⁶², Matteo Della Monica⁴⁶³, Carmelo Piscopo⁴⁶³, Mario Capasso^{464,465,466}, Roberta Russo^{464,465}, Immacolata Andolfo^{464,465}, Achille Iolascon^{464,465}, Giuseppe Fiorentino⁴⁶⁷, Massimo Carella⁴⁶⁸, Marco Castori⁴⁶⁸, Giuseppe Merla^{464,469}, Gabriella Maria Squeo⁴⁶⁹, Filippo Aucella⁴⁷⁰, Pamela Raggi⁴⁷¹, Carmen Marciano⁴⁷¹, Rita Perna⁴⁷¹, Matteo Bassetti^{472,473}, Antonio Di Biagio⁴⁷³, Maurizio Sanguinetti^{474,475}, Luca Masucci^{474,475}, Serafina Valente⁴⁷⁶, Marco Mandalà⁴⁷⁷, Alessia Giorli⁴⁷⁷, Lorenzo Salerni⁴⁷⁷, Patrizia Zucchi⁴⁷⁸, Pierpaolo Parravicini⁴⁷⁸, Elisabetta Menatti⁴⁷⁹, Tullio Trotta⁴⁸⁰, Ferdinando Giannattasio⁴⁸⁰, Gabriella Coiro⁴⁸⁰, Fabio Lena⁴⁸¹, Domenico A. Coviello⁴⁸², Cristina Mussini⁴⁸³, Enrico Martinelli⁴⁸⁴, Sandro Mancarella⁴³⁰, Luisa Tavecchia⁴³⁰, Lia Crotti^{485,486,487,487}, Chiara Gabizzi⁴⁸³, Marco Rizzi⁴⁸⁸, Franco Maggioletti⁴⁸⁸, Diego Ripamonti⁴⁸⁸, Tiziana Barchetti⁴⁸⁹, Maria Teresa La Rovere⁴⁹⁰, Simona Sarzi-Bagno⁴⁹¹, Maurizio Bussotti⁴⁹², Stefano Ceri⁴⁹³, Pietro Pinoli⁴⁹³, Francesco Raimondi⁴⁹⁴, Filippo Biscarini⁴⁹⁵, Alessandra Stella⁴⁹⁵, Kristina Zguro⁴⁹⁵, Katia Capitanì^{425,496}, Claudia Suardi⁴⁹⁷, Simona Dei⁴⁹⁸, Gianfranco Parati^{485,488}, Sabrina Ravaglia⁴⁹⁹, Rosangela Artuso⁵⁰⁰, Giordano Bottà⁵⁰¹, Paolo Di Domenico⁵⁰¹, Iliaria Rancan⁴⁴¹, Antonio Perrella⁵⁰², Francesco Bianchi^{426,502}, Davide Romani⁴⁵², Paola Bergomi⁵⁰³, Emanuele Catena⁵⁰³, Riccardo Colombo⁵⁰³, Marco Tanfonì⁴³², Antonella Vincenti⁵⁰⁴, Claudio Ferri⁵⁰⁵, Davide Grassi⁵⁰⁵, Gloria Pessina⁵⁰⁶, Mario Tumbarello^{425,507}, Massimo Di Pietro⁵⁰⁸, Ravaglia Sabrina⁴⁹⁹, Sauro Luchi⁵⁰⁹, Chiara Barbieri⁵¹⁰, Donatella Acquilini⁵¹¹, Elena Andreucci⁵⁰⁰, Francesco Vladimiro Segala⁵¹², Giusy Tiseo⁵¹⁰, Marco Falcone⁵¹⁰, Mirjam Lista^{423,425}, Monica Poscente⁵⁰⁶, Oreste De Vivo⁴⁷⁶,

Paola Petrocelli⁵⁰⁹, Alessandra Guarnaccia⁴⁷⁴, Silvia Baroni⁵¹³, Albert V. Smith²⁶⁵, Andrew P. Boughton²⁶⁵, Kevin W. Li²⁶⁵, Jonathon LeFaive²⁶⁵, Aubrey Annis²⁶⁵, Anne E. Justice⁵¹⁴, Tooraj Mirshahi⁵¹⁵, Geetha Chittoor⁵¹⁴, Navya Shilpa Josyula⁵¹⁴, Jack A. Kosmick⁵¹⁶, Manuel A. R. Ferreira⁵¹⁶, Joseph B. Leader⁵¹⁷, Dave J. Carey⁵¹⁵, Matthew C. Gass⁵¹⁷, Julie E. Horowitz⁵¹⁶, Michael N. Cantor⁵¹⁷, Ashish Yadav⁵¹⁶, Aris Baras⁵¹⁶, Goncalo R. Abecasis⁵¹⁶, David A. van Heel⁵¹⁸, Karen A. Hunt⁵¹⁸, Dan Mason⁵¹⁹, Qin Qin Huang⁵²⁰, Sarah Finer⁵¹⁸, Bhavi Trivedi⁵¹⁸, Christopher J. Griffiths⁵¹⁸, Hilary C. Martin⁵²⁰, John Wright⁵¹⁹, Richard C. Trembath⁵²¹, Nicole Soranzo^{522,523,524}, Jing Hua Zhao⁵²⁵, Adam S. Butterworth^{523,525,526,527}, John Danesh^{522,523,525,526,527}, Emanuele Di Angelantonio^{523,525,526,527}, Lude Franke⁵²⁸, Marike Boezen⁵²⁸, Patrick Deelen⁵²⁹, Annique Claringbould⁵²⁸, Esteban Lopera⁵²⁸, Robert Warmerdam⁵²⁸, Judith M. Vonk⁵³⁰, Irene van Blokland⁵²⁸, Pauline Lanting⁵³¹, Anil P. S. Ori^{528,532}, Sebastian Zollner²⁶⁵, Jiongming Wang²⁶⁵, Andrew Beck²⁶⁵, Gina Peloso^{533,534}, Yuk-Lam Ho⁵³⁵, Yan V. Sun⁵³⁶, Jennifer E. Huffman⁵³⁴, Christopher J. O'Donnell⁵³⁴, Kelly Cho⁵³⁵, Phil Tsao⁵³⁷, J. Michael Gaziano⁵³⁵, Michel Nivard⁵³⁵, Eco de Geus⁵³⁶, Meike Bartels⁵³⁸, Jouke Jan Hotteenga⁵³⁸, Scott T. Weiss³⁸², Elizabeth W. Karlson³⁸², Jordan W. Smoller⁴¹⁷, Robert C. Green⁵³⁹, Yen-Chen Anne Feng⁴¹⁷, Josep Mercader⁵³⁹, Shawn N. Murphy⁴¹⁷, James B. Meigs⁴¹⁷, Ann E. Woolley³⁸², Emma F. Perez⁴¹⁷, Daniel Rader⁵⁴⁰, Anurag Verma⁵⁴⁰, Marylyn D. Ritchie⁵⁴⁰, Binglan Li⁵³⁷, Shefali S. Verma⁵⁴⁰, Anastasia Lucas⁵⁴⁰, Yuki Bradford⁵⁴⁰, Hugo Zeberg^{541,542}, Robert Frithiof⁵⁴³, Michael Hultström⁵⁴³, Miklos Lipsey^{543,543}, Lindo Nkambul^{263,274,545}, Nicolas Tardif⁵⁴⁶, Olav Rooyackers⁵⁴⁶, Jonathan Grip⁵⁴⁶, Tomislav Maricic⁵⁴², Konrad J. Karczewski^{263,417}, Elizabeth G. Atkinson^{263,417}, Kristin Tsuo^{263,417}, Nikolas Baya^{263,417}, Patrick Turley^{263,417}, Rahul Gupta^{263,417}, Shawnequa Callier⁵⁴⁷, Raymond K. Walters^{263,417}, Duncan S. Palmer^{263,417}, Gopal Sarma^{263,417}, Nathan Cheng^{263,417}, Wenhan Lu^{263,417}, Sam Bryant^{263,417}, Claire Churchhouse^{263,417}, Caroline Cusick²⁶³, Jacqueline I. Goldstein^{263,417}, Daniel King^{263,417}, Cotton Seed^{263,417}, Hilary Finucane^{263,417}, Alicia R. Martin^{263,417}, F. Kyle Satterstrom^{263,417}, Daniel J. Wilson⁵⁴⁸, Jacob Armstrong⁵⁴⁸, Justine K. Rudkin⁵⁴⁸, Gavin Band⁵⁴⁹, Sarah G. Earle⁵⁴⁸, Shang-Kuan Lin⁵⁴⁸, Nicolas Arning⁵⁴⁸, Derrick W. Crook⁵⁵⁰, David H. Wyllie⁵⁵¹, Anne Marie O'Connell⁵⁵¹, Chris C. A. Spencer⁵⁵¹, Nils Koelling⁵⁵³, Mark J. Caulfield⁵⁵⁴, Richard H. Scott⁵⁵⁴, Tom Fowler⁵⁵⁴, Loukas Moutsianas⁵⁵⁴, Athanasios Kousathanas⁵⁵⁴, Dorota Pasko⁵⁵⁴, Susan Walker⁵⁵⁴, Augusto Rendon⁵⁵⁴, Alex Stuckey⁵⁵⁴, Christopher A. Odoms⁵⁵⁴, Daniel Rhodes⁵⁵⁴, Georgia Chan⁵⁵⁴, Prabhur Arumugam⁵⁵⁴, Catherine A. Ball⁵⁵⁵, Eurie L. Hong⁵⁵⁵, Kristin Rand⁵⁵⁵, Ahna Girshick⁵⁵⁵, Harendra Guturu⁵⁵⁵, Asher Haug Baltzell⁵⁵⁵, Genevieve Roberts⁵⁵⁵, Danny Park⁵⁵⁵, Marie Coignet⁵⁵⁵, Shannon McCurdy⁵⁵⁵, Spencer Knight⁵⁵⁵, Raghavendran Partha⁵⁵⁵, Brooke Rhead⁵⁵⁵, Miao Zhang⁵⁵⁵, Nathan Berkowitz⁵⁵⁵, Michael Gaddis⁵⁵⁵, Keith Noto⁵⁵⁵, Luong Ruiz⁵⁵⁵, Milos Pavlovic⁵⁵⁵, Laura G. Sloopman²⁶⁴, Alexander W. Charney²⁶⁴, Noam D. Beckmann²⁶⁴, Eric E. Schadt²⁶⁴, Daniel M. Jordan²⁶⁴, Ryan C. Thompson²⁶⁴, Kyle Gettler²⁶⁴, Noura S. Abul-Husn²⁶⁴, Steven Asanovic²⁶⁴, Joseph D. Buxbaum²⁶⁴, Kumardeep Chaudhary²⁶⁴, Judy H. Cho²⁶⁴, Yuval Itan²⁶⁴, Eimear E. Kenny²⁶⁴, Gillian M. Belbin²⁶⁴, Stuart C. Sealfon²⁶⁴, Robert P. Sebra²⁶⁴, Irene Salibi²⁶⁴, Brett L. Collins²⁶⁴, Tess Levy²⁶⁴, Bari Britvan²⁶⁴, Katherine Keller²⁶⁴, Lara Tang²⁶⁴, Michael Peruggia²⁶⁴, Liam L. Hieste²⁶⁴, Kristi Niblo²⁶⁴, Alexandra Aksentijevich²⁶⁴, Alexander Labkowsky²⁶⁴, Avromie Karp²⁶⁴, Menachem Zlatopolsky²⁶⁴, Michael Preuss²⁶⁴, Ruth J. F. Loos²⁶⁴, Girish N. Nadkarni²⁶⁴, Ron Do²⁶⁴, Clive Hoggart²⁶⁴, Sam Choi²⁶⁴, Slayton J. Underwood²⁶⁴, Paul O'Reill²⁶⁴, Laura M. Huckins²⁶⁴, Marissa Zyndorf²⁶⁴, Raff J. Daly^{262,263}, Benjamin M. Neale²⁶³ & Andrea Ganna^{262,263}

²⁶¹Yale University, New Haven, CT, USA. ²⁶²Institute for Molecular Medicine Finland (FIMM), University of Helsinki, Helsinki, Finland. ²⁶³Broad Institute of MIT and Harvard, Cambridge, MA, USA. ²⁶⁴Icahn School of Medicine at Mount Sinai, New York, NY, USA. ²⁶⁵University of Michigan, Ann Arbor, MI, USA. ²⁶⁶Centre for Bioinformatics and Data Analysis, Medical University of Białystok, Białystok, Poland. ²⁶⁷Institute of Genetics and Cancer, University of Edinburgh, Western General Hospital, Edinburgh, UK. ²⁶⁸University of Texas Health, Houston, TX, USA. ²⁶⁹Center for Applied Genomics, Children's Hospital of Philadelphia, Philadelphia, PA, USA. ²⁷⁰Department of Pediatrics, Perelman School of Medicine, University of Pennsylvania, Philadelphia, PA, USA. ²⁷¹Vanderbilt University Medical Center, Nashville, TN, USA. ²⁷²University of North Carolina at Chapel Hill, Chapel Hill, NC, USA. ²⁷³Roslin Institute, The Royal (Dick) School of Veterinary Studies, University of Edinburgh, Edinburgh, UK. ²⁷⁴Analytic and Translational Genetics Unit, Massachusetts General Hospital, Boston, MA, USA. ²⁷⁵Genolier Innovation Network and Hub, Swiss Medical Network, Genolier Healthcare Campus, Genolier, Switzerland. ²⁷⁶Department of Pediatrics, Faculty of Medicine, Mansoura University, Mansoura, Egypt. ²⁷⁷Department of Clinical Pathology, Faculty of Medicine, Tanta University, Tanta, Egypt. ²⁷⁸Department of Anaesthesia and Critical Care, Faculty of Medicine, Mansoura University, Mansoura, Egypt. ²⁷⁹Department of Surgery, Faculty of Medicine, Mansoura University, Mansoura, Egypt. ²⁸⁰Department of Internal Medicine, Faculty of Medicine, Tanta University, Tanta, Egypt. ²⁸¹Faculty of Science, Tanta University, Tanta, Egypt. ²⁸²Chest Department, Faculty of Medicine, Tanta University, Tanta, Egypt. ²⁸³Department of Clinical Pathology, Faculty of Medicine, Mansoura University, Mansoura, Egypt. ²⁸⁴Department of Biosciences, School of Science and Technology, Nottingham Trent University, Nottingham, UK. ²⁸⁵Chest Department, Faculty of Medicine, Mansoura University, Mansoura, Egypt. ²⁸⁶Anesthesia, Surgical Intensive Care and Pain Management Department, Faculty of Medicine, Tanta University, Tanta, Egypt. ²⁸⁷Department of Medical Biochemistry, Faculty of Medicine, Mansoura University, Mansoura, Egypt. ²⁸⁸Department of Tropical Medicine, Faculty of Medicine, Mansoura University, Mansoura, Egypt. ²⁸⁹Pediatric and Neonatology, Kafr El-Zayat General Hospital, Kafr El-Zayat, Egypt. ²⁹⁰Pediatrics Department, Faculty of Medicine, Tanta University, Tanta, Egypt. ²⁹¹Department of Health Sciences, University of Leicester, Leicester, UK. ²⁹²Leicester NIHR Biomedical Research Centre, Leicester, UK. ²⁹³Department of Respiratory Sciences, University of Leicester, Leicester, UK. ²⁹⁴University of Leicester, Leicester, UK. ²⁹⁵Digestive Oncology Research Center, Digestive Disease Research Institute, Shariati Hospital, Tehran University of Medical Sciences, Tehran, Iran. ²⁹⁶Department of Pulmonology, School of Medicine, Shariati Hospital, Tehran University of Medical Sciences, Tehran, Iran. ²⁹⁷Department of Critical Care Medicine, Noorafshar Hospital, Tehran, Iran. ²⁹⁸Department of Emergency Intensive Care Unit, School of Medicine, Shariati Hospital, Tehran University of Medical Sciences, Tehran, Iran. ²⁹⁹Department of Anesthesiology,

School of Medicine, Amir Alam Hospital, Tehran University of Medical Sciences, Tehran, Iran. ³⁰⁰Department of Pulmonology, School of Medicine, Tehran University of Medical Sciences, Tehran, Iran. ³⁰¹Department of Pathology, Parseh Pathobiology and Genetics Laboratory, Tehran, Iran. ³⁰²Department of Microbiology, Health and Family Research Center, NIOC Hospital, Tehran, Iran. ³⁰³Department of Emergency Medicine, School of Medicine, Shariati Hospital, Tehran University of Medical Sciences, Tehran, Iran. ³⁰⁴Department of Anesthesiology, School of Medicine, Tehran University of Medical Sciences, Tehran, Iran. ³⁰⁵Department of Pathology, Faculty of Medicine, Tehran Azad University, Tehran, Iran. ³⁰⁶Clinical Pharmacokinetics and Pharmacogenomics Research Unit, Faculty of Medicine, Chulalongkorn University, Bangkok, Thailand. ³⁰⁷Department of Pharmacology, Faculty of Medicine, Chulalongkorn University, Bangkok, Thailand. ³⁰⁸Department of Pathology, Faculty of Medicine, Nakornnayok, Srinakharinwirot University, Bangkok, Thailand. ³⁰⁹Center of Excellence for Medical Genomics, Medical Genomics Cluster, Faculty of Medicine, Chulalongkorn University, Bangkok, Thailand. ³¹⁰Excellence Center for Genomics and Precision Medicine, King Chulalongkorn Memorial Hospital, The Thai Red Cross Society, Bangkok, Thailand. ³¹¹Department of Mathematics and Computer Science, Faculty of Science, Chulalongkorn University, Bangkok, Thailand. ³¹²Omic Sciences and Bioinformatics Center, Faculty of Science, Chulalongkorn University, Bangkok, Thailand. ³¹³Research Affairs, Faculty of Medicine, Chulalongkorn University, Bangkok, Thailand. ³¹⁴Thai Red Cross Emerging Infectious Diseases Clinical Centre, King Chulalongkorn Memorial Hospital, Bangkok, Thailand. ³¹⁵Department of Pediatrics, Faculty of Medicine, Chulalongkorn University, Bangkok, Thailand. ³¹⁶Division of Infectious Diseases, Department of Medicine, Faculty of Medicine, Chulalongkorn University, Bangkok, Thailand. ³¹⁷Center of Excellence in Pediatric Infectious Diseases and Vaccines, Chulalongkorn University, Bangkok, Thailand. ³¹⁸Department of Microbiology, Faculty of Medicine, Chulalongkorn University, Bangkok, Thailand. ³¹⁹Immunology Division, Department of Microbiology, Faculty of Medicine, Chulalongkorn University, Bangkok, Thailand. ³²⁰Center of Excellence in Immunology and Immune-mediated Diseases, Department of Microbiology, Faculty of Medicine, Chulalongkorn University, Bangkok, Thailand. ³²¹Healthcare-associated Infection Research Group STAR (Special Task Force for Activating Research), Chulalongkorn University, Bangkok, Thailand. ³²²K.G. Jebesen Center for Genetic Epidemiology, Department of Public Health and Nursing, Norwegian University of Science and Technology (NTNU), Trondheim, Norway. ³²³HUNT Research Center, Department of Public Health and Nursing, Norwegian University of Science and Technology (NTNU), Levanger, Norway. ³²⁴Clinic of Medicine, St Olav's Hospital, Trondheim University Hospital, Trondheim, Norway. ³²⁵Division of Cardiovascular Medicine, Department of Internal Medicine, University of Michigan, Ann Arbor, MI, USA. ³²⁶Department of Computational Medicine and Bioinformatics, University of Michigan, Ann Arbor, MI, USA. ³²⁷Program in Medical and Population Genetics, Broad Institute of Harvard and MIT, Cambridge, MA, USA. ³²⁸Gemini Center for Sepsis Research, Department of Circulation and Medical Imaging, Norwegian University of Science and Technology (NTNU), Trondheim, Norway. ³²⁹Department of Chronic Disease Epidemiology and Center for Perinatal, Pediatric and Environmental Epidemiology, Yale School of Public Health, New Haven, CT, USA. ³³⁰Clinic of Anaesthesia and Intensive Care, St Olav's Hospital, Trondheim University Hospital, Trondheim, Norway. ³³¹Genomics Research Department, Saudi Human Genome Project, King Fahad Medical City and King Abdulaziz City for Science and Technology (KACST), Riyadh, Saudi Arabia. ³³²Developmental Medicine Department, King Abdullah International Medical Research Center, King Saud Bin Abdulaziz University for Health Sciences, Ministry of National Guard Health Affairs, Riyadh, Saudi Arabia. ³³³Saudi Human Genome Project (SHGP), King Abdulaziz City for Science and Technology (KACST), Satellite Lab at King Abdulaziz Medical City, Ministry of National Guard Health Affairs, Riyadh, Saudi Arabia. ³³⁴The Liver Transplant Unit, King Faisal Specialist Hospital and Research Centre, Riyadh, Saudi Arabia. ³³⁵The Division of Gastroenterology and Hepatology, Johns Hopkins University, Baltimore, MD, USA. ³³⁶Department of Pathology, College of Medicine, King Saud University, Riyadh, Saudi Arabia. ³³⁷Titus Family Department of Clinical Pharmacy, USC School of Pharmacy, University of Southern California, Los Angeles, CA, USA. ³³⁸College of Applied Medical Sciences, Taibah University, Madina, Saudi Arabia. ³³⁹Developmental Medicine Department, King Abdullah International Medical Research Center, King Saud Bin Abdulaziz University for Health Sciences, Ministry of National Guard Health Affairs, Riyadh, Saudi Arabia. ³⁴⁰KACST-BWH Centre of Excellence for Biomedicine, Joint Centers of Excellence Program, King Abdulaziz City for Science and Technology (KACST), Riyadh, Saudi Arabia. ³⁴¹Ministry of the National Guard Health Affairs, King Abdullah International Medical Research Center and King Saud Bin Abdulaziz University for Health Sciences, Riyadh, Saudi Arabia. ³⁴²Ohud Hospital, Ministry of Health, Madinah, Saudi Arabia. ³⁴³Pediatric Infectious Diseases, Children's Specialized Hospital, King Fahad Medical City, Riyadh, Saudi Arabia. ³⁴⁴The Saudi Biobank, King Abdullah International Medical Research Center, King Saud Bin Abdulaziz University for Health Sciences, Ministry of National Guard Health Affairs, Riyadh, Saudi Arabia. ³⁴⁵Developmental Medicine Department, King Abdullah International Medical Research Center and King Saud Bin Abdulaziz University for Health Sciences, King Abdulaziz Medical City, Ministry of National Guard Health Affairs, Riyadh, Saudi Arabia. ³⁴⁶Department of Pathology and Laboratory Medicine, King Abdulaziz Medical City, Ministry of National Guard Health Affairs, King Saud Bin Abdulaziz University for Health Sciences and King Abdullah International Medical Research Center, Riyadh, Saudi Arabia. ³⁴⁷Laboratory Department, Security Forces Hospital, General Directorate of Medical Services, Ministry of Interior, Riyadh, Saudi Arabia. ³⁴⁸Department of Clinical Laboratory Sciences, College of Applied Medical Sciences, King Saud University, Riyadh, Saudi Arabia. ³⁴⁹King Abdulaziz City for Science and Technology (KACST), Riyadh, Saudi Arabia. ³⁵⁰Life Science and Environmental Institute, King Abdulaziz City for Science and Technology (KACST), Riyadh, Saudi Arabia. ³⁵¹Department of Developmental Medicine, King Abdullah International Medical Research Center, King Saud Bin Abdulaziz University for Health Sciences, King Abdulaziz Medical City, Ministry of National Guard Health Affairs, Riyadh, Saudi Arabia. ³⁵²Titus Family Department of Clinical Pharmacy, USC School of Pharmacy University of Southern California, Los Angeles, CA, USA. ³⁵³Centre for Fertility and Health, Norwegian Institute of Public Health, Oslo, Norway. ³⁵⁴Department of Method Development and Analytics, Norwegian Institute of Public Health, Oslo, Norway. ³⁵⁵Department of Genetics and Bioinformatics, Norwegian Institute of Public Health, Oslo, Norway. ³⁵⁶Department of Twin Research and Genetic Epidemiology, King's College London, London, UK. ³⁵⁷NIHR Biomedical Research Centre at Guy's and St Thomas' Foundation Trust, London, UK. ³⁵⁸Vanda Pharmaceuticals, London, UK. ³⁵⁹Stroke Pharmacogenomics and Genetics, Biomedical Research Institute Sant Pau, Sant Pau Hospital, Barcelona, Spain. ³⁶⁰Institute of Biomedicine of Valencia (IBV), National Spanish Research Council (CSIC), València, Spain. ³⁶¹Network Center for Biomedical Research on Neurodegenerative Diseases (CIBERNED), València, Spain. ³⁶²Neurology and Genetic Mixed Unit, La Fe Health Research Institute, València, Spain. ³⁶³Institute for Biomedical Research of Barcelona (IIBB), National Spanish Research Council (CSIC), Barcelona, Spain. ³⁶⁴Department of Neurology, Hospital Universitari MútuaTerrassa, Fundació Docència i Recerca MútuaTerrassa, Terrassa, Spain. ³⁶⁵Department of Molecular and Cell Biology, Centro Nacional de Biotecnología (CNB-CSIC), Campus Universidad Autónoma de Madrid, Madrid, Spain. ³⁶⁶Instituto de Física de Cantabria (IFCA-CSIC), Santander, Spain. ³⁶⁷Institut d'Investigacions Biomèdiques August Pi i Sunyer (IDIBAPS), Barcelona, Spain. ³⁶⁸Hospital Clínic, Barcelona, Spain. ³⁶⁹Hospital Clínic, IDIBAPS, School of Medicine, University of Barcelona, Barcelona, Spain. ³⁷⁰IDIBAPS, Barcelona, Spain. ³⁷¹IIBB-CSIC, Barcelona, Spain. ³⁷²Servicio de Salud del Principado de Asturias, Oviedo, Spain. ³⁷³Hospital Mutua de Terrassa, Terrassa, Spain. ³⁷⁴Hospital Valle Hebrón, Barcelona, Spain. ³⁷⁵Instituto de Biomedicina y Genética Molecular (IBGM), CSIC-Universidad de Valladolid, Valladolid, Spain. ³⁷⁶Hospital Clínico Universitario de Valladolid (SACYL), Valladolid, Spain. ³⁷⁷University Hospital of Albacete, Albacete, Spain. ³⁷⁸Department of Neurology, Biomedical Research Institute Sant Pau (IB Sant Pau), Hospital de la Santa Creu i Sant Pau, Barcelona, Spain. ³⁷⁹Hospital Universitario Ramon y Cajal, IRYCIS, Madrid, Spain. ³⁸⁰Institute of Biomedicine of Seville (IBiS), Hospital Universitario Virgen del Rocío, CSIC and University of Seville, Seville, Spain. ³⁸¹Department of Neurology, Hospital Universitario Virgen Macarena, Seville, Spain. ³⁸²Brigham and Women's Hospital, Boston, MA, USA. ³⁸³Harvard Medical School, Boston, MA, USA. ³⁸⁴Division of Human Genetics, Department of Pediatrics, The Perelman School of Medicine, University of Pennsylvania, Philadelphia, PA, USA. ³⁸⁵Faculty of Medicine, University of Iceland, Reykjavik, Iceland. ³⁸⁶Erasmus MC, Rotterdam, The Netherlands. ³⁸⁷Finnish Institute for Health and Welfare (THL), Helsinki, Finland. ³⁸⁸University of Helsinki, Faculty of Medicine, Clinical and Molecular Metabolism Research Program, Helsinki, Finland. ³⁸⁹Public Health, Faculty of Medicine, University of Helsinki, Helsinki, Finland. ³⁹⁰Department of Human Genetics, McGill University, Montréal, Québec, Canada. ³⁹¹Lady Davis Institute, Jewish General Hospital, McGill University, Montréal, Québec, Canada. ³⁹²Kyoto-McGill International Collaborative School in Genomic Medicine, Graduate School of Medicine, Kyoto University, Kyoto, Japan. ³⁹³Research Fellow, Japan Society for the Promotion of Science, Kyoto, Japan. ³⁹⁴University of Liege, Liege, Belgium. ³⁹⁵CHU of Liege, Liege, Belgium. ³⁹⁶SBHUL (Liege Biobank), CHU of Liege, Liege, Belgium. ³⁹⁷CHC Mont-Légia, Liege, Belgium. ³⁹⁸University of Colorado Anschutz Medical Campus, Aurora, CO, USA. ³⁹⁹Estonian Genome Centre, Institute of Genomics, University of Tartu, Tartu, Estonia. ⁴⁰⁰University of Tartu, Tartu, Estonia. ⁴⁰¹Kuressaare Hospital, Kuressaare, Estonia. ⁴⁰²Tartu University Hospital, Tartu, Estonia. ⁴⁰³Institute of Biomedicine and Translational Medicine, University of Tartu, Tartu, Estonia. ⁴⁰⁴West Tallinn Central Hospital, Tallinn, Estonia. ⁴⁰⁵Estonian Health Insurance Fund, Tallinn, Estonia. ⁴⁰⁶Infectious Diseases Service, Department of Medicine, University Hospital and University of Lausanne, Lausanne, Switzerland. ⁴⁰⁷Institute of Molecular and Clinical Ophthalmology Basel (IOB), Basel, Switzerland. ⁴⁰⁸Department of Ophthalmology, University of Basel, Basel, Switzerland. ⁴⁰⁹Centre for Primary Care and Public Health, University of Lausanne, Lausanne, Switzerland. ⁴¹⁰Division of Infectious Diseases and Hospital Epidemiology, Cantonal Hospital St Gallen, St Gallen, Switzerland. ⁴¹¹Division of Intensive Care, Geneva University Hospitals and the University of Geneva Faculty of Medicine, Geneva, Switzerland. ⁴¹²Infectious Disease Service, Department of Internal Medicine, Geneva University Hospital, Geneva, Switzerland. ⁴¹³Clinique de Médecine et Spécialités, Infectiologie, HFR-Fribourg, Fribourg, Switzerland. ⁴¹⁴Infectious Diseases Division, University Hospital Centre of the canton of Vaud, Hospital of Valais, Sion, Switzerland. ⁴¹⁵GCAT-Genomes for Life, Germans Trias i Pujol Health Sciences Research Institute (IGTP), Badalona, Spain. ⁴¹⁶Catalan Institute of Oncology, Bellvitge Biomedical Research Institute, Consortium for Biomedical Research in Epidemiology and Public Health and University of Barcelona, Barcelona, Spain. ⁴¹⁷Massachusetts General Hospital, Boston, MA, USA. ⁴¹⁸Life and Medical Sciences, Barcelona Supercomputing Center-Centro Nacional de Supercomputación (BSC-CNS), Barcelona, Spain. ⁴¹⁹SGlobal, Barcelona, Spain. ⁴²⁰IMIM (Hospital del Mar Medical Research Institute), Barcelona, Spain. ⁴²¹Universitat Pompeu Fabra (UPF), Barcelona, Spain. ⁴²²CIBER Epidemiología y Salud Pública (CIBERESP), Madrid, Spain. ⁴²³Medical Genetics, University of Siena, Siena, Italy. ⁴²⁴Genetica Medica, Azienda Ospedaliero-Universitaria Senese, Siena, Italy. ⁴²⁵Med Biotech Hub and Competence Center, Department of Medical Biotechnologies, University of Siena, Siena, Italy. ⁴²⁶Infectious Diseases Clinic, Department of Medicine 2, Azienda Ospedaliera di Perugia and University of Perugia, Santa Maria Hospital, Perugia, Italy. ⁴²⁷Department of Anesthesia and Intensive Care, University of Modena and Reggio Emilia, Modena, Italy. ⁴²⁸Division of Infectious Diseases and Immunology, Fondazione IRCCS Policlinico San Matteo, Pavia, Italy. ⁴²⁹Department of Internal Medicine and Therapeutics, University of Pavia, Pavia, Italy. ⁴³⁰U.O.C. Medicina, ASST Nord Milano, Ospedale Bassini, Milan, Italy. ⁴³¹Department of Mathematics, University of Pavia, Pavia, Italy. ⁴³²University of Siena, DIISM-SAILAB, Siena, Italy. ⁴³³Independent researcher, Milan, Italy. ⁴³⁴Fondazione IRCCS Ca' Granda Ospedale Maggiore Policlinico, Milan, Italy. ⁴³⁵Department of Infectious and Tropical Diseases, University of Brescia and ASST Spedali Civili Hospital, Brescia, Italy. ⁴³⁶Department of Molecular and Translational Medicine, University of Brescia, Brescia, Italy. ⁴³⁷Clinical Chemistry Laboratory, Cytogenetics and Molecular Genetics Section, Diagnostic Department, ASST Spedali Civili di Brescia, Brescia, Italy. ⁴³⁸Chirurgia Vascolare, Ospedale Maggiore di Crema, Crema, Italy. ⁴³⁹III Infectious Diseases Unit, ASST-FFB-Sacco, Milan, Italy. ⁴⁴⁰Department of Biomedical and Clinical Sciences Luigi Sacco, University of Milan, Milan, Italy. ⁴⁴¹Department of Specialized and Internal Medicine, Tropical and Infectious Diseases Unit, Azienda Ospedaliera Universitaria Senese, Siena, Italy. ⁴⁴²HIV/AIDS Department, National Institute for Infectious Diseases Lazzaro Spallanzani, IRCCS, Rome, Italy. ⁴⁴³Unit of Respiratory Diseases and Lung Transplantation, Department of Internal and Specialist Medicine, University of Siena, Siena, Italy. ⁴⁴⁴Unit of Intensive Care Medicine, Departments of Emergency and Urgency, Medicine, Surgery and Neurosciences, Siena University Hospital, Siena, Italy. ⁴⁴⁵Unit of Diagnostic Imaging, Departments of Medical, Surgical and Neurosciences and Radiological Sciences, University of Siena, Siena, Italy. ⁴⁴⁶Rheumatology Unit, Department of Medicine, Surgery and Neurosciences, University of Siena, Policlinico Le Scotte, Siena, Italy. ⁴⁴⁷Infectious Diseases Unit, Department of Specialized and Internal Medicine, San Donato Hospital Arezzo, Arezzo, Italy. ⁴⁴⁸Anesthesia Unit, Department of Emergency, San Donato Hospital, Arezzo, Italy. ⁴⁴⁹Pneumology Unit and UTIP, Department of

Specialized and Internal Medicine, San Donato Hospital, Arezzo, Italy. ⁴⁵⁰Anesthesia Unit, Department of Emergency, Misericordia Hospital, Grosseto, Italy. ⁴⁵¹Infectious Diseases Unit, Department of Specialized and Internal Medicine, Misericordia Hospital, Grosseto, Italy. ⁴⁵²Department of Preventive Medicine, Azienda USL Toscana Sud Est, Tuscany, Italy. ⁴⁵³Clinical Chemical Analysis Laboratory, Misericordia Hospital, Grosseto, Italy. ⁴⁵⁴Territorial Scientific Technician Department, Azienda USL Toscana Sud Est, Arezzo, Italy. ⁴⁵⁵Clinical Chemical Analysis Laboratory, San Donato Hospital, Arezzo, Italy. ⁴⁵⁶Department of Health Sciences, Clinic of Infectious Diseases, ASST Santi Paolo e Carlo, University of Milan, Milan, Italy. ⁴⁵⁷Department of Medical and Surgical Sciences for Children and Adults, University of Modena and Reggio Emilia, Modena, Italy. ⁴⁵⁸Infectious Diseases Clinic, Santa Maria Hospital, University of Perugia, Perugia, Italy. ⁴⁵⁹Department of Infectious Diseases, Treviso Hospital, Treviso, Italy. ⁴⁶⁰Clinical Infectious Diseases, Mestre Hospital, Venezia, Italy. ⁴⁶¹Infectious Diseases Clinic, Belluno, Italy. ⁴⁶²Department of Molecular Medicine, University of Padova, Padua, Italy. ⁴⁶³Medical Genetics and Laboratory of Medical Genetics Unit, A.O.R.N. Antonio Cardarelli Hospital, Naples, Italy. ⁴⁶⁴Department of Molecular Medicine and Medical Biotechnology, University of Naples Federico II, Naples, Italy. ⁴⁶⁵CEINGE Biotechnology Avanzate, Naples, Italy. ⁴⁶⁶IRCCS SDN, Naples, Italy. ⁴⁶⁷Unit of Respiratory Physiopathology, AORN dei Colli, Monaldi Hospital, Naples, Italy. ⁴⁶⁸Division of Medical Genetics, Fondazione IRCCS Casa Sollievo della Sofferenza Hospital, San Giovanni Rotondo, Italy. ⁴⁶⁹Laboratory of Regulatory and Functional Genomics, Fondazione IRCCS Casa Sollievo della Sofferenza Hospital, San Giovanni Rotondo, Italy. ⁴⁷⁰Department of Medical Sciences, Fondazione IRCCS Casa Sollievo della Sofferenza Hospital, San Giovanni Rotondo, Italy. ⁴⁷¹Clinical Trial Office, Fondazione IRCCS Casa Sollievo della Sofferenza Hospital, San Giovanni Rotondo, Italy. ⁴⁷²Department of Health Sciences, University of Genova, Genova, Italy. ⁴⁷³Infectious Diseases Clinic, Policlinico San Martino Hospital, IRCCS for Cancer Research, Genova, Italy. ⁴⁷⁴Microbiology, Fondazione Policlinico Universitario Agostino Gemelli IRCCS, Catholic University of Medicine, Rome, Italy. ⁴⁷⁵Department of Laboratory Sciences and Infectious Diseases, Fondazione Policlinico Universitario A. Gemelli IRCCS, Rome, Italy. ⁴⁷⁶Department of Cardiovascular Diseases, University of Siena, Siena, Italy. ⁴⁷⁷Otolaryngology Unit, University of Siena, Siena, Italy. ⁴⁷⁸Department of Internal Medicine, ASST Valtellina e Alto Lario, Sondrio, Italy. ⁴⁷⁹Oncologia Medica e Ufficio Flussi Sondrio, Sondrio, Italy. ⁴⁸⁰First Aid Department, Luigi Curto Hospital, Polla, Salerno, Italy. ⁴⁸¹Local Health Unit, Pharmaceutical Department of Grosseto, Toscana Sud Est Local Health Unit, Grosseto, Italy. ⁴⁸²U.O.C. Laboratorio di Genetica Umana, IRCCS Istituto Giannina Gaslini, Genoa, Italy. ⁴⁸³Infectious Diseases Clinics, University of Modena and Reggio Emilia, Modena, Italy. ⁴⁸⁴Department of Respiratory Diseases, Azienda Ospedaliera di Cremona, Cremona, Italy. ⁴⁸⁵Department of Cardiovascular, Neural and Metabolic Sciences, Istituto Auxologico Italiano, IRCCS, San Luca Hospital, Milan, Italy. ⁴⁸⁶Department of Medicine and Surgery, University of Milano-Bicocca, Milan, Italy. ⁴⁸⁷Laboratory of Cardiovascular Genetics, Istituto Auxologico Italiano, IRCCS, Milan, Italy. ⁴⁸⁸Unit of Infectious Diseases, ASST Papa Giovanni XXIII Hospital, Bergamo, Italy. ⁴⁸⁹Direzione Scientifica, Istituti Clinici Scientifici Maugeri IRCCS, Pavia, Italy. ⁴⁹⁰Department of Cardiology, Istituti Clinici Scientifici Maugeri IRCCS, Institute of Montescano, Pavia, Italy. ⁴⁹¹Department of Cardiac Rehabilitation, Institute of Tradate (VA) and Istituti Clinici Scientifici Maugeri IRCCS, Pavia, Italy. ⁴⁹²Department of Cardiology, Istituti Clinici Scientifici Maugeri IRCCS, Institute of Milan, Milan, Italy. ⁴⁹³Department of Electronics, Information and Bioengineering (DEIB), Politecnico di Milano, Milan, Italy. ⁴⁹⁴Scuola Normale Superiore, Pisa, Italy. ⁴⁹⁵CNR-Consiglio Nazionale delle Ricerche, Istituto di Biologia e Biotecnologia Agraria (IBBA), Milano, Italy. ⁴⁹⁶Core Research Laboratory, ISPRO, Florence, Italy. ⁴⁹⁷Fondazione per la Ricerca Ospedale di Bergamo, Bergamo, Italy. ⁴⁹⁸Health Management, Azienda USL Toscana Sud Est, Tuscany, Italy. ⁴⁹⁹IRCCS Mondino Foundation, Pavia, Italy. ⁵⁰⁰Medical Genetics Unit, Meyer Children's University Hospital, Florence, Italy. ⁵⁰¹Allelica, New York, NY, USA. ⁵⁰²Pneumology Unit, Department of Medicine, Misericordia Hospital, Grosseto, Italy. ⁵⁰³Intensive Care Unit and Department of Anesthesia, ASST Fatebenefratelli Sacco, Luigi Sacco Hospital, Polo Universitario, University of Milan, Milan, Italy. ⁵⁰⁴Infectious Disease Unit, Hospital of Massa,

Massa, Italy. ⁵⁰⁵Department of Clinical Medicine, Public Health, Life and Environment Sciences, University of L'Aquila, L'Aquila, Italy. ⁵⁰⁶UOSD Laboratorio di Genetica Medica—ASL Viterbo, San Lorenzo, Italy. ⁵⁰⁷Department of Medical Sciences, Infectious and Tropical Diseases Unit, Azienda Ospedaliera Universitaria Senese, Siena, Italy. ⁵⁰⁸Unit of Infectious Diseases, Santa Maria Annunziata Hospital, Florence, Italy. ⁵⁰⁹Infectious Disease Unit, Hospital of Lucca, Lucca, Italy. ⁵¹⁰Infectious Diseases Unit, Department of Clinical and Experimental Medicine, University of Pisa, Pisa, Italy. ⁵¹¹Infectious Disease Unit, Santo Stefano Hospital, AUSL Toscana Centro, Prato, Italy. ⁵¹²Clinic of Infectious Diseases, Catholic University of the Sacred Heart, Rome, Italy. ⁵¹³Department of Diagnostic and Laboratory Medicine, Institute of Biochemistry and Clinical Biochemistry, Fondazione Policlinico Universitario A. Gemelli IRCCS, Catholic University of the Sacred Heart, Rome, Italy. ⁵¹⁴Department of Population Health Sciences, Geisinger Health System, Danville, PA, USA. ⁵¹⁵Department of Molecular and Functional Genomics, Geisinger Health System, Danville, PA, USA. ⁵¹⁶Regeneron Genetics Center, Tarrytown, NY, USA. ⁵¹⁷Phenomic Analytics and Clinical Data Core, Geisinger Health System, Danville, PA, USA. ⁵¹⁸Queen Mary University of London, London, UK. ⁵¹⁹Bradford Institute for Health Research, Bradford Teaching Hospitals National Health Service (NHS) Foundation Trust, Bradford, UK. ⁵²⁰Medical and Population Genomics, Wellcome Sanger Institute, Hinxton, UK. ⁵²¹School of Basic and Medical Biosciences, Faculty of Life Sciences and Medicine, King's College London, London, UK. ⁵²²Department of Human Genetics, Wellcome Sanger Institute, Hinxton, UK. ⁵²³National Institute for Health Research Blood and Transplant Research Unit in Donor Health and Genomics, University of Cambridge, Cambridge, UK. ⁵²⁴Department of Haematology, University of Cambridge, Cambridge, UK. ⁵²⁵British Heart Foundation Cardiovascular Epidemiology Unit, Department of Public Health and Primary Care, University of Cambridge, Cambridge, UK. ⁵²⁶British Heart Foundation Centre of Research Excellence, University of Cambridge, Cambridge, UK. ⁵²⁷Health Data Research UK Cambridge, Wellcome Genome Campus, University of Cambridge, Cambridge, UK. ⁵²⁸Department of Genetics, University Medical Centre Groningen, University of Groningen, Groningen, The Netherlands. ⁵²⁹Department of Genetics, University Medical Centre Utrecht, Utrecht, The Netherlands. ⁵³⁰Department of Epidemiology, University Medical Centre Groningen, University of Groningen, Groningen, The Netherlands. ⁵³¹Department of Genetics, University Medical Centre Groningen, University of Groningen, Groningen, The Netherlands. ⁵³²Department of Psychiatry, University Medical Center Groningen, Groningen, The Netherlands. ⁵³³Department of Biostatistics, Boston University School of Public Health, Boston, MA, USA. ⁵³⁴Center for Population Genomics, MAVERIC, VA Boston Healthcare System, Boston, MA, USA. ⁵³⁵MAVERIC, VA Boston Healthcare System, Boston, MA, USA. ⁵³⁶Department of Epidemiology, Emory University Rollins School of Public Health, Atlanta, GA, USA. ⁵³⁷Stanford University, Stanford, CA, USA. ⁵³⁸Vrije Universiteit Amsterdam, Amsterdam, The Netherlands. ⁵³⁹Broad Institute of MIT and Harvard, Boston, MA, USA. ⁵⁴⁰Department of Genetics, University of Pennsylvania Perelman School of Medicine, Philadelphia, PA, USA. ⁵⁴¹Department of Neuroscience, Karolinska Institutet, Stockholm, Sweden. ⁵⁴²Max Planck Institute for Evolutionary Anthropology, Leipzig, Germany. ⁵⁴³Anaesthesiology and Intensive Care Medicine, Department of Surgical Sciences, Uppsala University, Uppsala, Sweden. ⁵⁴⁴Integrative Physiology, Department of Medical Cell Biology, Uppsala University, Uppsala, Sweden. ⁵⁴⁵Stanley Center for Psychiatric Research and Program in Medical and Population Genetics, Muscatine, IA, USA. ⁵⁴⁶Division Anesthesiology and Intensive Care, CLINTEC, Karolinska Institutet, Stockholm, Sweden. ⁵⁴⁷Department of Clinical Research and Leadership, George Washington University, Washington, DC, USA. ⁵⁴⁸Big Data Institute, Nuffield Department of Population Health, University of Oxford, Oxford, UK. ⁵⁴⁹Wellcome Centre for Human Genetics, University of Oxford, Oxford, UK. ⁵⁵⁰Nuffield Department of Medicine, Experimental Medicine Division, University of Oxford, John Radcliffe Hospital, Oxford, UK. ⁵⁵¹Public Health England, Field Service, Addenbrooke's Hospital, Cambridge, UK. ⁵⁵²Public Health England, Data and Analytical Services, National Infection Service, London, UK. ⁵⁵³Genomics PLC, Oxford, UK. ⁵⁵⁴Genomics England, London, UK. ⁵⁵⁵Ancestry, Lehi, UT, USA. ⁵⁵⁶e-mail: dbaraka90@hotmail.com

Methods

Ethics

GenOMICC study: GenOMICC was approved by the following research ethics committees: Scotland 'A' Research Ethics Committee (15/SS/0110) and Coventry and Warwickshire Research Ethics Committee (England, Wales and Northern Ireland) (19/WM/0247). Current and previous versions of the study protocol are available at <https://genomicc.org/protocol/>. 100,000 Genomes project: the 100,000 Genomes project was approved by the East of England–Cambridge Central Research Ethics Committee (REF 20/EE/0035). Only individuals from the 100,000 Genomes project for whom WGS data were available and who consented for their data to be used for research purposes were included in the analyses. UK Biobank study: ethical approval for the UK Biobank was previously obtained from the North West Centre for Research Ethics Committee (11/NW/0382). The work described herein was approved by UK Biobank under application number 26041. Geisinger Health Systems (GHS) study: approval for DiscovEHR analyses was provided by the GHS Institutional Review Board under project number 2006-0258. AncestryDNA study: all data for this research project were from individuals who provided prior informed consent to participate in AncestryDNA's Human Diversity Project, as reviewed and approved by our external institutional review board, Advarra (formerly Quorum). All data were de-identified before use. Penn Medicine Biobank study: appropriate consent was obtained from each participant regarding the storage of biological specimens, genetic sequencing and genotyping, and access to all available EHR data. This study was approved by the institutional review board of the University of Pennsylvania and complied with the principles set out in the Declaration of Helsinki. Informed consent was obtained for all study participants. 23andMe study: participants in this study were recruited from the customer base of 23andMe, a personal genetics company. All individuals included in the analyses provided informed consent and answered surveys online according to the 23andMe protocol for research in humans, which was reviewed and approved by Ethical and Independent Review Services, a private institutional review board (<http://www.eandireview.com>).

Recruitment of cases (patients with COVID-19)

Patients were recruited to the GenOMICC study in 224 UK intensive care units (<https://genomicc.org>). All individuals had confirmed COVID-19 according to local clinical testing and were deemed, in the view of the treating clinician, to require continuous cardiorespiratory monitoring. In UK practice this kind of monitoring is undertaken in high-dependency or intensive care units.

Recruitment of control individuals

Mild or asymptomatic control individuals. Participants were recruited to the mild COVID-19 cohort on the basis of having experienced mild (non-hospitalized) or asymptomatic COVID-19. Participants volunteered to take part in the study via a microsite and were required to self-report the details of a positive COVID-19 test. Volunteers were prioritized for genome sequencing on the basis of demographic matching with the critical COVID-19 cohort considering self-reported ancestry, sex, age and location within the UK. We refer to this cohort as the COVID-19 mild cohort.

Control individuals from the 100,000 Genomes project. Participants were enrolled in the 100,000 Genomes Project from families with a broad range of rare diseases, cancers and infection by 13 regional NHS Genomic Medicine Centres across England and in Northern Ireland, Scotland and Wales. For this analysis, participants for whom a positive SARS-CoV-2 test had been recorded as of March 2021 were not included owing to uncertainty in the severity of COVID-19 symptoms.

Only participants for whom genome sequencing was performed from blood-derived DNA were included and participants with haematological malignancies were excluded to avoid potential tumour contamination.

DNA extraction

For severe cases of COVID-19 and mild cohort controls, DNA was extracted from whole blood either manually using a Nucleon Kit (Cytiva) and resuspended in 1 ml TE buffer pH 7.5 (10 mM Tris-Cl pH 7.5, 1 mM EDTA pH 8.0), or automated on the Chemagic 360 platform using the Chemagic DNA blood kit (PerkinElmer) and re-suspended in 400 µl elution buffer. The yield of the DNA was measured using Qubit and normalized to 50 ng µl⁻¹ before sequencing. For the 100,000 Genomes Project samples, DNA was extracted from whole blood at designated extraction centres following sample handling guidance provided by Genomics England and NHS England.

WGS

Sequencing libraries were generated using the Illumina TruSeq DNA PCR-Free High Throughput Sample Preparation kit and sequenced with 150-bp paired-end reads in a single lane of an Illumina HiSeq X instrument (for 100,000 Genomes Project samples) or a NovaSeq instrument (for the COVID-19 critical and mild cohorts).

Sequencing data quality control. All genome sequencing data were required to meet minimum quality metrics and quality control measures were applied for all genomes as part of the bioinformatics pipeline. The minimum data requirements for all genomes were: more than 85 × 10⁹ bases with Q ≥ 30 and at least 95% of the autosomal genome covered at 15× or higher calculated from reads with mapping quality greater than 10 after removing duplicate reads and overlapping bases, after adaptor and quality trimming. Assessment of germline cross-sample contamination was performed using VerifyBamID and samples with more than 3% contamination were excluded. Sex checks were performed to confirm that the sex reported for a participant was concordant with the sex inferred from the genomic data.

WGS alignment and variant calling

COVID-19 cohorts. For the critical and mild COVID-19 cohorts, sequencing data alignment and variant calling were performed with Genomics England pipeline 2.0, which uses the DRAGEN software (v.3.2.22). Alignment was performed to genome reference GRCh38 including decoy contigs and alternative haplotypes (ALT contigs), with ALT-aware mapping and variant calling to improve specificity.

100,000 Genomes Project cohort. All genomes from the 100,000 Genomes Project cohort were analysed with the Illumina North Star Version 4 Whole Genome Sequencing Workflow (NSV4, v.2.6.53.23); which comprises the iSAAC Aligner (v.03.16.02.19) and Starling Small Variant Caller (v.2.4.7). Samples were aligned to the Homo Sapiens NCBI GRCh38 assembly with decoys.

A subset of the genomes from the cancer program of the 100,000 Genomes Project were reprocessed (alignment and variant calling) using the same pipeline used for the COVID-19 cohorts (DRAGEN v.3.2.22) for equity of alignment and variant calling.

Aggregation

Aggregation was conducted separately for the samples analysed with Genomics England pipeline 2.0 (severe cohort, mild cohort, cancer-realigned 100,000 Genomes Project) and those analysed with the Illumina North Star Version 4 pipeline (100,000 Genomes Project).

For the first three, the WGS data were aggregated from single-sample gVCF files to multi-sample VCF files using GVCFGenotyper (GG) v.3.8.1, which accepts gVCF files generated by the DRAGEN pipeline as input. GG

Article

outputs multi-allelic variants (several ALT variants per position on the same row), and for downstream analyses the output was decomposed to bi-allelic variants per row using the software vt v.0.57721. We refer to the aggregate as aggCOVID_vX, in which X is the specific freeze. The analysis in this manuscript uses data from freeze v.4.2 and the respective aggregate is referred to as aggCOVID_v4.2.

Aggregation for the 100,000 Genomes Project cohort was performed using Illumina's gvcfgenotyper v.2019.02.26, merged with bcftools v.1.10.2 and normalized with vt v.0.57721.

Sample quality control

Samples that failed any of the following four BAM-level quality control filters: freemix contamination > 3%, mean autosomal coverage < 25×, per cent mapped reads < 90% or per cent chimeric reads > 5% were excluded from the analysis.

In addition, a set of VCF-level quality control filters were applied after aggregation on all autosomal bi-allelic single-nucleotide variants (SNVs) (akin to gnomAD v.3.1)¹⁸. Samples were filtered out on the basis of the residuals of eleven quality control metrics (calculated using bcftools) after regressing out the effects of sequencing platform and the first three ancestry assignment principal components (PCs) (including all linear, quadratic and interaction terms) taken from the sample projections onto the SNP loadings from the individuals of 1000 Genomes Project phase 3 (1KGP3). Samples were removed that were four median absolute deviations (MADs) above or below the median for the following metrics: ratio of heterozygous to homozygous, ratio of insertions to deletions, ratio of transitions to transversions, total deletions, total insertions, total heterozygous SNPs, total homozygous SNPs, total transitions and total transversions. For the number of total singletons (SNPs), samples were removed that were more than 8 MADs above the median. For the ratio of heterozygous to homozygous alternative SNPs, samples were removed that were more than 4 MADs above the median.

After quality control, 79,803 individuals were included in the analysis with the breakdown according to cohort shown in Supplementary Table 2.

Selection of high-quality independent SNPs

We selected high-quality independent variants for inferring kinship coefficients, performing PCA, assigning ancestry and for the conditioning on the genetic relatedness matrix by the logistic mixed model of SAIGE and SAIGE-GENE. To avoid capturing platform and/or analysis pipeline effects for these analyses, we performed very stringent variant quality control as described below.

High-quality common SNPs. We started with autosomal, bi-allelic SNPs which had a frequency of higher than 5% in aggV2 (100,000 Genomes Project participant aggregate) and in the 1KGP3. We then restricted to variants that had missingness < 1%, median genotype quality control > 30, median depth (DP) ≥ 30 and at least 90% of heterozygote genotypes passing an ABratio binomial test with P value > 10^{-2} for aggV2 participants. We also excluded variants in complex regions from the list available in [https://genome.sph.umich.edu/wiki/Regions_of_high_linkage_disequilibrium_\(LD\)](https://genome.sph.umich.edu/wiki/Regions_of_high_linkage_disequilibrium_(LD)) (lifted over for GRCh38), and variants where the REF/ALT combination was CG or AT (C/G, G/C, A/T, T/A). We also removed all SNPs that were out of Hardy-Weinberg equilibrium (HWE) in any of the AFR, EAS, EUR or SAS super-populations of aggV2, with a P value cut-off of $P_{HWE} < 10^{-5}$. We then LD-pruned using PLINK v.1.9 with $r^2 = 0.1$ and in 500-kb windows. This resulted in a total of 63,523 high-quality sites from aggV2.

We then extracted these high-quality sites from the aggCOVID_v4.2 aggregate and further applied variant quality filters (missingness < 1%, median quality control > 30, median depth ≥ 30 and at least 90% of heterozygote genotypes passing an ABratio binomial test with P value > 10^{-2}), per batch of sequencing platform (that is, HiseqX, NovaSeq6000).

After applying variant filters in aggV2 and aggCOVID_v4.2, we merged the genomic data from the two aggregates for the intersection of the variants, which resulted in a final total of 58,925 sites.

High-quality rare SNPs. We selected high-quality rare (MAF < 0.005) bi-allelic SNPs to be used with SAIGE for aggregate variant testing (AVT) analysis. To create this set, we applied the same variant quality control procedure as with the common variants: We selected variants that had missingness < 1%, median quality control > 30, median depth ≥ 30 and at least 90% of heterozygote genotypes passing an ABratio binomial test with P value > 10^{-2} per batch of sequencing and genotyping platform (that is, HiSeq + NSV4, HiSeq + Pipeline 2.0, NovaSeq + Pipeline 2.0). We then subsetted those to the following groups of minor allele count (MAC) and MAF categories: MAC 1, 2, 3, 4, 5, 6–10, 11–20, MAC 20–MAF 0.001, MAF 0.001–0.005.

Relatedness, ancestry and principal components

Kinship. We calculated kinship coefficients among all pairs of samples using the software PLINK v.2.0 and its implementation of the KING robust algorithm. We used a kinship cut-off of < 0.0442 to select unrelated individuals with argument “-king-cutoff”.

Genetic ancestry prediction. To infer the ancestry of each individual, we performed principal component analysis (PCA) on unrelated 1KGP3 individuals with GCTA v.1.93.1 beta software using high-quality common SNPs⁴³, and inferred the first 20 PCs. We calculated loadings for each SNP, which we used to project aggV2 and aggCOVID_v4.2 individuals onto the 1KGP3 PCs. We then trained a random forest algorithm from the R package randomForest with the first 10 1KGP3 PCs as features and the super-population ancestry of each individual as labels. These were ‘AFR’ for individuals of African ancestry, ‘AMR’ for individuals of American ancestry, ‘EAS’ for individuals of East Asian ancestry, ‘EUR’ for individuals of European ancestry and ‘SAS’ for individuals of South Asian ancestry. We used 500 trees for the training. We then used the trained model to assign a probability of belonging to a certain super-population class for each individual in our cohorts. We assigned individuals to a super-population when class probability ≥ 0.8. Individuals for whom no class had probability ≥ 0.8 were labelled as ‘unassigned’ and were not included in the analyses.

PCA. After labelling each individual with predicted genetic ancestry, we calculated ancestry-specific PCs using GCTA v.1.93.1_beta⁴³. We computed 20 PCs for each of the ancestries that were used in the association analyses (AFR, EAS, EUR and SAS).

Variant quality control

Variant quality control was performed to ensure high quality of variants and to minimize batch effects due to using samples from different sequencing platforms (NovaSeq6000 and HiseqX) and different variant callers (Strelka2 and DRAGEN). We first masked low-quality genotypes setting them to missing, merged aggregate files and then performed additional variant quality control separately for the two major types of association analyses, GWAS and AVT, which concerned common and rare variants, respectively.

Masking. Before any analysis, we masked low-quality genotypes using the bcftools setGT module. Genotypes with DP < 10, genotype quality (GQ) < 20 and heterozygote genotypes failing an ABratio binomial test with P value < 10^{-3} were set to missing.

We then converted the masked VCF files to PLINK and bgen format using PLINK v.2.0.

Merging of aggregate samples. Merging of aggV2 and aggCOVID_v4.2 samples was done using PLINK files with masked genotypes and the merge function of PLINK v.1.9⁴⁴. For variants that were found in both aggregates.

GWAS analyses

Variation quality control. We restricted all GWAS analyses to common variants applying the following filters using PLINK v.1.9: $MAF > 0$ in both cases and controls, $MAF > 0.5\%$ and $MAC > 20$, missingness $< 2\%$, differential missingness between cases and controls, $mid-Pvalue < 10^{-5}$, HWE deviations on unrelated controls, $mid-Pvalue < 10^{-6}$. Multi-allelic variants were in addition required to have $MAF > 0.1\%$ in both aggV2 and aggCOVID_v4.2.

Control-control quality control filter. 100,000 Genomes Project aggV2 samples that were aligned and genotype called with the Illumina North Star version 4 pipeline represented the majority of control samples in our GWAS analyses, whereas all of the cases were aligned and called with Genomics England pipeline 2.0 (Supplementary Table 1). Therefore, the alignment and genotyping pipelines partially match the case-control status, which necessitates additional filtering for adjusting for between-pipeline differences in alignment and variant calling. To control for potential batch effects, we used the overlap of 3,954 samples from the Genomics England 100,000 Genomes Project participants that were aligned and called with both pipelines. For each variant, we computed and compared between platforms the inferred allele frequency for the population samples. We then filtered out all variants that had $>1\%$ relative difference in allele frequency between platforms. The relative difference was computed on a per-population basis for EUR ($n = 3,157$), SAS ($n = 373$), AFR ($n = 354$) and EAS ($n = 81$).

Model. We used a two-step logistic mixed model regression approach as implemented in SAIGE v.0.44.5 for single-variant association analyses. In step 1, SAIGE fits the null mixed model and covariates. In step 2, single-variant association tests are performed with the saddlepoint approximation (SPA) correction to calibrate unbalanced case-control ratios. We used the high-quality common variant sites for fitting the null model and sex, age, age^2 , age-by-sex and 20 PCs as covariates in step 1. The PCs were computed separately by predicted genetic ancestry (that is, EUR-specific, AFR-specific and so on), to capture subtle structure effects.

Analyses. All analyses were done on unrelated individuals with a pairwise kinship coefficient < 0.0442 . We conducted GWAS analyses per predicted genetic ancestry, for all populations for which we had more than 100 cases and more than 100 controls (AFR, EAS, EUR and SAS).

Multiple testing correction. As our study is testing variants that were directly sequenced by WGS and not imputed, we calculated the P value significance threshold by estimating the effective number of tests. After selecting the final filtered set of tested variants for each population, we LD-pruned in a window of 250 kb and $r^2 = 0.8$ with PLINK 1.9. We then computed the Bonferroni-corrected P value threshold as 0.05 divided by the number of LD-pruned variants tested in the GWAS. The P value thresholds that were used for declaring statistical significance are provided in Supplementary Table 5.

LD-clumping. We used PLINK v.1.9 to do clumping of variants that were genome-wide significant for each analysis with $P1$ set to per-population P value from Supplementary Table 5, $P2 = 0.01$, clump distance 1,500 kb and $r^2 = 0.1$.

Conditional analysis and signal independence. To find the set of independent variants in the per-population analyses, we performed a step-wise conditional analysis with the GWAS summary statistics for each population using GCTA 1.9.3-cojo-slct function⁴³. The parameters for the function were $pval = 2.2 \times 10^{-8}$, a distance of 10,000 kb and a colinear threshold of 0.9 (ref. ⁴⁵). For establishing independence of multi-ancestry meta-analysis signals from per-population discovered signals, we performed LD-clumping using the meta-analysis summaries

and identified signals with no overlap with the LD-clumped results from the per-population analyses. In addition to the GCTA-cojo analysis, we also performed confirmatory individual-level conditional analysis as implemented in SAIGE. For every lead variant signal (including the multi-ancestry meta-analysis signals), we conditioned on the lead variants of all other signals identified as independent by GCTA-cojo and located on the same chromosome with option -condition of SAIGE (Supplementary Table 6).

Fine-mapping. We performed fine-mapping for genome-wide-significant signals using the R package SusieR v.0.11.42⁴³. For each genome-wide-significant variant locus, we selected the variants 1.5 Mbp on each side and computed the correlation matrix among them with PLINK v.1.9. We then ran the susieR summary-statistics-based function susie_rss and provided the summary z scores from SAIGE (that is, effect size divided by its standard error) and the correlation matrix computed with the same samples that were used for the corresponding GWAS. We required coverage ≥ 0.95 for each identified credible set and minimum and median absolute correlation coefficients (purity) of $r = 0.1$ and 0.5, respectively.

Functional annotation of credible sets. We annotated all variants included in each credible set identified by SusieR using the online Variant Effect Predictor (VEP) v.104 and selected the worst consequence across GENCODE basic transcripts (Supplementary Information). We also ranked each variant within each credible set according to the predicted consequence and the ranking was based on the table provided by Ensembl: https://www.ensembl.org/info/genome/variation/prediction/predicted_data.html.

Multi-ancestry meta-analysis. We performed a meta-analysis across all ancestries using an inverse-variance weighting method and control for population stratification for each separate analysis in the METAL software⁴⁶. The meta-analysed variants were filtered for variants with heterogeneity P value $P < 2.22 \times 10^{-8}$ and variants that are not present in at least half of the individuals. We used the meta R package to plot forest plots of the clumped multi-ancestry meta-analysis variants⁴⁷.

LD-based validation of lead GWAS signals. To quantify the support for genome-wide-significant signals from nearby variants in LD, we assessed the internal consistency of GWAS results of the lead variants and their surroundings. To this end, we compared observed z -scores at lead variants with the expected z -scores based on those observed at neighbouring variants. Specifically, we computed the observed z -score for a variant i as $s_i = \hat{\beta}/\hat{\sigma}_{\beta}$ and, following a previous approach⁴⁸, the imputed z -score at a target variant t as

$$\hat{s}_t = \mathbf{\Sigma}_{t,P}(\mathbf{\Sigma}_{P,P} + \lambda \mathbf{I})^{-1} \mathbf{s}_P$$

where \mathbf{s}_P are the observed z -scores at a set P of predictor variants, $\mathbf{\Sigma}_{x,y}$ is the empirical correlation matrix of dosage coded genotypes computed on the GWAS sample between the variants in x and y , and λ is a regularization parameter set to 10^{-5} . The set P of predictor variants consisted of all variants within 100 kb of the target variant with a genotype correlation with the target variant greater than 0.25. This approach is similar to one proposed recently⁴⁹.

Stratified analysis. We performed sex-specific analysis (male and female individuals separately) as well as analysis stratified by age (that is, participants of younger than 60 years old and 60 years old or above) for the EUR ancestry group. To compare the effect of variants within groups for the age- and sex-stratified analysis we first adjusted the effect and error of each variant for the standard deviation of the trait in each stratified group and then used the following t -statistic, as in previous studies^{50,51}

$$t = \frac{b_1 - b_2}{\sqrt{se_1^2 + se_2^2 - 2 \times rse_1 \times rse_2}}$$

where b_1 is the adjusted effect for group 1, b_2 is the adjusted effect for group 2, se_1 and se_2 are the adjusted standard errors for groups 1 and 2, respectively, and r is the Spearman rank correlation between groups across all genetic variants.

Replication. To generate a replication set, we conducted a meta-analysis of data from 23andMe, together with a meta-analysis of the COVID-19 HGI data freeze 6 (hospitalized COVID versus population) GWAS (B2 analysis), including all genetic ancestries. Although the HGI programme included an analysis designed to mirror the GenOMICC study (analysis 'A2'), most of these cases come from GenOMICC and are already included in the discovery cohort. We therefore used the broader hospitalized phenotype ('B2') for replication.

To account for signal due to sample overlap we performed a mathematical subtraction from HGI v.6 B2, of the GenOMICC GWAS of European genetic ancestry. Publicly available HGI data were downloaded from <https://www.covid19hg.org/results/r6/>. The subtraction was performed using the MetaSubtract package (v.1.60) for R (v.4.0.2) after removing variants with the same genomic position and using the lambda.cohorts with genomic inflation calculated on the GenOMICC summary statistics.

We calculated a multi-ancestry meta-analysis for the three ancestries with summary statistics in 23andMe—African, Latino and European—using variants that passed the 23andMe ancestry quality control, with imputation score > 0.6 and with MAF > 0.005, before performing a final meta-analysis of 23andMe and HGI B2 without GenOMICC to create the final replication set. Meta-analysis was performed using METAL⁴⁶, with the inverse-variance weighting method (STDERR mode) and genomic control ON. We considered that a hit was replicated if the direction of effect in the GenOMICC-subtracted HGI summary statistics was the same as in our GWAS, and the P value was significant after Bonferroni correction for the number of attempted replications ($pval < 0.05/25$). If the main hit was not present in the HGI–23andMe meta-analysis or if the hit was not replicating, we looked for replication in variants in high LD with the top variant ($r^2 > 0.9$), which helped replicate two regions.

To attempt additional replication of two associations, we performed a multi-ancestry meta-analysis across five continental ancestry groups in the UK Biobank, AncestryDNA, Penn Medicine Biobank and GHS, totalling 9,937 hospitalized cases of COVID-19 and 1,059,390 controls (COVID-19 negative or unknown). Hospitalization status (positive, negative or unknown) was determined on the basis of COVID-19-related ICD10 codes U071, U072, U073 in variable 'diag_icd10' (table 'hesin_diag') in the UK Biobank study; self-reported hospitalization due to COVID-19 in the AncestryDNA study; and medical records in the GHS and Penn Medicine Biobank studies. Association analyses in each study were performed using the genome-wide Firth logistic regression test implemented in REGENIE. In this implementation, Firth's approach is applied when the P value from a standard logistic regression score test is less than 0.05. We included in step 1 of REGENIE (that is, prediction of individual trait values based on the genetic data) directly genotyped variants with MAF > 1%, missingness < 10%, HWE test $P > 1 \times 10^{-15}$ and LD-pruning (1,000 variant windows, 100 variant sliding windows and $r^2 < 0.9$). The association model used in step 2 of REGENIE included as covariates age, age², sex, age-by-sex, and the first 10 ancestry-informative PCs derived from the analysis of a stricter set of LD-pruned (50 variant windows, 5 variant sliding windows and $r^2 < 0.5$) common variants from the array (imputed for the GHS study) data. Within each study, association analyses were performed separately for five different continental ancestries defined on the basis of the array data: African (AFR), Hispanic or Latin American (HLA),

East Asian (EAS), European (EUR) and South Asian (SAS). Results were subsequently meta-analysed across studies and ancestries using an inverse-variance-weighted fixed-effects meta-analysis.

HLA imputation and association analysis

HLA types were imputed at two-field (four-digit) resolution for all samples within aggV2 and aggCOVID_v4.2 for the following seven loci: HLA-A, HLA-C, HLA-B, HLA-DRB1, HLA-DQA1, HLA-DQB1 and HLA-DPB1, using the HIBAG package in R¹⁵. At the time of writing, HLA types were also imputed for 82% of samples using HLA*LA⁵². Inferred HLA alleles between HIBAG and HLA*LA were more than 96% identical at four-digit resolution. HLA association analysis was run under an additive model using SAIGE, in an identical manner to the SNV GWAS. The multi-sample VCF of aggregated HLA type calls from HIBAG was used as input in cases in which any allele call with posterior probability (T) < 0.5 were set to missing.

AVT

AVT on aggCOVID_v4.2 was performed using SKAT-O as implemented in SAIGE-GENE v.0.44.5¹⁷ on all protein-coding genes. Variant and sample quality control for the preparation and masking of the aggregate files have been described elsewhere. We further excluded SNPs with differential missingness between cases and controls (mid- P value < 10^{-5}) or a site-wide missingness above 5%. Only bi-allelic SNPs with MAF < 0.5% were included.

We filtered the variants to include in the AVT by applying two functional annotation filters: a putative loss of function (pLoF) filter, in which only variants that are annotated by LOFTEE¹⁸ as high-confidence loss of function were included; and a more lenient (missense) filter, in which variants that have a consequence of missense or worse as annotated by VEP, with a CADD_PHRED score of ≥ 10 , were also included. All variants were annotated using VEP v99. SAIGE-GENE was run with the same covariates used in the single variant analysis: sex, age, age², age-by-sex and 20 (population-specific) PCs generated from common variants (MAF $\geq 5\%$).

We ran the tests separately by genetically predicted ancestry, as well as across all four ancestries as a mega-analysis. We considered a gene-wide-significant threshold on the basis of the genes tested per ancestry, correcting for the two masks (pLoF and missense; Supplementary Table 14).

Post-GWAS analysis

TWASs. We performed TWASs in the MetaXcan framework and the GTEx v.8 eQTL and splicing quantitative trait loci (sQTL) MASHR-M models available for download in <http://predictdb.org/>. We first calculated, using the European summary statistics, individual TWASs for whole blood and lung with the S-PrediXcan function^{53,54}. Then we performed a metaTWAS including data from all tissues to increase statistical power using s-MultiXcan⁵⁵. We applied the Bonferroni correction to the results to choose significant genes and introns for each analysis.

Colocalization analysis. Significant genes from the TWAS, splicing TWAS, metaTWAS and splicing metaTWAS, as well as genes for which one of the top variants was a significant eQTL or sQTL, were selected for a colocalization analysis using the coloc R package⁵⁶. We chose the lead SNPs from the European ancestry GWAS summary statistics and a region of ± 200 kb around each SNP to do the colocalization with the identified genes in the region. GTEx v.8 whole-blood and lung tissue summary statistics and eqtlGen (which has blood eQTL summary statistics for more than 30,000 individuals) were used for the analysis^{22,57}. We first performed a sensitivity analysis of the posterior probability of colocalization (PP_{H4}) on the prior probability of colocalization (P_{12}), going from $P_{12} = 10^{-8}$ to $P_{12} = 10^{-4}$, with the default threshold being $P_{12} = 10^{-5}$. eQTL signal and GWAS signals were deemed to colocalize if these two criteria were met: (1) at $P_{12} = 5 \times 10^{-5}$ the probability of colocalization

$PP_{H4} > 0.5$; and (2) at $P_{12} = 10^{-5}$ the probability of independent signal (PP_{H3}) was not the main hypothesis ($PP_{H3} < 0.5$). These criteria were chosen to allow eQTLs with weaker P values, owing to lack of power in GTEx v.8, to be colocalized with the signal when the main hypothesis using small priors was that there was not any signal in the eQTL data.

As the chromosome 3-associated interval is larger than 200 kb, we performed additional colocalization including a region up to 500 kb, but no further colocalizations were found.

Mendelian randomization. We performed GSMR²³ in a replicated outcome study design. As exposures, we used the pQTLs from the INTERVAL study²⁴. We used the 1000 Genomes Project imputed data of the Health and Retirement Study (HRS) ($n = 8,557$) as the LD reference data required for GSMR analysis. The HRS data are available from dbGap (accession number: phs000428).

GSMR was undertaken using all exposures for which we were able to identify two or more independent SNPs associated with the exposure (P value(exposure) $< 5 \times 10^{-8}$; LD clumping ± 1 Mb, $r^2 < 0.05$; HEIDI-outlier filtering test, for the removal of SNPs with evidence of horizontal pleiotropy, was performed at the default threshold value of 0.01). Using GSMR, we identified those proteins implicated in determining COVID-19 severity in the new GenOMICC results (following genomic-control correction for inflation) at a false discovery rate (FDR) of less than 0.05, and attempted replication in the GWAS of ‘Hospitalized COVID versus population’ (phenotype B2) of the COVID-19 HGI (ref. ⁵⁸) having excluded the previous GenOMICC results. We achieved this by mathematically removing the contribution of GenOMICC¹ from the meta-analysis. We considered as replicated those results that passed a Bonferroni-corrected P value threshold, correcting for the total number of replication tests attempted (that is, the number of observations from the discovery set with $FDR < 0.05$).

Heritability. For the SNP-based narrow-sense heritabilities of severe COVID-19 and HGI COVID phenotypes, both high-definition likelihood (HDL) and LD score regression (LDSC)⁵⁹ methods were applied. The HGI summary statistics were based on the GWAS analysis of all available samples, in which the majority were European populations (see <https://www.covid19hg.org/results/r6/>). The munge_sumstats.py procedure in the LDSC software was used to harmonize the summary statistics, and in LDSC, the reference panel was built using the 1000 Genome European samples with SNPs that have $MAF > 0.05$. As both HDL and LDSC are based on GWAS summary z -score statistics, the estimated heritabilities are thus on the observed scale.

Enrichment analysis. Enrichment analysis was performed to identify ontologies in which discovery genes were overrepresented. Using the XGR algorithm (<http://galahad.well.ox.ac.uk/XGR>)⁶⁰, 19 genes identified through lead variant proximity, credible variant sets, mutation consequence and TWAS analyses were tested for enrichment in disease ontology⁶¹, gene ontologies (biological process, molecular function and cellular component)⁶² and KEGG⁶³ and Reactome⁶⁴ pathways using default settings. This generated a P value and FDR for overrepresentation of genes within each of the ontologies (Supplementary Table 15).

Reporting summary

Further information on research design is available in the Nature Research Reporting Summary linked to this paper.

Data availability

All data are available through <https://genomicc.org/data>. This includes downloadable summary data tables and instructions for applying to access individual-level data. Individual-level genome sequence data for the COVID-19 severe and mild cohorts can be analysed by qualified researchers in the UK Outbreak Data Analysis Platform at the University

of Edinburgh by application at <https://genomicc.org/data>. Genomic data for the 100,000 Genomes Project participants and a subset of COVID-19 cases are also available through the Genomics England research environment, which can be accessed by application at <https://www.genomicsengland.co.uk/join-a-gecip-domain>. The full GWAS summary statistics for the 23andMe discovery dataset are available through 23andMe to qualified researchers under an agreement with 23andMe that protects the privacy of the 23andMe participants. More information and access to the data are provided at <https://research.23andMe.com/dataset-access/>.

Code availability

Code to calculate the imputation of P values based on LD SNPs is available at https://github.com/baillielab/GenOMICC_GWAS.

43. Yang, J., Lee, S. H., Goddard, M. E. & Visscher, P. M. GCTA: a tool for genome-wide complex trait analysis. *Am. J. Hum. Genet.* **88**, 76–82 (2011).
44. Purcell, S. et al. PLINK: a tool set for whole-genome association and population-based linkage analyses. *Am. J. Hum. Genet.* **81**, 559–575 (2007).
45. Yang, J. et al. Conditional and joint multiple-SNP analysis of GWAS summary statistics identifies additional variants influencing complex traits. *Nat. Genet.* **44**, 369–375 (2012).
46. Willer, C. J., Li, Y. & Abecasis, G. R. METAL: fast and efficient meta-analysis of genomewide association scans. *Bioinformatics* **26**, 2190–2191 (2010).
47. Balduzzi, S., Rücker, G. & Schwarzer, G. How to perform a meta-analysis with R: a practical tutorial. *Evid. Based Ment. Health* **22**, 153–160 (2019).
48. Pasaniuc, B. et al. Fast and accurate imputation of summary statistics enhances evidence of functional enrichment. *Bioinformatics* **30**, 2906–2914 (2014).
49. Chen, W. et al. Improved analyses of GWAS summary statistics by reducing data heterogeneity and errors. *Nat. Commun.* **12**, 7117 (2021).
50. Bernabeu, E. et al. Sex differences in genetic architecture in the UK biobank. *Nat. Genet.* **53**, 1283–1289 (2021).
51. Winkler, T. W. et al. The influence of age and sex on genetic associations with adult body size and shape: a large-scale genome-wide interaction study. *PLoS Genet.* **11**, e1005378 (2015).
52. Dilthey, A. T. et al. HLA*LA—HLA typing from linearly projected graph alignments. *Bioinformatics* **35**, 4394–4396 (2019).
53. Gamazon, E. R. et al. A gene-based association method for mapping traits using reference transcriptome data. *Nat. Genet.* **47**, 1091–1098 (2015).
54. Barbeira, A. N. et al. Exploring the phenotypic consequences of tissue specific gene expression variation inferred from GWAS summary statistics. *Nat. Commun.* **9**, 1825 (2018).
55. Barbeira, A. N. et al. Integrating predicted transcriptome from multiple tissues improves association detection. *PLoS Genet.* **15**, e1007889 (2019).
56. Giambartolomei, C. et al. Bayesian test for colocalisation between pairs of genetic association studies using summary statistics. *PLoS Genet.* **10**, e1004383 (2014).
57. Vösa, U. et al. Large-scale cis- and trans-eQTL analyses identify thousands of genetic loci and polygenic scores that regulate blood gene expression. *Nat. Genet.* **53**, 1300–1310 (2021).
58. The COVID-19 Host Genetics Initiative. The COVID-19 Host Genetics Initiative, a global initiative to elucidate the role of host genetic factors in susceptibility and severity of the SARS-CoV-2 virus pandemic. *Eur. J. Hum. Genet.* **28**, 715–718 (2020).
59. Bulik-Sullivan, B. K. et al. LD score regression distinguishes confounding from polygenicity in genome-wide association studies. *Nat. Genet.* **47**, 291–295 (2015).
60. Fang, H., Knezevic, B., Burnham, K. L. & Knight, J. C. XGR software for enhanced interpretation of genomic summary data, illustrated by application to immunological traits. *Genome Med.* **8**, 129 (2016).
61. Schriml, L. M. et al. Disease Ontology: a backbone for disease semantic integration. *Nucleic Acids Res.* **40**, D940–D946 (2012).
62. Ashburner, M. et al. Gene Ontology: tool for the unification of biology. *Nat. Genet.* **25**, 25–29 (2000).
63. Kanehisa, M. & Goto, S. KEGG: Kyoto Encyclopedia of Genes and Genomes. *Nucleic Acids Res.* **28**, 27–30 (2000).
64. Jassal, B. et al. The reactome pathway knowledgebase. *Nucleic Acids Res.* **48**, D498–D503 (2020).
65. Chen, M.-H. et al. Phospholipid scramblase 1 contains a nonclassical nuclear localization signal with unique binding site in importin α . *J. Biol. Chem.* **280**, 10599–10606 (2005).
66. Chen, C.-W., Sowden, M., Zhao, Q., Wiedmer, T. & Sims, P. J. Nuclear phospholipid scramblase 1 prolongs the mitotic expansion of granulocyte precursors during G-CSF-induced granulopoiesis. *J. Leukocyte Biol.* **90**, 221–233 (2011).
67. Thomas, C. et al. Structural linkage between ligand discrimination and receptor activation by type I interferons. *Cell* **146**, 621–632 (2011).

Acknowledgements We thank the patients and their loved ones who volunteered to contribute to this study at one of the most difficult times in their lives, and the research staff in every intensive care unit who recruited patients at personal risk under challenging conditions. GenOMICC was funded by the Department of Health and Social Care (DHSC), Illumina, LifeArc, the Medical Research Council (MRC), UKRI, Sepsis Research (the Fiona Elizabeth Agnew Trust), the Intensive Care Society, a Wellcome Trust Senior Research Fellowship (J.K.B., 223164/Z/21/Z) a BBSRC Institute Program Support Grant to the Roslin Institute (BBS/E/D/20002172, BBS/E/D/10002070 and BBS/E/D/30002275) and UKRI grants MC_PC_20004, MC_PC_19025, MC_PC_1905 and MRN02995X/1. WGS was performed by Illumina

Article

at Illumina Laboratory Services and was overseen by Genomics England. We would like to thank all at Genomics England who have contributed to the sequencing, clinical and genomic data analysis. This research is supported in part by the Data and Connectivity National Core Study, led by Health Data Research UK in partnership with the Office for National Statistics and funded by UK Research and Innovation (grant ref. MC_PC_20029). A.D.B. would like to acknowledge funding from the Wellcome PhD training fellowship for clinicians (204979/Z/16/Z) and the Edinburgh Clinical Academic Track (ECAT) programme. We thank the research participants and employees of 23andMe for making this work possible. Genomics England and the 100,000 Genomes Project were funded by the National Institute for Health Research, the Wellcome Trust, the MRC, Cancer Research UK, the DHSC and NHS England. We are grateful for the support from S. Hill and the team in NHS England and the 13 Genomic Medicine Centres that delivered the 100,000 Genomes Project, which provided most of the control genome sequences for this study. We thank the participants in the 100,000 Genomes Project, who made this study possible, and the Genomics England Participant Panel for their strategic advice, involvement and engagement. We acknowledge NHS Digital, Public Health England and the Intensive Care National Audit and Research Centre, who provided life-course longitudinal clinical data on the participants. This work forms part of the portfolio of research of the National Institute for Health Research Barts Biomedical Research Centre. Mark Caulfield is an NIHR Senior Investigator. This study owes a great deal to the National Institute for Healthcare Research Clinical Research Network (NIHR CRN) and the Chief Scientist's Office (Scotland), who facilitate recruitment into research studies in NHS hospitals, and to the global ISARIC and InFACT consortia. Additional replication was conducted using the UK Biobank Resource (project 26041). The Penn Medicine BioBank is funded by a gift from the Smilow family; the National Center for Advancing Translational Sciences of the National Institutes of Health under CTSA award number UL1TR001878; and the Perelman School of Medicine at the University of Pennsylvania. We thank the AncestryDNA customers who voluntarily contributed information in the COVID-19 survey. HRS (dbGaP accession: phs000428.v1.p1): HRS was supported by the National Institute on Aging (NIA U01AG009740). The genotyping was funded separately by the National Institute on Aging (RC2 AG036495, RC4 AG039029). Genotyping was conducted by the NIH Center for Inherited Disease Research (CIDR) at Johns Hopkins University. Genotyping quality control and final preparation of the data were performed by the Genetics Coordinating Center at the University of Washington. The Genotype-Tissue Expression (GTEx) Project was supported by the Common Fund of the Office of the Director of the National Institutes of Health, and by the NCI, NHGRI, NHLBI, NIDA, NIMH and NINDS. The data used for the analyses described in this manuscript were obtained from the GTEx Portal on 22 August 2021 (GTEx Analysis Release v.8 (dbGaP Accession phs000424.v8.p2)). We thank the research participants and employees of 23andMe for making this work possible. A full list of contributors who have provided data that were collated in the HGI project, including previous

iterations, is available at <https://www.covid19hg.org/acknowledgements>. The views expressed are those of the authors and not necessarily those of the DHSC, NHS, Department for International Development (DfID), NIHR, MRC, Wellcome Trust or Public Health England.

Author contributions A.K., E.P.-C., K. Rawlik, A. Stuckey, C.A.O., S.W., T. Malinauskas, Y.W., X.S., K.S.E., B.W., D.R., L.K., M.Z., N.P., J.A.K., J.E.H., A.B., G.R.A., M.A.R.F., A.J., T. Mirshahi, M.O., D.J.R., M.D.R., A.V., J.Y., A.D.B., S.C.H., L. Moutsianas, A.L. and J.K.B. contributed to data analysis. A.K., E.P.-C., K. Rawlik, A. Stuckey, C.A.O., S.W., C.D.R., J.M., A.R., S.C.H., L. Moutsianas and A.L. contributed to bioinformatics. A.K., E.P.-C., K. Rawlik, C.D.R., J.M., D.M., A.N., M.G.S., S.C.H., L. Moutsianas, M.J.C. and J.K.B. contributed to writing and reviewing the manuscript. E.P.-C., K. Rawlik, K.M., S.K., A.F., L. Murphy, K. Rowan, C.P.P., V.V., J.F.W., S.C.H., A.L., M.J.C. and J.K.B. contributed to design. S.W., F.G., W.O., P.G. and S.D. contributed to project management. F.G., W.O., K.M., S.K., P.G., S.D., D.M., A.N., M.G.S., S.S., J.K., T.A.F., M.S.-H., C.S., C.H., P.H., L.L., D. McAuley, H.M., P.J.O., P.E., T.W., A.T., A.F., L. Murphy, K. Rowan, C.P.P., R.H.S., S.C.H. and A.L. contributed to oversight. F.G., W.O., F.M.-C. and J.K.B. contributed to ethics and governance. K.M., A. Siddiq, A.F. and L. Murphy contributed to sample handling and sequencing. A. Siddiq contributed to data collection. T.Z. contributed to sample handling. T.Z., G.E., C.P., D.B. and C.K. contributed to sequencing. L.T. contributed to the recruitment of controls. G.C., P.A., K. Rowan and A.L. contributed to clinical data management. K. Rowan, C.P.P., S.C.H. and J.K.B. contributed to conception. K. Rowan, C.P.P., V.V. and J.F.W. contributed to reviewing the manuscript. M.J.C. and J.K.B. contributed to scientific leadership.

Competing interests J.A.K., J.E.H., A.B., G.R.A. and M.A.R.F. are current employees and/or stockholders of Regeneron Genetics Center or Regeneron Pharmaceuticals. Genomics England is a wholly owned Department of Health and Social Care company created in 2013 to work with the NHS to introduce advanced genomic technologies and analytics into healthcare. All Genomics England affiliated authors are, or were, salaried by Genomics England during this programme. All other authors declare that they have no competing interests relating to this work.

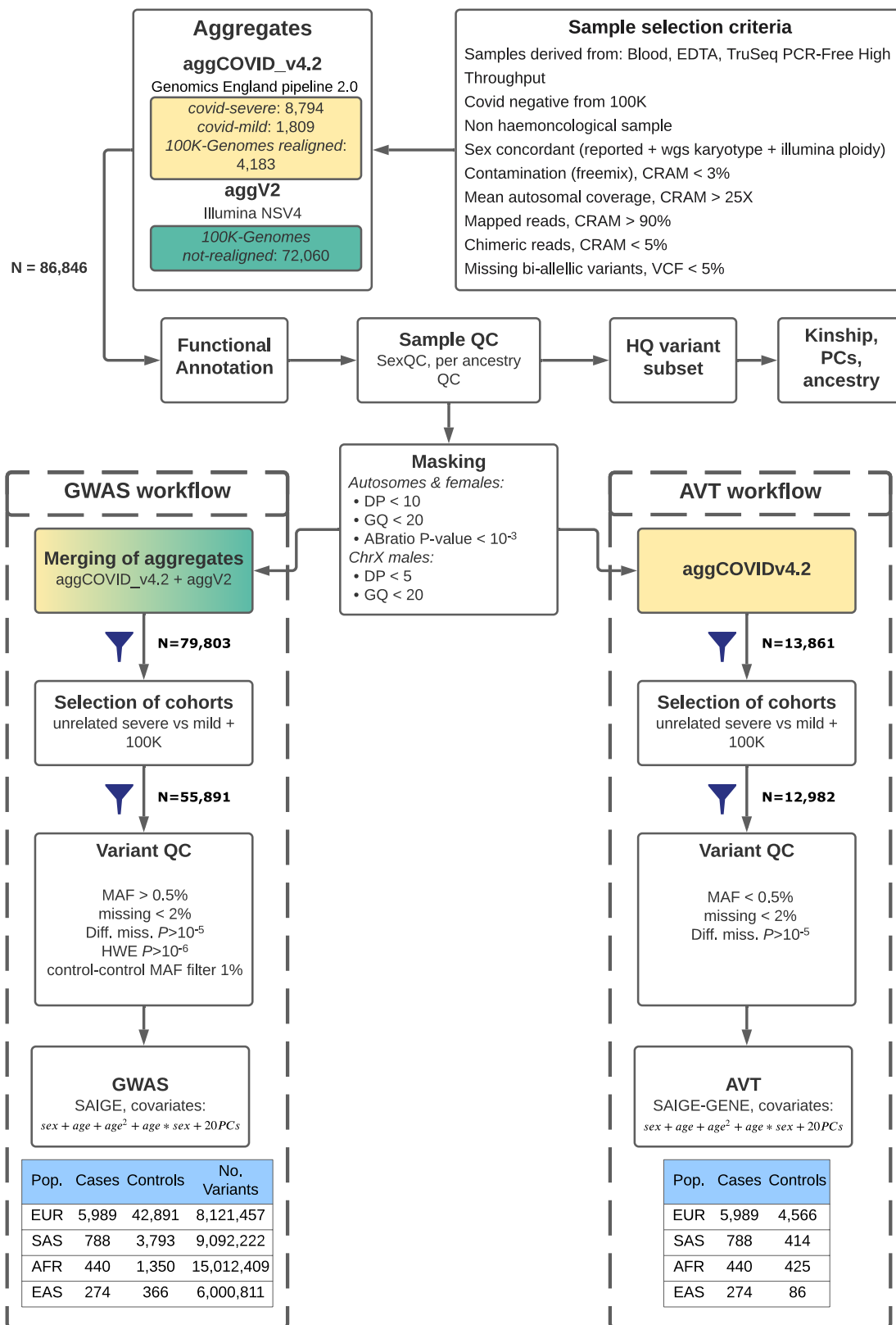
Additional information

Supplementary information The online version contains supplementary material available at <https://doi.org/10.1038/s41586-022-04576-6>.

Correspondence and requests for materials should be addressed to Mark J. Caulfield, J. Kenneth Bailie or Duna Barakeh.

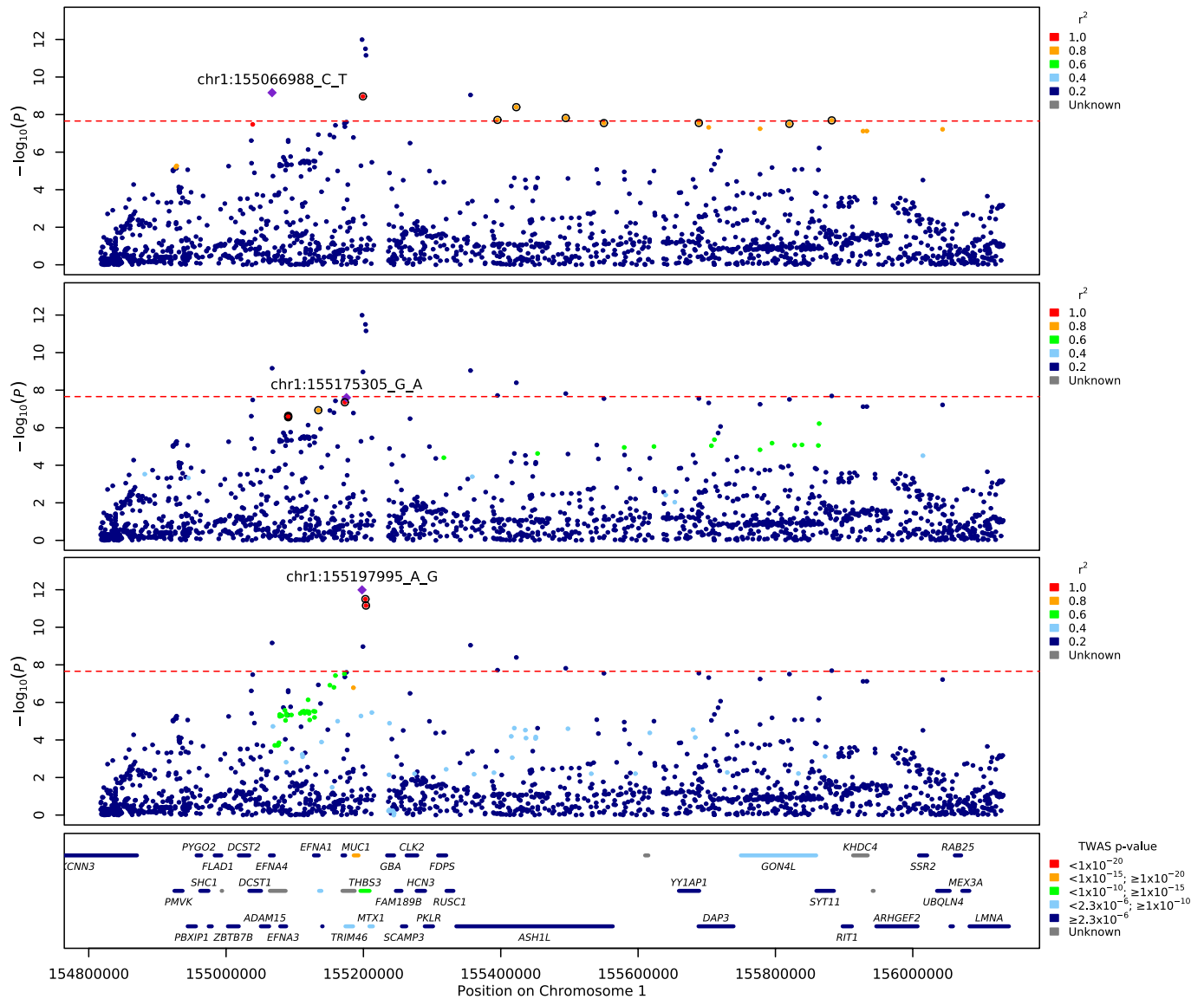
Peer review information *Nature* thanks Jacques Fellay and the other, anonymous, reviewer(s) for their contribution to the peer review of this work. Peer reviewer reports are available.

Reprints and permissions information is available at <http://www.nature.com/reprints>.



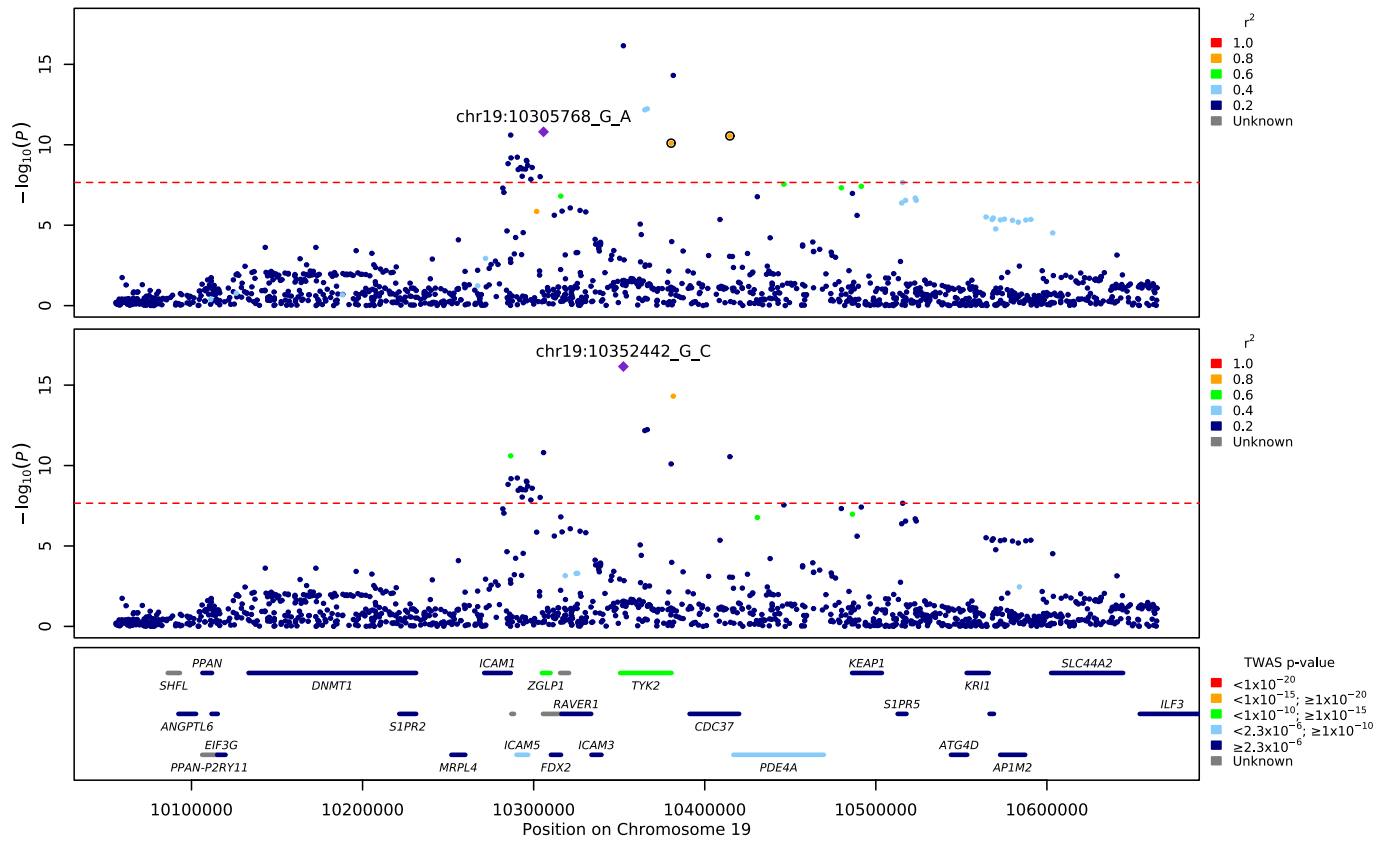
Extended Data Fig. 1 | Analysis workflow for GWAS and AVT analyses of this study. The cohorts displayed in yellow and green in the top box were processed with Genomics England Pipeline 2.0 and Illumina NSV4, respectively (see Methods on WGS Alignment and variant calling for details on differences between pipelines). We used individuals that were processed with either pipeline for the GWAS analyses and individuals processed only with Genomics

England Pipeline 2.0 for the AVT analyses. The definition of the cases and controls was the same for GWAS and AVT, cases were the COVID-19 severe individuals for both, and controls included individuals from the 100,000 Genomes Project (100,000 Genomes Project) and also COVID-19 positive individuals that were recruited for this study and experienced only mild symptoms (COVID-mild).



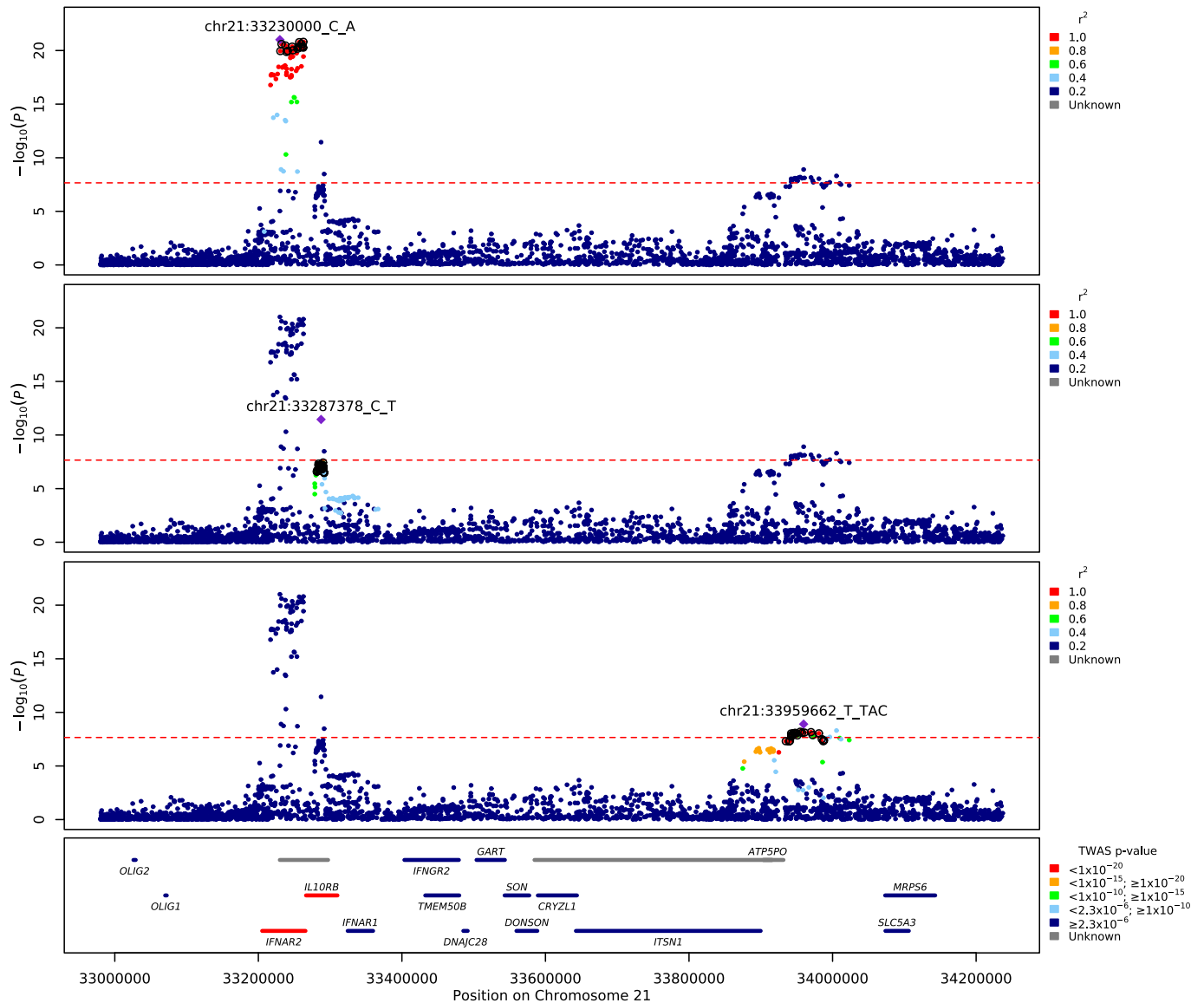
Extended Data Fig. 2 | Regional detail showing fine-mapping to identify three adjacent independent signals on chromosome 1. Top two panels: variants in LD with the lead variants shown. The variants that are included in two independent credible sets are displayed with black outline circles. r^2 values

in the legend denote upper limits, $0.2=[0.0,0.2]$, $0.4=[0.2,0.4]$, $0.6=[0.4,0.6]$, $0.8=[0.6,0.8]$, $1=[0.8,1]$. Bottom panel: locations of protein-coding genes, coloured by TWAS P -value. The red dashed line shows the Bonferroni-corrected P -value= 2.2×10^{-8} for Europeans.



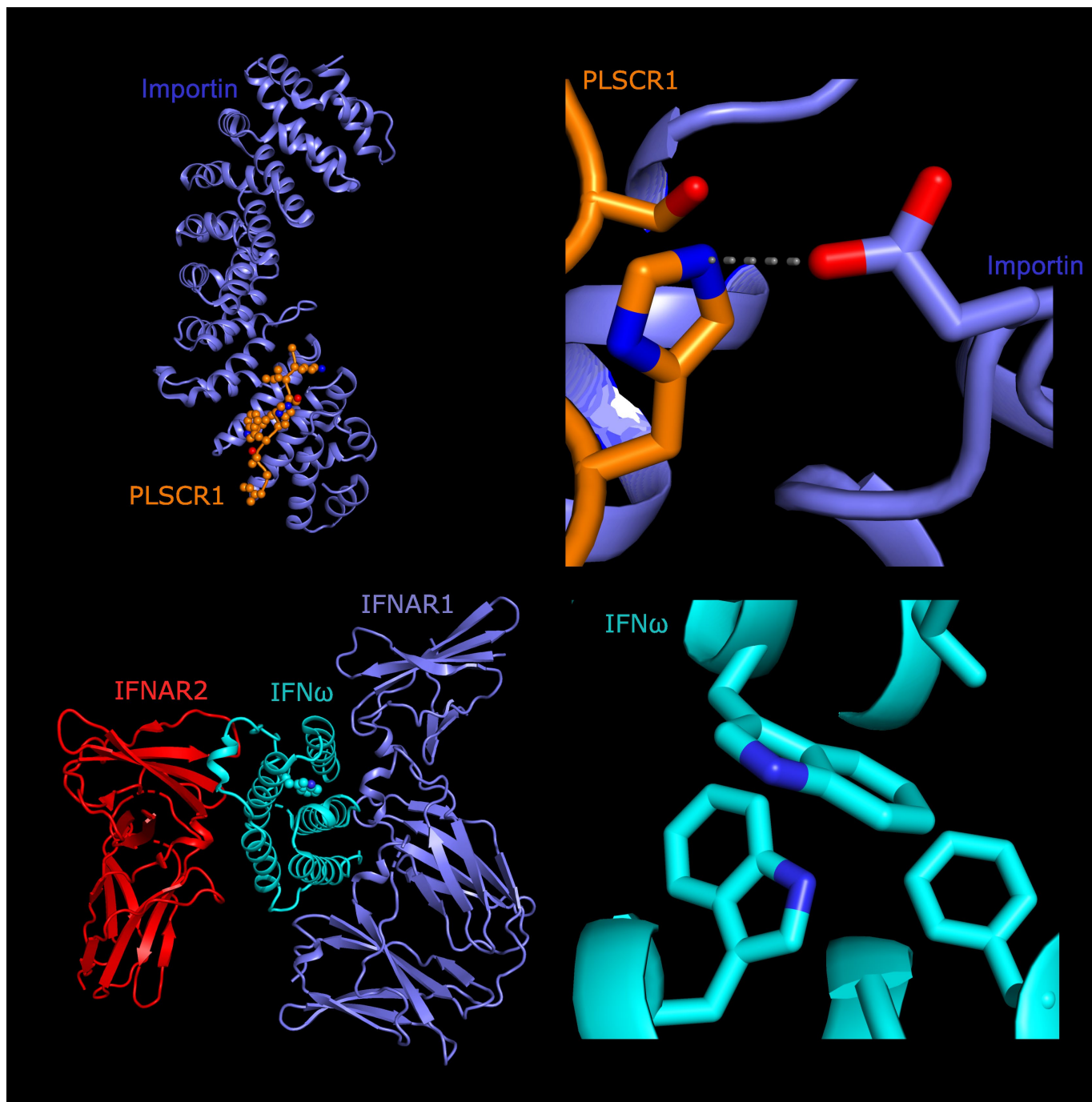
Extended Data Fig. 3 | Regional detail showing fine-mapping to identify two adjacent independent signals on chromosome 19. Top two panels: variants in LD with the lead variants shown. The variants that are included in two independent credible sets are displayed with black outline circles. r^2 values

in the legend denote upper limits, $0.2=[0.2,0.2]$, $0.4=[0.2,0.4]$, $0.6=[0.4,0.6]$, $0.8=[0.6,0.8]$, $1=[0.8,1]$. Bottom panel: locations of protein-coding genes, coloured by TWAS P -value. The red dashed line shows the Bonferroni-corrected P -value= 2.2×10^{-8} for Europeans.



Extended Data Fig. 4 | Regional detail showing fine-mapping to identify three adjacent independent signals on chromosome 21. Top three panels: variants in LD with the lead variants shown. The variants that are included in three independent credible sets are displayed with black outline circles.

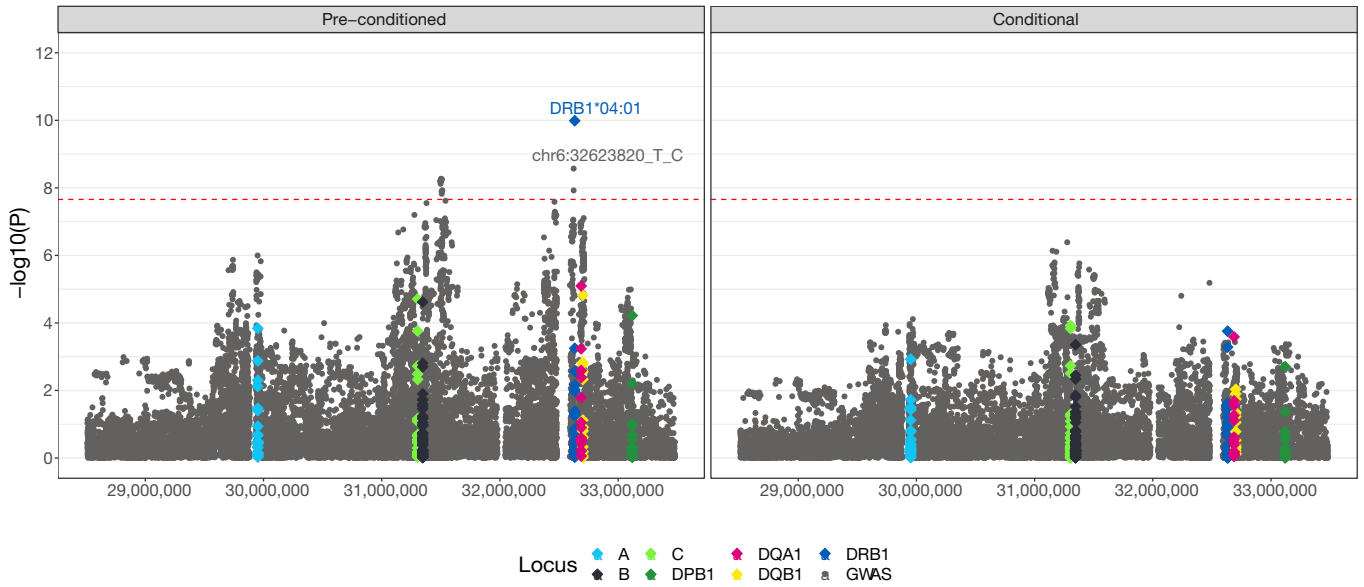
r^2 values in the legend denote upper limits, $0.2=[0,0.2]$, $0.4=[0.2,0.4]$, $0.6=[0.4,0.6]$, $0.8=[0.6,0.8]$, $1=[0.8,1]$. Bottom panel: locations of protein-coding genes, coloured by TWAS P -value. The red dashed line shows the Bonferroni-corrected P -value= 2.2×10^{-8} for Europeans.



Extended Data Fig. 5 | Predicted structural consequences of lead variants at PLSCR1 and IFNA10. (a) Crystal structure of PLSCR1 nuclear localization signal (orange, Gly257–Ile266, numbering correspond to UniProt entry O15162) in complex with Importin α (blue), Protein Data Bank (PDB) ID 1Y2A (ref. ⁶⁵). Side chains of PLSCR1 are shown as connected spheres with carbon atoms coloured in orange, nitrogens in blue and oxygens in red. Hydrogen atoms were not determined at this resolution (2.20) and are not shown. (b) Close-up view showing side chains of PLSCR1 Ser260, His262 and Importin Glu107 as sticks. Distance (in) between selected atoms (PLSCR1 His262 Ne2 and Importin Glu107 carboxyl O) is indicated. A hydrogen bond between PLSCR1 His262 and Importin Glu107 is indicated with a dashed line. The risk variant is predicted to eliminate this bond, disrupting nuclear import, an essential step for effect on antiviral signalling²⁷ and neutrophil maturation⁶⁶. (c) Because there is very

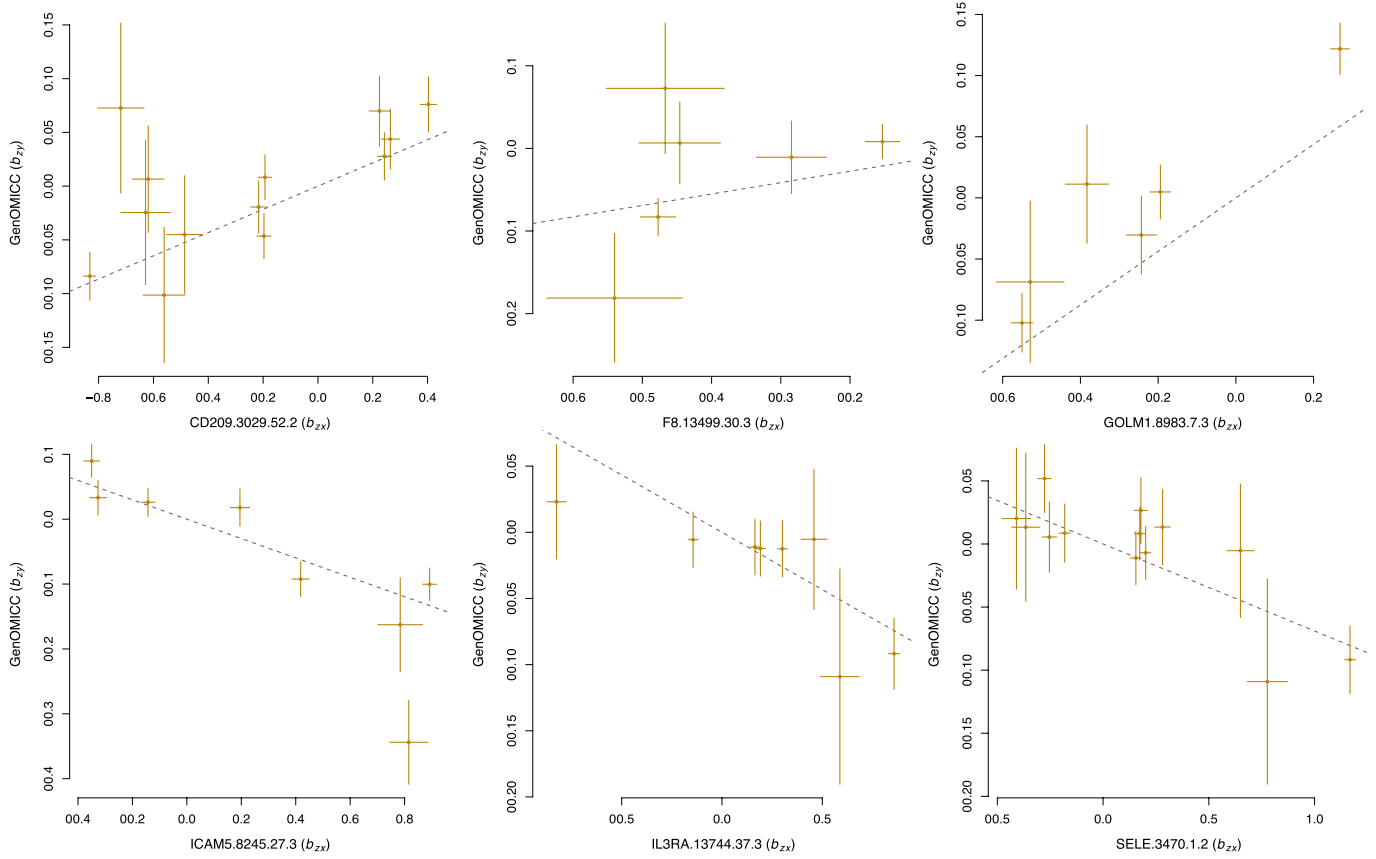
strong sequence conservation between IFNA10 and the gene encoding IFN ω , we used existing crystal structure data (Protein Data Bank ID 3SE4 (ref. ⁶⁷)) for IFN ω (cyan) to display a ternary complex with interferon α/β receptor IFNAR1 (blue), IFNAR2 (red). The side chain of Trp164 is shown as spheres and indicated with a black line. (d) The hydrophobic core of IFN ω with Trp164 shielded from the solvent in the center. Trp164-surrounding residues of IFN ω are numbered and correspond to UniProt entry P05000. Trp164 and surrounding residues are conserved in IFNA10 (UniProt ID P01566) and share the same numbering as in IFN ω (P05000). Side chains of four residues are shown as sticks. Carbon and nitrogen atoms coloured in cyan and blue, respectively. The critical COVID-19-associated mutation, Trp164Cys, would replace an evolutionarily conserved, bulky side chain in the hydrophobic core of IFNA10 with a smaller one, which may destabilize IFNA10.

Overlaid GWAS and HLA associations: conditioned on DRB1*04:01
(Europeans $s_{\text{e}}_{\text{vs_mld_aggV2}}$)



Extended Data Fig. 6 | Manhattan plot of HLA and GWAS signal across the extended MHC region for the EUR cohort. Grey circles mark the GWAS (small variant) associations and diamonds represent the HLA each allele association, coloured by locus. The lead variant from the GWAS and lead allele from HLA are

labelled. The left-panel shows the raw association $-\log_{10}(P\text{values})$ per variant-prior to conditional analysis. The right-panel shows the $-\log_{10}(P\text{values})$ per variant following conditioning on DRB1*04:01. The dashed red line shows the Bonferroni-corrected genome-wide significance threshold for Europeans.



Extended Data Fig. 7 | Effect-effect plots for Mendelian randomization analyses to assess causal evidence for circulating proteins in critical COVID-19. Each plot shows effect size (β) of variants associated with protein

concentration (x axis) and critical COVID-19 (y axis). A full list of instruments is found in Supplementary Table 13.

Article

Extended Data Table 1 | Fine-mapping results for lead variants and worst consequence variant in each credible set

| Lead variant | Pop | Focal CS | nCS | Worst variant | Worst variant Pval | Lead variant CADD | Worst variant CADD | Worst Consequence | Worst gene |
|-----------------------|------|-----------------------|------|---------------------|------------------------|-------------------|--------------------|----------------------------|------------------|
| chr1:155066988:C:T | EUR | chr1:155197995:A:G | 9 | chr1:155066988:C:T | 6.8×10^{-10} | 10.3 | 10.3 | synonymous | <i>EFNA4</i> |
| chr1:155175305:G:A | META | chr1:155197995:A:G | 5 | chr1:155134292:T:C | 1.17×10^{-07} | 8.34 | 1.37 | 3' UTR | <i>EFNA1</i> |
| chr1:155197995:A:G | EUR | chr1:155197995:A:G | 3 | chr1:155202934:T:C | 3.15×10^{-12} | 2.1 | 21.2 | missense | <i>THBS3</i> |
| chr3:45796521:G:T | EUR | chr3:45859597:C:T | 1 | chr3:45796521:G:T | 9.9×10^{-17} | 9.19 | 9.19 | 5' UTR | <i>SLC6A20</i> |
| chr3:45859597:C:T | EUR | chr3:45859597:C:T | 9 | chr3:45825948:A:G | 6.1×10^{-132} | 0.143 | 7.96 | 3' UTR | <i>LZTFL1</i> |
| chr3:146517122:G:A | EUR | chr3:146517122:G:A | 9 | chr3:146517122:G:A | 4.94×10^{-09} | 22.6 | 22.6 | missense | <i>PLSCR1</i> |
| chr5:131995059:C:T | EUR | chr5:131995059:C:T | 32 | chr5:132075767:T:C | 1.48×10^{-09} | 0.206 | 6.09 | missense | <i>CSF2</i> |
| chr6:32623820:T:C | EUR | chr6:32623820:T:C | 33 | chr6:32467073:G:C | 6.65×10^{-08} | 10.1 | 8.12 | intron | <i>HLA-DRB9</i> |
| chr6:41515007:A:C | META | chr6:41515652:G:C | 8 | chr6:41515652:G:C | 5.17×10^{-08} | 4.11 | 4.17 | intron | <i>LINC01276</i> |
| chr9:21206606:C:G | EUR | chr9:21206606:C:G | 3 | chr9:21206606:C:G | 1.93×10^{-09} | 23.9 | 23.9 | missense | <i>IFNA10</i> |
| chr11:34482745:G:A | EUR | chr11:34482745:G:A | 4 | chr11:34479140:G:A | 2.56×10^{-10} | 0.073 | 1.32 | 3' UTR | <i>ELF5</i> |
| chr12:132489230:G:C:G | EUR | chr12:132489230:G:C:G | 25 | chr12:132565387:T:C | 1.42×10^{-07} | 4.91 | 4.64 | non coding transcript exon | - |
| chr13:112889041:C:T | EUR | chr13:112889041:C:T | 4 | chr13:112886111:C:T | 5.36×10^{-11} | 0.676 | 5.5 | 3' UTR | <i>ATP11A</i> |
| chr15:93046840:T:A | EUR | chr15:93046840:T:A | 2 | chr15:93046840:T:A | 8.61×10^{-13} | 4.45 | 4.45 | intron | <i>RGMA</i> |
| chr16:89196249:G:A | EUR | chr16:89196249:G:A | 4 | chr16:89196249:G:A | 4.4×10^{-09} | 22.8 | 22.8 | missense | <i>SLC22A31</i> |
| chr17:46152620:T:C | EUR | chr17:46152620:T:C | 1430 | chr17:45830530:T:C | 1.14×10^{-07} | 5.27 | 3.96 | stop lost | <i>CRHR1</i> |
| chr17:49863260:C:A | EUR | chr17:49863260:C:A | 5 | chr17:49880589:C:T | 1.91×10^{-09} | 5.38 | 7.22 | TF binding site | - |
| chr19:4717660:A:G | EUR | chr19:4717660:A:G | 1 | chr19:4717660:A:G | 3.91×10^{-36} | 16.3 | 16.3 | intron | <i>DPP9</i> |
| chr19:10305768:G:A | EUR | chr19:10352442:G:C | 3 | chr19:10380329:C:G | 7.93×10^{-11} | 0.422 | 7.91 | intron | <i>TYK2</i> |
| chr19:10352442:G:C | EUR | chr19:10352442:G:C | 1 | chr19:10352442:G:C | 6.98×10^{-17} | 25.1 | 25.1 | missense | <i>TYK2</i> |
| chr19:48697960:C:T | EUR | chr19:48697960:C:T | 10 | chr19:48703346:C:T | 6.75×10^{-10} | 2.44 | 7.02 | synonymous | <i>FUT2</i> |
| chr21:33230000:C:A | EUR | chr21:33230000:C:A | 16 | chr21:33262573:G:A | 5.35×10^{-21} | 10.1 | 3.43 | missense | <i>IFNAR2</i> |
| chr21:33287378:C:T | EUR | chr21:33230000:C:A | 33 | chr21:33288868:T:G | 1.59×10^{-07} | 3.63 | 5.84 | intron | <i>IL10RB</i> |
| chr21:33959662:T:TAC | EUR | chr21:33230000:C:A | 23 | chr21:33972178:G:A | 1.32×10^{-08} | 0.246 | 0.282 | non coding transcript exon | <i>LINC00649</i> |

Fine-mapping was performed in EUR for all variants except chr6:41515007:A:C, which was fine-mapped in the SAS population for which the signal was strongest among the per-population analyses. The lead variant chr2:60480453:A:G (rs1123573) that was discovered in multi-ancestry meta-analysis is not included in the table as fine-mapping did not generate any credible sets with the required posterior inclusion probability of >0.95 for any of the populations. Focal CS is the index SNP that was used for fine-mapping with SusieR, 1.5Mb on each side. nCS indicates the number of variants included in each credible set. Consequence annotation for all variants across credible sets was generated using VEP v.104 and the worst consequence across GENCODE basic transcripts was chosen. All variants were ranked according to their consequence type and chr:pos_{hg38}:ref_{hg38}:alt, P value and CADD score are provided for the variant with the worst consequence across all variants in each credible set.

Extended Data Table 2 | Identification of 16 proteins by the GSMR analysis for COVID-19 severity at FDR < 0.05

| Gene | <i>BETA</i> | <i>SE</i> | <i>P</i> | <i>BETA</i> _{hgib2.23m} | <i>SE</i> _{hgib2.23m} | <i>P</i> _{hgib2.23m} |
|-----------|-------------|-----------|-----------------------|----------------------------------|--------------------------------|-------------------------------|
| ICAM5 | -0.15 | 0.025 | 2.82×10^{-9} | -0.07 | 0.013 | 7.65×10^{-8} * |
| GOLM1 | 0.22 | 0.037 | 2.92×10^{-9} | 0.20 | 0.021 | 1.04×10^{-21} * |
| ICAM1 | 0.10 | 0.017 | 6.33×10^{-9} | 0.013 | 0.009 | 0.14 |
| ICAM5 | -0.19 | 0.033 | 1.58×10^{-8} | -0.048 | 0.017 | 0.0054 |
| FAM3D | 0.13 | 0.024 | 2.12×10^{-8} | 0.12 | 0.013 | 3.12×10^{-18} * |
| PDGFRL | 0.10 | 0.021 | 1.85×10^{-6} | 0.021 | 0.010 | 0.041 |
| CD209 | 0.11 | 0.024 | 6.58×10^{-6} | 0.11 | 0.014 | 1.88×10^{-15} * |
| ABO | 0.064 | 0.017 | 0.00012 | 0.084 | 0.0088 | 7.76×10^{-22} * |
| C1GALT1C1 | 0.13 | 0.037 | 0.00026 | 0.055 | 0.030 | 0.063 |
| CCL25 | 0.15 | 0.040 | 0.00026 | 0.035 | 0.023 | 0.13 |
| F8 | 0.14 | 0.042 | 0.0011 | 0.16 | 0.020 | 1.46×10^{-14} * |
| TLR4:LY96 | -0.12 | 0.038 | 0.0014 | - | - | - |
| IL3RA | -0.087 | 0.028 | 0.0019 | -0.065 | 0.014 | 4.33×10^{-6} * |
| SELE | -0.069 | 0.022 | 0.0019 | -0.095 | 0.013 | 3.76×10^{-14} * |
| CAMK1 | -0.064 | 0.021 | 0.00205 | 0.0047 | 0.0110 | 0.664 |
| IL27RA | -0.084 | 0.028 | 0.00229 | 0.0020 | 0.0150 | 0.892 |

We report the effect size *BETA*, the standard error *SE* and the *P* value *P* for the GenOMICC analysis and the replication with HGI B2 and 23andme meta-analysis. An asterisk (*) next to the replication *P* value (*P*_{hgib2.23m}) indicates that the protein result is replicated with concordant direction of effect. We considered as replicated those results that passed a Bonferroni correction of the *P* values of the replicated outcome Mendelian randomization.

Reporting Summary

Nature Portfolio wishes to improve the reproducibility of the work that we publish. This form provides structure for consistency and transparency in reporting. For further information on Nature Portfolio policies, see our [Editorial Policies](#) and the [Editorial Policy Checklist](#).

Statistics

For all statistical analyses, confirm that the following items are present in the figure legend, table legend, main text, or Methods section.

n/a Confirmed

- The exact sample size (n) for each experimental group/condition, given as a discrete number and unit of measurement
- A statement on whether measurements were taken from distinct samples or whether the same sample was measured repeatedly
- The statistical test(s) used AND whether they are one- or two-sided
Only common tests should be described solely by name; describe more complex techniques in the Methods section.
- A description of all covariates tested
- A description of any assumptions or corrections, such as tests of normality and adjustment for multiple comparisons
- A full description of the statistical parameters including central tendency (e.g. means) or other basic estimates (e.g. regression coefficient) AND variation (e.g. standard deviation) or associated estimates of uncertainty (e.g. confidence intervals)
- For null hypothesis testing, the test statistic (e.g. F , t , r) with confidence intervals, effect sizes, degrees of freedom and P value noted
Give P values as exact values whenever suitable.
- For Bayesian analysis, information on the choice of priors and Markov chain Monte Carlo settings
- For hierarchical and complex designs, identification of the appropriate level for tests and full reporting of outcomes
- Estimates of effect sizes (e.g. Cohen's d , Pearson's r), indicating how they were calculated

Our web collection on [statistics for biologists](#) contains articles on many of the points above.

Software and code

Policy information about [availability of computer code](#)

Data collection Nucleon Kit (Cytiva), Chemagic 360 platform using Chemagic DNA blood kit (Perkin Elmer) . T Qubit and normalised Illumina TruSeq DNA PCR-Free High Throughput Sample Preparation kit, Illumina HiSeq X instrument (for 100,000 Genomes Project samples), NovaSeq instrument (for the COVID-19 critical and mild cohorts).

Data analysis VerifyBAMID, DRAGEN(v3.2.22), Illumina North Star Version 4 Whole Genome Sequencing Workflow (NSV4, version 2.6.53.23), ISAAC Aligner (version 03.16.02.19), Starling Small Variant Caller (version 2.4.7), GVGCFGenotyper (GG) v3.8.1, vt v0.57721, gvcfgenotyper v2019.02.26, bcftools v1.10.2, plink 1.9, HiSeq+NSV4, HiSeq+Pipeline 2.0, NovaSeq+Pipeline 2.0, KING 2.1, plink2, GCTA v1.93.1_beta, Strelka2, SAIGE v0.44.5, GCTA 1.9.3, SusieR v0.11.42, VEPv104, metal 2018-08-28, MetaSubtract package (v1.60), R(v4.0.2), SAIGE-GENE v0.44.5, LOFTEE, VEPv99, MetaXCan (v0.6.5), coloc R package 5.1.0, R 3.6.3, GSMR, Heidi, HIBAG R package 1.8.3, XGR package (20-Apr-2020), LDSC (v1.0.1), HDL(v.1.4.0), REGENIEv2.2

For manuscripts utilizing custom algorithms or software that are central to the research but not yet described in published literature, software must be made available to editors and reviewers. We strongly encourage code deposition in a community repository (e.g. GitHub). See the Nature Portfolio [guidelines for submitting code & software](#) for further information.

Data

Policy information about [availability of data](#)

All manuscripts must include a [data availability statement](#). This statement should provide the following information, where applicable:

- Accession codes, unique identifiers, or web links for publicly available datasets
- A description of any restrictions on data availability
- For clinical datasets or third party data, please ensure that the statement adheres to our [policy](#)

Full summary data in support of the findings of this study will be available for download from <https://genomicc.org/data> concurrently with publication. Individual-level data can be analysed by qualified researchers in the UK Outbreak Data Analysis Platform at the University of Edinburgh by application at <https://genomicc.org/data>. Genomic data for 1000,000 genomes participants and cases are available through the Genomics England research environment. The full GWAS summary statistics for the 23andMe discovery data set will be made available through 23andMe to qualified researchers under an agreement with 23andMe that protects the privacy of the 23andMe participants. Please visit <https://research.23andme.com/dataset-access/> for more information and to apply to access the data.

Field-specific reporting

Please select the one below that is the best fit for your research. If you are not sure, read the appropriate sections before making your selection.

- Life sciences Behavioural & social sciences Ecological, evolutionary & environmental sciences

For a reference copy of the document with all sections, see [nature.com/documents/nr-reporting-summary-flat.pdf](https://www.nature.com/documents/nr-reporting-summary-flat.pdf)

Life sciences study design

All studies must disclose on these points even when the disclosure is negative.

| | |
|-----------------|---|
| Sample size | Cases: n=7,491, controls n=48,400 (mild cases n=1630, 100k controls n=46,770). European ancestry ncases=5,989 ncontrols=41,891 South Asian ancestry ncases=788, ncontrols=3,793 African ancestry ncases=440, ncontrols=1,350 East Asian ancestry ncases=274, ncontrols=366 |
| Data exclusions | no exclusions |
| Replication | Data from the Host Genetics Initiative (HGI) data freeze 6 B2 analysis (hospitalised cases) were combined in a meta-analysis with data shared by 23andMe.Inc . We removed signals in HGI derived from GenOMICC cases for independence. 22 of the 25 independent GWAS signals were replicated. Replication of rs28368148 and rs4424872 was attempted using a trans-ancestry meta-analysis UKB, AncestryDNA, Penn Medicine Biobank (PMBB), and Geisinger Health Systems (GHS) totaling 9937 hospitalized COVID-19 cases and 1,059,390 controls (COVID-19 negative or unknown). 1 extra loci (rs28368148) was replicated using this method. The loci not replicated correspond to the lead snps: rs9271609 in HLA region and rs4424872 next to RGMA. |
| Randomization | Not relevant to the study. There wasn't any allocation to experimental groups |
| Blinding | Not relevant to the study. |

Reporting for specific materials, systems and methods

We require information from authors about some types of materials, experimental systems and methods used in many studies. Here, indicate whether each material, system or method listed is relevant to your study. If you are not sure if a list item applies to your research, read the appropriate section before selecting a response.

Materials & experimental systems

| | |
|-------------------------------------|---|
| n/a | Involved in the study |
| <input checked="" type="checkbox"/> | <input type="checkbox"/> Antibodies |
| <input checked="" type="checkbox"/> | <input type="checkbox"/> Eukaryotic cell lines |
| <input checked="" type="checkbox"/> | <input type="checkbox"/> Palaeontology and archaeology |
| <input checked="" type="checkbox"/> | <input type="checkbox"/> Animals and other organisms |
| <input type="checkbox"/> | <input checked="" type="checkbox"/> Human research participants |
| <input checked="" type="checkbox"/> | <input type="checkbox"/> Clinical data |
| <input checked="" type="checkbox"/> | <input type="checkbox"/> Dual use research of concern |

Methods

| | |
|-------------------------------------|---|
| n/a | Involved in the study |
| <input checked="" type="checkbox"/> | <input type="checkbox"/> ChIP-seq |
| <input checked="" type="checkbox"/> | <input type="checkbox"/> Flow cytometry |
| <input checked="" type="checkbox"/> | <input type="checkbox"/> MRI-based neuroimaging |

Human research participants

Policy information about [studies involving human research participants](#)

Population characteristics

Severe COVID-19 (n=7491). Significant comorbidities: 1,605. Died(60 days) 2154, Invasive Ventilation 4028.
 mean age=60, mean BMI=29.9
 European ancestry (n=5,989): males 4,062 females 1,927.
 South Asian ancestry (n=788): males:586, females:202
 East Asian ancestry(n=274) males:162, females:112
 African ancestry(n=440) males:286, females 154
 100K controls: 18,915 unaffected family members of rare diseases participants. 14,701 affected rare diseases participants, 1,005 not assessed for disease status, 12,149 cancer participants.
 mean age: 51
 mean BMI: 26.1
 European ancestry (n=41,384): males 18,971females 22,413
 South Asian ancestry (n=3698): males:1802, females:1896
 East Asian ancestry(n=352) males:138, females:224
 African ancestry(n=1,236) males:632, females:704
 Mild COVID-19 cohort. mean age: 46.
 European ancestry (n=1507): males:410, females:1,097
 South Asian ancestry (n=95): males:43, females:52
 East Asian ancestry(n=14) males:8, females:6
 African ancestry(n=14) males:6, females:8

Recruitment

Critically ill patients recruited to the GenOMICC study (genomicc.org) had confirmed COVID-19 according to local clinical testing and were deemed, in the view of the treating clinician, to require continuous cardiorespiratory monitoring. In UK practice this kind of monitoring is undertaken in high dependency or intensive care units. Patients were recruited from 224 ICU across the UK.
 Participants were recruited to the mild COVID-19 cohort on the basis of having experienced mild (non-hospitalised) or asymptomatic COVID-19. Participants volunteered to take part in the study via a microsite and were required to self-report the details of a positive COVID-19 test. Volunteers were prioritised for genome sequencing based on demographic matching with the critical COVID-19 cohort considering self-reported ancestry, sex, age and location within the UK.
 Participants were enrolled in the 100,000 Genomes Project from families with a broad range of rare diseases, cancers and infection by 13 regional NHS Genomic Medicine Centres across England and in Northern Ireland, Scotland and Wales. For this analysis, participants for whom a positive SARS-CoV-2 test had been recorded as of March, 2021 were not included due to uncertainty in the severity of COVID-19 symptoms. Only participants for whom genome sequencing was performed from blood derived DNA were included and participants with haematological malignancies were excluded to avoid potential tumour contamination.

Ethics oversight

Research ethics committees (Scotland 15/SS/0110, England, Wales and Northern Ireland: 19/WM/0247. Current and previous versions of the study protocol are available at genomicc.org/protocol.
 UKBiobank Study: ethical approval for the UK Biobank was previously obtained from the North West Centre for Research Ethics Committee(11/NW/0382). The work described herein was approved by UK Biobank under application number 26041.
 GHS study: approval for DiscovEHR analyses was provided by the Geisinger Health System Institutional Review Board under project number 2006-0258.
 AncestryDNA study: all data for this research project was from subjects who provided prior informed consent to participate in AncestryDNA's Human Diversity Project, as reviewed and approved by our external institutional review board, Advarra (formerlyQuorum). All data was de-identified prior to use.
 PMBBstudy: appropriate consent was obtained from each participant regarding storage of biological specimens, genetic sequencing and genotyping, and access to all available EHR data. This study was approved by the Institutional Review Board of the University of Pennsylvania and complied with the principles set out in the Declaration of Helsinki. Informed consent was obtained for all study participants.

Note that full information on the approval of the study protocol must also be provided in the manuscript.